AMBIENT VIBRATION TESTING AND SEISMIC PERFORMANCE ASSESSMENT OF HAGIA IRENE

by

Cem Şentay

B.Sc., Civil Engineering, Boğaziçi University, 2016

Submitted to the Institute for Graduate Studies in
Science and Engineering in partial fulfillment of
the requirements for the degree of
Master of Science

Graduate Program in Civil Engineering

Boğaziçi University

2021

ACKNOWLEDGEMENTS

First and foremost, I would like to express my sincere and deep gratitude to my thesis supervisor, Professor Serdar Soyöz for giving me the opportunity to do research on this extraordinary structure and topic and for his invaluable guidance throughout this thesis. Not only during my master's studies but also during the research works of this thesis, he has provided me with invaluable information about the methodology of this research. I am also very grateful for his patience, ease of mind, kindness and friendship.

Besides my supervisor, I would also like thank the rest of my thesis committee: Professor Cem Yalçın and Associate Professor Ufuk Yazgan for their encouragement and insightful comments. I am also thankful to Professor Cem Yalçın for his valuable teachings throughout my bachelor's degree.

I am extremely grateful to the teaching assistants of my supervisor, Emre Aytulun and Semih Gönen for their friendship, sense of humour and continuous support and guidance throughout my research. Apart from my supervisor, they were the two greatest contributors to my research.

I would also like thank my classmates Mert Güner, Aykut Onursal, Özlem Adalı, Onur Manat, Kaan Aytekin, Ali Atilla Arısoy and many others for their support and friendship during my master's studies. I also want to thank my coworkers for their understanding and patience during this research.

Last but not least, I humbly thank my mother, my father and my brother for their continuous support and encouragement, and my partner in crime, Ezgi İlhan for her deep care and love, understanding and support no matter the situation through this process. They made me who I am today.

ABSTRACT

AMBIENT VIBRATION TESTING AND SEISMIC PERFORMANCE ASSESSMENT OF HAGIA IRENE

This thesis investigates the applicable methods for ambient vibration testing and seismic assessment to the cultural heritage buildings by using the Hagia Irene Church in Istanbul as the case study. The city of Istanbul is home to hundreds of cultural heritage buildings. These buildings suffered numerous damages throughout history due to environmental conditions, human-caused incidents and natural disasters. Due to these facts, it is important to know the current condition of these buildings. It is especially important to conduct such studies in Turkey, due to the fact that Turkey is in an active earthquake zone. There are many challenges to tackle during the seismic assessment of heritage buildings. One of these challenges is the construction techniques and material properties. It is difficult to model the behaviour of a masonry structure. To counter this, the proposed methodology includes using a small-scale test to lay a foundation for the greater work ahead. In this small-scale test, a masonry panel wall was subjected to non-destructive identification tests and a cyclic loading test. After conducting the lab-tests, a finite element model of the wall was made to imitate the conditions of the lab-test. Then the experimental and numerical results were compared to determine the viability of the proposed methodology. Satisfied with the obtained results, an ambient vibration test was made to Hagia Irene and a finite element model of the structure was created and calibrated according to the vibration data. The results obtained from this model were used to determine the seismic performance of Hagia Irene.

ÖZET

AYA İRİNİ'NİN ORTAM TİTREŞİM TESTİ VE DEPREM PERFORMANS DEĞERLENDİRMESİ

Bu tez, İstanbul'daki Aya İrini Kilisesi'ni örnek olay incelemesi olarak kullanarak kültürel miras yapılarına ortam titreşim testi ve sismik değerlendirme için uygulanabilir yöntemleri araştırmaktadır. İstanbul şehri yüzlerce kültürel mirasa ev sahipliği yapmaktadır. Bu binalar, çevre koşulları, insan kaynaklı olaylar ve doğal afetler nedeniyle tarih boyunca sayısız zarara uğramıştır. Bu sebeplerden dolayı bu binaların mevcut durumunun bilinmesi önemlidir. Türkiye aktif deprem bölgesinde olduğu için Türkiye'de bu tür çalışmaların yapılması özellikle önemlidir. Tarihi binaların sismik değerlendirmesi sırasında üstesinden gelinmesi gereken birçok zorluk vardır. Bu zorluklardan biri inşaat yöntemleri ve malzeme özellikleridir. Bir yığma yapının davranışını modellemek zordur. Bununla mücadele etmek için önerilen metodoloji, ilerideki daha büyük işler için bir temel oluşturmak üzere küçük ölçekli bir test kullanmayı içerir. Bu küçük ölçekli testte, bir yığma panel duvar tahribatsız tanımlama testlerine ve döngüsel yükleme testine tabi tutulmuştur. Laboratuar testleri yapıldıktan sonra, laboratuar testinin koşullarını taklit etmek için duvarın sonlu eleman modeli yapılmıştır. Daha sonra önerilen metodolojinin uygulanabilirliğini belirlemek için deneysel ve sayısal sonuçlar karşılaştırılmıştır. Elde edilen sonuçlardan memnun kalınarak Aya İrini'ye ortam titreşim testi yapılmış ve titreşim verilerine göre yapının sonlu eleman modeli oluşturularake kalibre edilmiştir. Bu modelden elde edilen sonuçlar Aya İrini'nin sismik performansını belirlemek için kullanılmıştır.

TABLE OF CONTENTS

ACKNOWLEDGEMENTS iii
ABSTRACT iv
ÖZET v
LIST OF FIGURES ix
LIST OF TABLES xv
LIST OF SYMBOLS xvi
LIST OF ACRONYMS/ABBREVIATIONS xvii
1. INTRODUCTION 1
1.1. Global Context 1
1.2. Seismic Performance Assessment of Cultural Heritage Buildings 2
1.3. Research Motivation and Objective 3
2. LITERATURE REVIEW 4
2.1. Structural Health Monitoring 4
2.1.1. General Definition 4
2.1.2. Motivation 5
2.1.3. Brief History of Structural Health Monitoring 6
2.1.4. Conclusion 7
2.2. Structural Health Monitoring of Masonry Structures 7
2.2.1. Introduction 7
2.2.2. Case Studies 8
2.2.2.1. Masonry Towers 8
2.2.2.2. Religious Structures 12
2.2.2.3. Bridges 15
2.2.3. Conclusion and Remarks 19
2.3. Finite Element Modelling of Masonry Structures 20
2.3.1. Introduction 20
2.3.1.1. Micro-Modelling 21
2.3.1.2. Mezzo-Modelling 22
2.3.1.3. Macro-Modelling 23

2.3.2. Conclusion 24
3. METHODOLOGY 25
3.1. Introduction 25
3.2. On-Site Test 25
3.3. Finite Element Analysis 26
4. SMALL SCALE TEST 28
4.1. Introduction 28
4.2. Laboratory Tests 28
4.3. Finite Element Model 35
4.3.1. Creating the Model 35
4.3.2. Modal Analysis and Results 35
4.3.3. Cyclic Loading Analysis and Results 38
4.4. Results Comparison and Interpretation 42
4.5. Conclusion 48
5. ON-SITE TEST 49
5.1. Hagia Irene 49
5.1.1. History 49
5.1.2. Architecture 50
5.2. Ambient Vibration Test 52
5.2.1. Introduction 52
5.2.2. Procedure 52
5.2.3. Signal Analysis and Results 57
6. FINITE ELEMENT MODEL 60
6.1. Creating the Model 60
6.2. Summary of FEM Results 67
6.2.1. Modal Results 67
6.2.2. Response Spectrum Analysis and Results 76
7. RESULTS DISCUSSION 87
7.1. Possible Damage Zones 87
7.2. Comparing the Results with the Damages in Hagia Irene 96
8. CONCLUSION 107

REFERENCES 111

LIST OF FIGURES

Figure 2.1. Typical Structural Health Monitoring System 4

Figure 2.2. Micro-Modelling Method 22

Figure 2.3. Mezzo-Modelling Method 23

Figure 2.4. Macro-Modelling Method 24

Figure 4.1. The Wall Under Construction 29

Figure 4.2. Masonry Wall During Flat Jack Test 30

Figure 4.3. Accelerometer Layout 31

Figure 4.4. Final Testing System 32

Figure 4.5. Final Testing System Sketch 33

Figure 4.6. Damaged Wall After The Test 34

Figure 4.7. First Mode, 17.09 Hz 37

Figure 4.8. Second Mode, 38.74 Hz 37

Figure 4.9. Third Mode, 57.50 HZ 37

Figure 4.10. Hysteresis Curve obtained from Cyclic Test 38

Figure 4.11. Stress-Strain Curve Of Masonry Model 39

Figure 4.12. Meshed FEM Of The Wall 40

Figure 4.13. Surface Displacement Case 41

Figure 4.14. Nodal Displacement Case 42

Figure 4.15. Stair Cracking Pattern 43

Figure 4.16. Nodal Displacement Result 44

Figure 4.17. Surface Displacement Result 44

Figure 4.18. Experimental and Numerical Pushover Curves 46

Figure 4.19. Young's Modulus Change 47

Figure 5.1. Hagia Irene from Outside 50

Figure 5.2. Hagia Irene Inside 51

Figure 5.3. Recording Station 53

Figure 5.4. Accelerometers on the Ground, in Two Different Directions 54

Figure 5.5. Accelerometer on the Wall 55

Figure 5.6. Layout of the Accelerometers 56

Figure 5.7. Peaks with Filter in Longitudinal Direction 58

Figure 5.8. Peaks with Filter in Transverse Direction 59

Figure 6.1. Base Plan of the FEM 61

Figure 6.2. Main Structure Model 1 63

Figure 6.3. Main Structure Model 2 63

Figure 6.4. Main Structure Model 3 63

Figure 6.5. Model of the Narthex 64

Figure 6.6. Model of the Small Dome 65

Figure 6.7. Model of the Large Dome 65

Figure 6.8. Model of the Entire Structure 66

Figure 6.9. Longitudinal Cross Section 66

Figure 6.10. Mode 1, 2.34 Hz 69

Figure 6.11. Mode 2, 2.71 Hz 70

Figure 6.12. Mode 3, 3.28 Hz 70

Figure 6.13. Mode 4, 3.68 Hz 71

Figure 6.14. Mode 5, 3.86 Hz 71

Figure 6.15. Mode 6, 4.43 Hz 71

Figure 6.16. Support Conditions for Set 2 72

Figure 6.17. Spectra Comparison and Modal Frequencies 77

Figure 6.18. Horizontal Acceleration Spectrum DD-2 Earthquake 78

Figure 6.19. Vertical Acceleration Spectrum DD-2 Earthquake 78

Figure 6.20. Shear Stress 80

Figure 6.21. Total Deformation 80

Figure 6.22. Maximum Principal Stress 81

Figure 6.23. Minimum Principal Stress 81

Figure 6.24. Shear Stress 82

Figure 6.25. Total Deformation 82

Figure 6.26. Maximum Principal Stress 83

Figure 6.27. Minimum Principal Stress 83

Figure 6.28. Shear Stress 84

Figure 6.29. Total Deformation 84

Figure 6.30. Maximum Principal Stress 85

Figure 6.31. Minimum Principal Stress 85

Figure 7.1. Total Deformation (mm) 88

Figure 7.2. Longitudinal Cross-Section 89

Figure 7.3. Maximum Principal Stress 90

Figure 7.4. Minimum Principal Stress 91

Figure 7.5. Shear Stresses 92

Figure 7.6. Entry 1 Damages 96

Figure 7.7. Entry 1 Damages FEM Results 97

Figure 7.8. Entry 2 Damages 97

Figure 7.9. Entry 2 Damages, Compressive Stresses 98

Figure 7.10. Entry 2 Damages, Tensile Stresses 98

Figure 7.11. Entry 2 Damages, Shear Stresses 99

Figure 7.12. Entry 3 Damages 99

Figure 7.13. Entry 3 Damages FEM Results 100

Figure 7.14. Narthex Shear Stresses, XY Plane 100

Figure 7.15. Narthex Damages, Longitudinal Cross Section 101

Figure 7.16. Narthex FEM Results, Longitudinal Cross Section 101

Figure 7.17. Entries 4,5 and 6 Damages 102

Figure 7.18. Entries 4,5 and 6 FEM Results 103

Figure 7.19. Damages on the Pillars 104

Figure 7.20. Damages on the Arches 105

Figure 7.21. Damages on the Arches FEM Results 105

LIST OF TABLES

Table 4.1. Modal Results Comparison 36

Table 6.1. Preliminary Results Comparison 68

Table 6.2. Final Results Comparison 69

Table 6.3. Trial Frequency Results 74

Table 6.4. Set 2 Results Comparison 75

Table 6.5. Set 3 Results Comparison 76

Table 6.6. Response Spectrum Results Peak Values 86

LIST OF SYMBOLS

E	Young's Modulus
f_b	Normalised mean compressive strength of a masonry unit
f_k	Characteristic compressive strength of masonry
f_m	Compressive strength of masonry mortar
f_{vk}	Characteristic shear strength of masonry
f_{vko}	Characteristic initial shear strength under zero compressive stress
f_{vlt}	Limit to the value of f_{vk}
K	Constant according to EUROCODE 6 Section 3.6.1
α	Constant according to EUROCODE 6 Section 3.6.1
β	Constant according to EUROCODE 6 Section 3.6.1
ν	Poisson's Ratio
ρ	Density
σ_d	Design compressive stress perpendicular to the shear in the masonry member

LIST OF ACRONYMS/ABBREVIATIONS

3D	Three Dimensional
DD-2	Design earthquake with a 10% probability of exceeding in 50 years, corresponding to a return period of 475 years. It is the "*standard design earthquake ground motion level*".
FEM	Finite Element Method
GPS	Global Positioning System
LVDT	Linear Variable Differential Transformer
SHM	Structural Health Monitoring
ZC	Local Soil Class C, according to 2018 Turkish Seismic Code

1. INTRODUCTION

1.1. Global Context

Architectural heritage is irreplaceable due to its power to define the historical richness and cultural diversity of societies of our time. All countries have their own history and culture and heritage buildings are one of the most commonly used ways to pass on that history and culture through the centuries. Depending on the era in which they were built in, these structures can show great differences although being in the same city. Therefore, cultural heritage buildings are usually defined according to their era they were built in and not according to their usage.

There are many factors threatening the cultural heritage buildings of a country. Some of these factors are weather conditions, age of the structure, wars in the previous centuries and natural disasters. The most important risk factor for Turkey, Italy, Greece and many other countries which are located in seismic regions is earthquakes. Heritage buildings such as churches and arch bridges are made of masonry. The definition of masonry is "the art and craft of building and fabricating in stone, clay, brick or concrete block". Masonry was the most commonly used construction method throughout the history. The technique is still being used nowadays. Masonry structures were designed and constructed considering mainly the static gravitational loads of the structure. Due to this reason, they perform poorly under shear and tension stresses created during earthquakes. This effect is also amplified by the material characteristics of masonry.

Earthquakes in Europe causing damage to historical structures showed that seismic performance assessment and in some cases installation of monitoring systems for heritage buildings is of great importance. There were researches following these earthquakes on the damaged buildings trying to determine the state of the structures. Some of these structures were severely damaged and required immediate diagnosis and rehabilitation to ensure the structural integrity and safety of the structure. There are also

researches made in Turkey, however the number of them is relatively small considering the vast amount of historical heritage buildings our country owns.

1.2. Seismic Performance Assessment of Cultural Heritage Buildings

Why is there a need to determine the seismic performance of cultural heritage buildings? First, although they are structures which have been standing tall throughout the centuries, nothing can prevail against time. These structures, some more than thousand years old, have experienced earthquakes, fires, wars and many other outside effects which can severely damage the structure. Especially Istanbul has seen has its fair share of wars and fires. Sack of Constantinople in April 1204 during the Fourth Crusade and the Fall of Constantinople in May 1453 are some of the historical events in which the city was pillaged and most of its structures damaged. Almost every cultural heritage building in the city has an accumulated damage. Studying and learning about these damages before retrofitting the structures is a must.

Second, safety is a big concern. Almost every cultural heritage building in the world, especially in Istanbul is a tourist attraction. Some of them are still being used for their original purpose, in addition to their touristic purposes. Considering the tourist population in the ancient city of Istanbul, maintaining the structural integrity of cultural heritage buildings is of paramount importance for the safety of the people.

Third, Istanbul is in a seismic zone, which means all of the structures in the city are under the threat of earthquakes. As previously mentioned, most of the cultural heritage buildings are masonry structures and they perform poorly under seismic loads. Seismic performance analysis can also give us an insight on how the structure would perform during a potential earthquake.

Finally, cultural heritage buildings show the history of a city. As the name says, they are heritage and they will be inherited by the future generations. The state of these structures show the value a country gives to its history and culture. It is important to remember that these structures are not national but international heritages.

1.3. Research Motivation and Objective

As previously mentioned, the study to preserve cultural heritage buildings is an international pursuit. In this context, the general motivation for this thesis is provided:

- Istanbul is a global treasure. All of the cultural heritage buildings in Istanbul must be protected and maintained in the most precise way.
- There is an imminent earthquake danger for Istanbul. The seismic assessment and general condition of these cultural heritage buildings must be known and adequate precautions must be taken.
- Due to the sheer number of heritage buildings, a vast number of them are sadly left unmaintained. Some of them require immediate action, such as Hagia Irene.
- Personal interest in architecture and history.

Based on these factors, the objective of this thesis is:

To determine the seismic performance of a complex masonry structure by implementing a multidisciplinary method and to show that masonry structures can be analysed using macro finite element models.

To complete this objective, different methods will be used throughout this thesis. These methods are chosen considering the structure, loading types and analysis types. Analytical, numerical and experimental approaches are used together. In Chapter 2, structural health monitoring, seismic performance analysis, ambient vibration testing, finite element models and their different applications to various historical structures will be inspected. After that, in Chapter 3, the methodology of this thesis will be explained. Chapter 4 and Chapter 5 explain the application of the methodology to a small scale model and Hagia Irene. In Chapter 6, the finite element model of the structure and the details of the finite element method analysis will be discussed. After comparing the results of the finite element model and on-site tests in Chapter 7, all of the works will be summarized and the thesis will be concluded in Chapter 8.

2. LITERATURE REVIEW

2.1. Structural Health Monitoring

2.1.1. General Definition

Implementation of a damage detection strategy for civil engineering structures is called as *Structural Health Monitoring (SHM)* [1]. Thanks to the time-dimension of monitoring, it can be said that SHM provides both a diagnosis and a prognosis (evolution of damage, residual life, etc.) for a structure, with a focus on damage identification. The main focus of this thesis is seismic assessment, however the installation of a permanent monitoring system is the next step after the seismic assessment of a cultural heritage structure, therefore SHM systems will shortly be explained in this chapter.

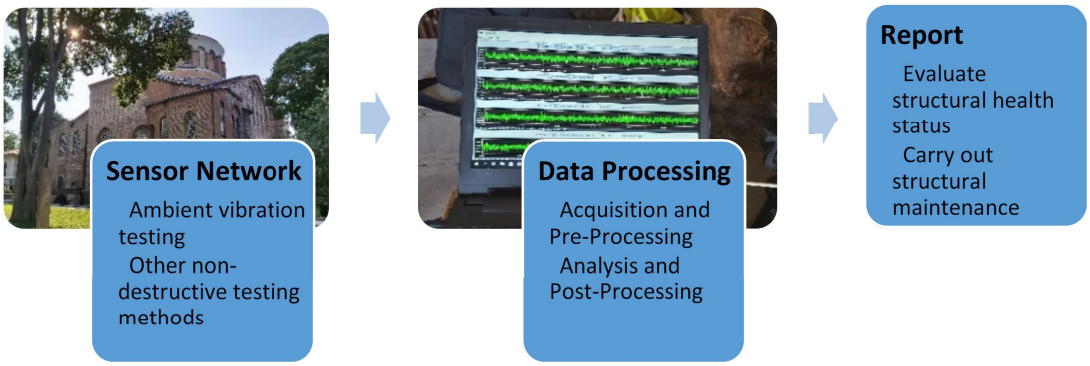

Figure 2.1. Typical Structural Health Monitoring System

In Figure 2.1, a typical structural health monitoring system is shown. There are three main steps in a structural health monitoring system. These are the sensor network, the data processing tool and the final evaluation or report. The sensor network depends on different variables such as the type of damage, the architecture of the structure and even weather conditions. The sensor network is created by using several sensors of the same type, for example accelerometers. The raw data obtained from these

sensors are stored for processing. Apart from these sensors, others are used to monitor the environmental conditions in order to perform usage monitoring. After acquiring and storing the data, they are calibrated and processed using signal analysis methods in order to be analysed. The most important part of a structural health monitoring system is the analysis. The interpretation of the data, filtering useless information from the crucial ones and creating situational and ample algorithms to process the acquired data is heavily reliant on the engineering judgement of the analyser and the correctness of the used analysis methods.

The last part of the structural health monitoring and seismic assessment process is the report and evaluation. The raw results do not mean anything without an interpretation. After the interpretation of the data, a report about the health status of the structure is prepared. According to this report, an action plan is prepared regarding the maintenance of the structure in question.

2.1.2. Motivation

SHM is needed to monitor a structure and detect damages at the earliest possible stage to ensure the safety of structures [2]. Especially private and government industries want to predict risks as soon and accurate as possible to protect their investments [1].

For civil engineers, one of the most important usage of structural health monitoring is damage detection. The most common cause of damages in a structure is earthquakes. This is especially important, since almost one third of the world population lives in earthquake prone zones. SHM can be used to minimize the uncertainties in post-earthquake damage assessments. By minimizing these uncertainties, the reoccupation of buildings would be easier and safer.

Aside from residential buildings, civil infrastructures were also a great development for the condition-based maintenance and seismic assessment systems. Dams, bridges, offshore installations, towers, nuclear installations and tunnels and excavations are examples for civil infrastructures which require constant monitoring in order

to ensure the safety of the said facility.

Nowadays, SHM is being used to extend the lifetime of a structure, detect damages, reduce maintenance costs and ensure the safety of the structures during their entire lifetime.

2.1.3. Brief History of Structural Health Monitoring

Damage identification was practised by measuring the changes in the dynamic response of a system using acoustic techniques since the start of the usage of tools. Observational methods were being used even before that. Nowadays, damage identification methods have become mostly digitalized, leading to the concept of Structural Health Monitoring with the development of stronger, cheaper and smaller computer hardware.

Civil, mechanical and aerospace engineers are the main pursuers in the field of SHM. In the case of civil engineering, major construction projects, such as large dams, long-span cable-supported bridges and offshore gas/oil production installations contributed significantly to the development of SHM technologies [3]. Civil engineers started studying vibration-based damage detection technologies in the early 1980s. Studies in this field were mainly focused on bridge structures and other infrastructures. While identifying damages in the structures, the main parameters are modal properties, mode shapes and other quantities derived from these properties. For a long time, bridges were the main focus of the damage identification technologies.

Apart from bridges, dams are also important structures which require regular inspection. For the dams, structural health monitoring is mainly used for surveillance. Buildings and towers form a major group as a target for the structural health monitoring technologies. The main motivation for the monitoring of buildings was the need to determine or predict the building performance during an earthquake. Determining the performance of a building subjected to certain types of ground motion is crucial for the improvement of structure designs. Most of the monitoring studies are aimed

to understand loading and response mechanisms better, not only for earthquakes, but also for wind loads [3].

For four decades, SHM and seismic performance analysis methods have been evolving into more refined processes. With the continuous development of sensor and data acquisition technologies, better predictions and assessments are being made.

2.1.4. Conclusion

It is without doubt that there will be future developments in this technology, considering its multidisciplinary nature. Signal processing, structural dynamics, different geometry and vibration sensing technologies, data analysis, computational hardware and smart materials are only some of the disciplines which create SHM. Integrating such different technologies and advancing the methods takes a lot of time. Due to these reasons, the development of SHM technologies would only be possible by focused and coordinated research efforts over long periods of time, but slowly and surely, SHM will become an inseparable part of our lives in the future, be it in the civil engineering or any other field of study.

2.2. Structural Health Monitoring of Masonry Structures

2.2.1. Introduction

Masonry structures have been built for thousands of years. Even today, masonry is a very popular material in the construction industry. Although concrete technologies greatly simplified the construction processes and replaced masonry techniques, they are still being used in rural areas or for artistic reasons. The main reason for pursuing research in this field is cultural heritage structures. Many historical structures are made of masonry. These structures include bridges, towers, castles, mosques, churches and even walls. In this part, the different approaches, techniques and the vast application area of this theme will be explained through case studies.

2.2.2. Case Studies

The case studies will be studied in groups according to the type of the structures. These groups are masonry towers, churches and bridges. This will make it easier to compare the methods and results used in different studies regarding similar structures.

2.2.2.1. Masonry Towers. The first case regarding the masonry towers is about the results of an ambient-vibration based methodology used to assess the health conditions of a masonry bell-tower [4]. The tower in question dates back to the 17th century, is 74 meters high and has major cracks on its load-bearing walls. The tower is the historic masonry bell-tower next to the Cathedral of Monza, in a town 20 km far from Milan, Italy. The seismic assessment involves both experimental and theoretical modal analysis. The analysis includes these main steps:

- Ambient vibration testing.
- Operational modal analysis. In the operational modal analysis, using only the output from an ambient vibration test, the modal parameters like natural frequencies and modal shapes are determined.
- Finite element model analysis and its calibration and comparison with the experimental results.
- Identification of the unknown structural parameters of the model updating the model by comparing its results with the experimental data. [4]

It is important to note here that the methodology of this thesis has these same main steps. Before the ambient vibration testing, on-site investigations were carried out in order to determine material properties and to locate damages and crack patterns. Then ambient vibration tests on the tower were conducted to measure the dynamic response. The vibration data was collected at 20 different points, located at different heights on the tower and using these data, the modal parameters are extracted using two different procedures, namely the *Frequency Domain Decomposition* and the *Peak Picking* method. Using these two methods, the natural frequencies and the mode

shapes are determined. After the determination of the modal behaviour of the tower leads to the next step, which is finite element modelling of the structure and structural identification. Some assumptions were made during the modelling which include the type of footing of the tower and the structural parameters like unit weight and Poisson's ratio. The structural parameters were estimated by comparing the theoretical and experimental natural frequencies. The last step was to compare the experimental results with the theoretical results, showing that the results correlate well with each other.

In another paper, a similar methodology as the previous one, which utilizes experimentally identified modal parameters, is used on the San Felice sul Panaro medieval fortress. The fortress was struck a heavy blow by the 2012 Emilia earthquake [5]. In this case, only the main tower of the fortress, with a height of 32 meters and a square plan was studied. Firstly, ambient vibration analysis on the tower was conducted identifying 5 experimental modes of the structure. After the determination of the modal parameters, the finite element of the tower is created using a non-standard mesh generation procedure called CLOUD2FEM. In this method, 3D points cloud generated by laser scanners is transformed into 3D finite element meshes, an almost automatic procedure which minimizes user-time investment. Preliminary material properties (Young's Modulus, Poisson's Ratio) were adopted and according to the experimental results, these parameters were updated. The model updating and structural parameter identification procedures differ from the previous case, however the goal remains the same. There was one problem with the model, which is the severe damages. These damages couldn't be simply modelled using a different elastic modulus for the damaged masonry. Therefore, the cracks were surveyed accurately and the elements corresponding to the damaged areas on the finite element model were calibrated accordingly. After this, it was seen that the actual behaviour of the tower in operational conditions can be fully characterized and the effect of damage and cracks can be accounted for.

The next article explains different finite element modelling strategies used in the seismic assessment of masonry structures. A finite element model updating method using vibration data is also explained. Finite-discrete element modelling was used

in this research, which considers the structure as a sum of blocks [6]. This makes transitions between continua and discontinua, like masonry interfaces, making it an appropriate method for the finite element modelling of masonry. The most important part of the modelling process was the determination of contact properties. There are also models which consider the entire structure to be a rigid body. This cuts down the computational time drastically, however material properties must be chosen accordingly. This theme will be further discussed in the following chapters involving the finite element modelling of masonry structures.

Two structures, 57th Regiment Monument in Çanakkale and M6 minaret of Sultan Ahmed Mosque were modelled for the tests. Before the model updating procedure, ambient vibration tests were conducted on the structures to define the modal parameters experimentally. The monument was modelled discreetly with abundant masonry elements, whereas four different finite element models were created for the minaret. The first model is a continuous model, the second and the third models are discrete models which also consider the actual layout of the masonry elements. The fourth model is also a discrete model, but the units are assumed to be rigid. After updating according to the experimental results, the models were used for seismic assessment. Regarding the results obtained from the tests, it was concluded that for a linear analysis, continuous models and bonded discrete models yield similar results for seismic assessment. In the model updating of discrete models, it is better to update only the joint stiffness values and stick with the experimentally obtained material properties.

In all of the papers until now, ambient vibration analysis and modal extraction are used as tools, however in this next paper, it is the main research focus. To determine the dynamic characteristics of the city hall in L'Aquila, Italy was the main focus of the research. The city hall and its tower was severely damaged during the L'Aquila earthquake in April 2009. The researched dynamic characteristics were the natural frequencies, mode shapes and damping ratios [7]. In order to analyse the ambient vibration responses, three different output-only identification methods were used, which include the frequency-domain decomposition, random decrement technique and the natural excitation technique. Following the explanation of the techniques, the data

collection method and analysis results were shown. The results obtained from the individual analysis methods were compared for the first five modes in both directions of the Civic Tower. After comparing the results of the output-only analysis methods, a finite element model of the structure was created, calibrated according to the previously obtained modal results and then all of the results are compared. In conclusion, all three methods for modal identification showed good agreement, confirming the reliability of the methods and the results.

Apart from short-termed analysis which heavily focuses on modal identification, there are also masonry towers which were analysed using long-term analysis. In the next case, seismic damages on a bell-tower due to the 2016 Central Italy seismic sequence were recorded by utilizing a previously installed SHM system in 2014. The San Pietro monumental bell tower is located in Perugia, Italy [8]. A simple vibration-based structural health monitoring system consisting of 3 accelerometers was already present on the structure to continuously monitor it to detect small damages caused by low return period earthquakes. One year after the start of the test, an ambient vibration test was conducted to define the vibration modes and their natural frequencies. Three major earthquakes made up the 2016 Central Italy seismic sequence. In order to determine the severity of the earthquakes at the site, the structural responses were compared to the responses calculated by applying elastic response spectra, showing that the earthquakes of 2016 Central Italy seismic sequence can be considered small intensity events. The natural frequency changes after the seismic events were clearly visible after the interpretation of the data. Lastly, a finite element model of the structure was created, calibrated using the experimental data and then used for seismic assessment. The most important result obtained from this research is that earthquake-induced damages can be detected using structural health monitoring systems while they are not visible.

There are studies which focus on multiple structures to tackle the differences in the modelling and experimenting methods. The next paper inspects two case monuments in Portugal: the Clock Tower of Mogadouro and the Church of Jeronimos Monastery, in Lisbon. The main focus is the identification of the modal and structural parameters of these monuments [9]. In this part, only the Clock Tower will be in-

spected. The damages on the tower were severe in 2004. A visual inspection mapping the damages and a modal identification test were made before the restoration works in 2006. Another dynamic modal identification test was carried out after the restoration works, revealing an increase in the natural frequencies of the mode shapes. For the structural assessment, a finite element model of the structure after the restoration was created and then updated using the data obtained from the dynamic modal analysis. In conclusion, using the explained methodology, viable seismic assessment for masonry structures can be made. Monitoring of natural frequencies was found out to be a reliable method for damage detection on its own.

2.2.2.2. Religious Structures. Churches and critical parts of the churches are very important cases when it comes to structural health monitoring of historical buildings. Many papers were written about structural health monitoring of churches and their parts. In this next paper, the structure of interest was monitored for 10 years. Between the years 2004 and 2014, the "Regina Montis Regalis" Basilica of Vicoforte was constantly monitored and the data acquired through this monitoring was analyzed [10]. The basilica houses the world's largest oval dome with internal axes of 37.23 by 24.89 meters.

The first step of this research was the automatization of the first monitoring system, which was installed in the early 1980s. To this extent, one hundred twelve instruments were installed on the Basilica. These instruments include crack meters, load cells, pressure cells, temperature sensors, wire gauges, hygrometer, piezometers and hydrometer. The sensors were divided into two groups, one group measuring strains, stresses and cracks and the other group measuring the environmental conditions. The data acquisition took place from November 2004 to November 2014. The first step of data analysis was to determine a correlation between the seasonal temperature changes and the structural behaviour. The crack magnitudes oscillate depending on the temperature, in a range of 0.01 mm to 0.2 mm. Apart from the cracks, the performance of the strengthening interventions were also analysed, depending on the temperature changes. The load cells installed on the tie bars showed an oscillation in the range of

± 5 kN. The second step was to analyse the data according to time. Over the entire testing period, the crack magnitudes increased whereas the loads on the tie bars decreased. In conclusion, apart from one or two exceptions, the analysis of the recorded data proved that there was no significant damage progression and there was no change in the efficiency of the strengthening system.

The main discussion topic of the next paper is the integration of structural health monitoring systems to the analysis and seismic assessment of structures [11]. The first step is always survey of the site. The Comillas Seminary is a modernist building constructed at the end of the 19th century. After the explanation of the geometry of the church and the damages, the integration of the health monitoring system is explained. The monitoring system consisted of sensors connected to remote terminal units. Those remote terminal units were connected to the master terminal unit and the user could remotely access and analyse the data obtained from another location due to the constant streaming of the data over the internet. With the help of this system, the evolution of inclinations and cracks were monitored over a time period of 1.5 years. At the end, the data obtained from the system were compared with in-situ measurements for validation. It was concluded that remote monitoring systems will be very useful for data acquisition and analysis in the future.

The case of Fossanova Church is more different than the previous case. In this paper, the seismic vulnerability assessment of the church is explained. First, the structure and the building materials and their mechanical properties were thoroughly investigated. Then, ambient vibration tests were conducted to determine the seismic behaviour of the church, accompanied by a finite element model using the results obtained from both the preliminary investigations and ambient vibration tests [12]. The finite element model was then updated to better simulate the dynamic behaviour of the church. The numerical analysis was accompanied by a limit analysis to better identify the vulnerable locations of the church, leading to a better estimation of the seismic vulnerability of the church. At last, a shaking table test was conducted on a model to check the dynamic response of the church and compare the results to the ones obtained from numerical analysis. The results obtained from the updated finite element model

showed good agreement with the results obtained from the shaking-table model results.

In the next research, the design and development of a monitoring system for the main spire of the Duomo di Milano is explained. The reason for this research is to ensure safety of the scaffolding on the spire during the restoration works [13]. The main purpose of the system was to detect any possible dangerous situations which may be caused due to the wind or other environmental conditions and alert the occupants. The spire is a very slender marble structure with a height of 30 meters and an octagonal cross-section. Due to this, a special scaffolding was modelled and installed for the restoration of the structure. This resulted in the need of a system which can identify the static and dynamic behaviours of both the spire and the scaffolding. The system consisted of different types of sensors, including high sensitivity accelerometers, biaxial tilt-meters, wire potentiometers and a weather station. Using these sensors and a suitable data acquisition system, the data obtained from the scaffolding and the spire were analysed to determine peak acceleration values, relative displacements between the scaffolding and the spire and tilts at the top of the spire. The system operated for four years during the restoration and even operates now after the restoration has been completed, serving as a semi-automatic monitoring system checking the structural integrity and reacting to any unconventional situation.

Seismic assessment is very crucial for the safety of the cultural heritage buildings. Santa Maria Assunta Cathedral in Reggio Emilia, Italy, was studied to determine the seismic performance of the structure. Apart from the seismic assessment of the structure, the methods and results of two different finite element modelling strategies, namely the limit analysis and numerical approach were also compared [14]. The analysis considered the cathedrals constructive history and the evolution of the structure, accumulated damage on the building after historic seismic events and the cracks and damages in present time. Firstly, the history of the cathedral was researched, because the cathedral underwent numerous changes during its lifetime. After that, the damages due to past seismic events were recorded. Then, in order to learn about the material properties of the masonry elements, destructive and non-destructive tests, including core extraction and flat-jack tests, were carried out. Sonic pulse velocity tests were

carried out to determine if the masonry elements could be modelled as rigid bodies and ambient vibration measurements were made for the extraction of modal properties using operational modal analysis. The modal results were compared with the results obtained from the finite element model to update the model parameters. After the calibration of the finite element model, limit analysis and finite element method analysis were conducted to determine the performance of the structure and its important parts under earthquake loads. In conclusion, both the limit analysis kinematic approach and the finite element model analysis provided satisfactory results.

In the last paper regarding religious structures three examples were discussed. It is a methodological discussion about the SHM process of the heritage buildings, which uses many methods from numerous disciplines. This discussion was made by applying this process to three different architectural heritage structures [15]. The structures under discussion are the Church of S. Caterina, the Fossano's Bell Tower and the Church of Madonnina della Neve. In this part only the churches will be inspected. Like every other vibration-based damage identification and seismic assessment study, the procedure started with historical research and building survey. Firstly, 3D finite element models of the churches were created by making assumptions for the material properties. From these models, preliminary modal analysis of the churches were made to determine the modal properties. After that, dynamic testings were made, determining the modal properties experimentally. These modal properties were used for model updating. For the Church of S. Caterina, 6 modes and their frequencies and damping ratios were found and updated. For the church of Madonnina Della Neve, 12 modes and their respective frequencies and damping ratios were found. It was concluded that updated finite element models can be used to predict the actual material properties of the historical structures and allow structural engineers to make difficult decisions regarding the conservation of the structure.

2.2.2.3. Bridges. Bridges, whether they are historical or modern, require constant monitoring because they are important components of a nation's infrastructure.

In the first paper regarding the SHM of bridges, two real cases are studied. The bridges in this paper are in two villages called S. Marcello Pistoiese and Cutigliano, in Northern Italy. These stone bridges were both built after the Second World War to cross the same river [16]. The bridges are built using sandstone blocks obtained from the rocks of the surroundings and the S. Marcello Pistoiese Bridge has brick-made vaults, whereas the Cutigliano Bridge has concrete-made vaults. The first step was to collect geometrical data and material properties. The geometrical data was collected by visual inspections, whereas material properties were determined according to laboratory and field testing results. Compressive and tensile strength and elastic modulus values were determined by laboratory tests. After determining these values, a Drucker-Prager model was selected to represent the materials in the non-linear finite element models. After creating the non-linear model, pushover analysis of the bridges were made for seismic performance analysis. At the end of the tests it was concluded that the seismic capacities of the bridges were higher than the seismic demands of the sites. The attractive part of this methodology is that non-linear behaviour of the materials and structures can be predicted using updated finite element models before any damage to the actual structure happens.

The next case regarding the structural assessment of masonry arch bridges comes from Spain. A methodology for the structural assessment of masonry arch bridges is explained by using it on the Vilanova Bridge in Galicia [17]. The bridge, built in the 13th-14th centuries has undergone many restorations during its lifetime. It is a classical medieval bridge with a length of 63 m. As in every SHM campaign, the bridge is inspected visually as the first step. After that, the geometry of the bridge is mapped using a terrestrial laser scanning survey. To characterize the inner structure of the bridge, a Ground Penetrating Radar survey was conducted. Material characterization was done by using sonic testing. Using the results obtained from the sonic testing, Poisson's ratio, density of the masonry and Young's modulus are determined. Lastly, an ambient vibration test was conducted to determine the mode shapes and natural frequencies accompanying those mode shapes. After the site testing, the finite element model of the bridge was created. The model was then updated according to the data obtained from the site. A structural assessment using a non-

linear approach was conducted using a pushover analysis. The performance of the bridge was also tested under static gravity loads and live loads. Lastly, after conducting a sensitivity analysis, it was concluded that the bridge has an acceptable safety level.

Next, two researches over masonry arch bridges in Turkey will be discussed. The first of them inspects a bridge in Sivas, Turkey. The bridge in question was constructed between 1926 and 1932 and spans over a river with a length of 59.3 m and with a width of 4.3 m [18]. After a detailed explanation of the bridge geometry and material properties of the bridge and its structural components, the process of system identification and modal updating was explained. First of all, ambient vibration data was collected from the bridge. The modal parameters of the bridge were extracted using Enhanced Frequency Domain Decomposition and Auto-Regressive Model methods. The obtained modal properties were used to update the numerical model of the bridge. The modelling strategy was to create a non-linear finite-element macro model but before creating the non-linear model, a working linear model was created. The non-linearity was incorporated to the model by changing the behaviour of the materials and by defining frictional contact surfaces between the parts of the bridge. After successfully creating the non-linear model, nonlinear static and dynamic analyses were conducted. For these analyses, numerous earthquake records were used. Comparing the static and dynamic model results, it is stated that they both show similar behaviours in stress and strain distributions. However, the static analysis gives smaller displacement values than the dynamic analysis, because it does not consider higher modes and therefore might not be suitable for a seismic response analysis. Lastly, incremental dynamic analysis was applied on the model by using numerous ground motion records. In conclusion, the results of this study shows the importance of determining modal parameters before creating a finite element model for further seismic performance analysis. Similarities and differences between static and dynamic models were also shown. Dynamic models were said to be more precise in determining the seismic behaviour of masonry arch bridges, however they require more computational effort. Incremental dynamic analysis was said to give even better results, but it requires even more computational effort compared to nonlinear dynamic analysis. Finally, the importance of the determination of performance criteria was pointed out, to make damage quantification and decision

making more precise.

The second article explains the process of system identification and seismic performance of masonry arch bridges in northeastern part of Turkey [19]. There are 12 bridges in this research and all of them located on a railway route. The need for this research arises from the fact that this railway line passes through the North Anatolian Fault. The main reason for the extraction of modal parameters of these 12 bridges is the validation of the finite element models of the bridges. The bridges were divided into four groups according to their geometries and a single bridge was chosen from each group for the ambient vibration tests. However, in the rest of the paper, the main focus was only one bridge. Accelerometers were placed on the piers and the spans of the bridge in both vertical and horizontal directions. After the measurements were done, the modal parameters were extracted using Enhanced Frequency Domain Decomposition. 6 mode shapes, of them 3 are transverse, 1 is longitudinal and 2 are vertical, their accompanying modal frequencies and modal damping ratios were determined. After determining the modal parameters of the bridge, the finite element model was updated in accordance to these modal parameters. The updating was done with the help of an error function. The seismic performance assessment of the bridge was done firstly with a pushover analysis. After the pushover analysis, non-linear time history analysis using numerous earthquakes was also conducted. In conclusion, both of the seismic assessment methods gave similar results. The results showed no global structural deficiency, however some cracks occurred in the middle arch barrel.

The last article about masonry arch bridges focuses on updating models by operational modal analysis. Three bridges are inspected in this research. Two bridges which can be considered architectural heritage, namely the St. Lazaro and the Lagoncinha bridges, and a more recently constructed bridge in Vila Fria, Portugal. The bridge models were updated by comparing the numerically and experimentally found modal parameters [20]. After briefly describing the bridges and their geometries, the numerical modelling of the structures are explained. CAST3M software was used for the finite element modelling of the bridges, using micro modelling strategies with zero thickness joint elements at critical parts of the bridges like the arches. Preliminary material

properties were chosen according to the available lab tests and typical values for masonry. The chosen material properties are the elastic modulus, Poisson's ratio and unit weight. Using these material properties, linear modal analysis of the bridges were made to determine natural frequencies and mode shapes of the bridges. After the numerical analyses were completed, ambient vibration tests were conducted on the bridges. Peak picking, Frequency Domain Decomposition, Extended Frequency Domain Decomposition and Stochastic Subspace Identification methods were used for the signal processing of the obtained data to determine the natural frequencies. After obtaining the frequencies from the experiments, they were compared with the numerical results. The models were then updated and calibrated by changing the initial material properties, achieving good agreement between the models and experimental results. Lastly, it is important to note that the performance of the experiments is of paramount importance in the process of updating finite element models. However, there are still difficulties to be tackled in the process of ambient vibration testing arising due to the type of structures.

2.2.3. Conclusion and Remarks

There are many different approaches while assessing the seismic performance of cultural heritage structures. The main steps used in all of the cases above were ambient vibration testing to obtain the modal parameters of the structures, finite element modelling and updating. Apart from some of the cases presented above, almost none of them used a small model of the structure made in a laboratory. Small scale models can give very good results regarding the seismic assessment of structures. Soil parameters were also rarely used while determining the seismic performance of a structure. The soil properties affect the intensity of earthquakes used in the seismic assessment of the structures.

Apart from the soil properties, there is also a very crucial element to consider while modelling the structures. In the case of Reggio Emilia Cathedral [14], different material properties were used for the different parts of the structure. This method was not used for many of the other cases. It is important to assign different material properties to different parts of the structure which are made of different materials.

However, it is also important to assign the material properties according to the location in the structure.

Another important thing that wasn't mentioned in the cases were that the cracks in the structures cause discontinuities. Cracks can be modelled as holes in the structure, similar to the windows and other holes and shafts in a structure. Restoration works must also be accounted for. Different construction materials were used through history, so this would also affect the material properties. Instead of using different material properties, the structural elements can be modelled in multiple parts. Increasing the complexity of the model also increases the time needed to run an analysis. It is important to try different approaches to a problem and find an optimal solution by comparing the individual results obtained from different methods. Most of the cases used a single approach to the task at hand.

It is important to always search for alternatives to get better or similar results. Masonry structures are by nature very complicated to model in finite element programs, so it is important to try different approaches and modelling techniques to the most optimal and correct solution to a problem. The lack of an established guideline for seismic assessment of cultural heritage buildings also makes it harder to determine a precise method. Every heritage building is unique in its own and therefore may require methods unique for themselves. That is another reason that makes this research area so interesting.

2.3. Finite Element Modelling of Masonry Structures

2.3.1. Introduction

The oldest, most used, and stable building method is stone masonry. The reliability of masonry structures mainly depends on the craftsmanship of the mason, gravity and friction. Stone structures have been used throughout history due to their high resistance against fire, water and other environmental effects. If designed and built correctly, they can easily withstand earthquakes. Another benefit of masonry struc-

tures is that they require less effort compared to other building materials in their era, like timber. Raw materials for construction are always available, the need for tools is minimal and the work is easily prepared, it is like building houses with LEGO bricks. Due to the simplicity of the method, masonry structures have been constructed for thousands of years.

Most of the masonry historical buildings are built with either cut dry-stone masonry without mortar, irregular stones with mortar, rubble with filling mortar in between or a combination of these three techniques [21]. The main function of masonry structures is to withstand vertical gravity loads. However, they are also required to withstand shear, torsional and tensile stresses under earthquake loads.

The modelling of masonry elements is a very tricky subject. As previously explained, masonry usually is made from bricks or stones as the building units and mortar as the gluing material, making it a composite material. Mortar and bricks are bonded together at an interface, therefore the properties of a masonry structure is heavily determined by the material properties of its constituents, brick and mortar. To model the behaviour of masonry numerically, the material properties and geometrical features of brick and mortar must be utilised.

There are different techniques used while creating masonry models. The main purpose of using different methods is to find a way to best mimic the behaviour of composite masonry. There are three main types of modelling for masonry: Micro-modelling, simplified micro-modelling (also called mezzo-modelling) and macro-modelling.

2.3.1.1. Micro-Modelling. The masonry elements, as previously mentioned, are made of 2 components, brick as the unit and mortar to bind the units together. However, there exists another component which should be considered while modelling masonry. That is the interface between the mortar and the unit. In micro modelling, all of these components are defined in the finite element model.

In micro-modelling, mortar-joints and unit-mortar interfaces can be modelled. These parts are mainly responsible for cracking and slip failures. Material properties like Young's Modulus and Poisson's Ratio of both the unit and mortar are taken into consideration while creating a micro-model of a masonry structure. The interface can also be taken as a potential failure zone for crack and slip modes. Micro-modelling is not very viable for two main reasons. First, the computation time increases exponentially as the structure grows in size or the number of units increases. Secondly, large structures are too difficult, even impossible to model using micro-modelling. Lastly, historical structures are hard to model due to the irregular geometries of the units.

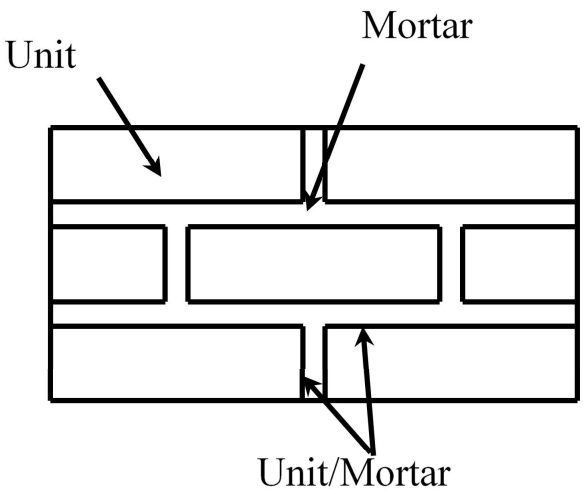

Figure 2.2. Micro-Modelling Method

2.3.1.2. Mezzo-Modelling. The difference between a mezzo-model and a micro-model is that in a mezzo-model, the interface between units and mortar is omitted. The interface elements have zero thickness and to incorporate them, the thickness of the units are increased. After this, the units and mortar between them become the only two elements in the model. The units are still called units, however the mortar is modelled as a contact element.

Mezzo-modelling has similar setbacks like micro-modelling. Too large structures or irregular unit geometries make it difficult, even impossible, to create a model.

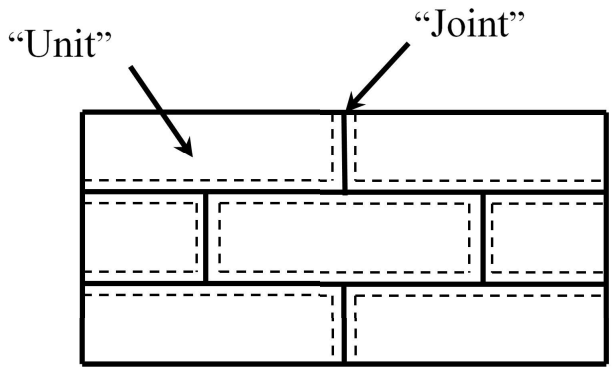

Figure 2.3. Mezzo-Modelling Method

2.3.1.3. Macro-Modelling. Macro-modelling is the simplest technique among these three modelling methods for masonry. Bricks, masonry and interface are all omitted. Instead, the structure is modelled like it is made from a composite material. There are mathematical formulae used to determine the material properties of the composite material depending on the material properties of the units and the mortar.

Due to this homogenisation of different material, some failure modes may disappear during the analysis. Therefore, macro modelling may not be a good option when modelling small wall specimens like arches or panel walls but similar results may still be obtained. The best part of macro-modelling is that it shortens the analysis duration by huge margins and makes the modelling easier. For huge structures like churches or towers, it is simply not possible to create a micro or mezzo-model.

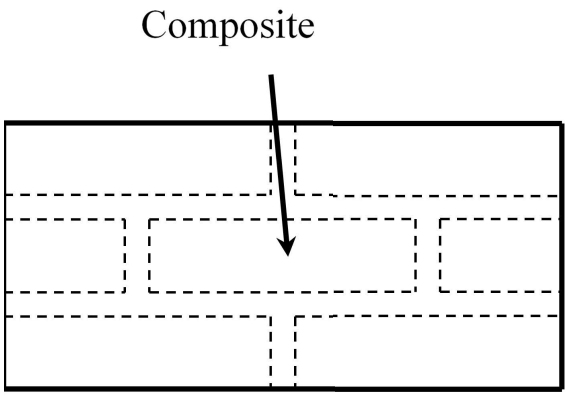

Figure 2.4. Macro-Modelling Method

2.3.2. Conclusion

The techniques used while modelling masonry structures is heavily dependent on the geometry and condition of the structure. Every modelling technique has its best place to be used. The aim of an engineer is to achieve the best possible results in the least amount of time.

3. METHODOLOGY

3.1. Introduction

It is not a simple task to assess the seismic performance of a masonry cultural heritage building. This requires through preparation, different experiments, models and numerous analyses. There are many approaches to consider while conducting seismic performance analysis on a cultural heritage building. In this chapter, the proposed data acquiring and modelling techniques will be discussed.

3.2. On-Site Test

Before trying to determine the seismic performance of a structure, actual data from the site is required. To achieve this, first of all the structure in question had to be inspected. After the inspection comes the models and analyses.

The inspection of the structure is a crucial part of the overall process, as it helps the engineer determine an approach for the upcoming work. First of all, the structure must be visually inspected, determining important parts, damaged zones and the overall geometry of the structure. Cultural heritage buildings usually have undergone numerous rehabilitation and modifications during their lifetimes. These also have to be taken into account. Having a thorough knowledge about the geometry of the structure makes the next step, which is the sensor placement relatively easier. As a simple example, a tower and a church can be compared. Churches usually have one or two storeys, therefore a measurement on the basement floor would suffice. However, measurements should be taken at every storey of a tower to determine the critical modes of the structure.

After the inspections, the data acquisition method or tool is determined. For cultural heritage buildings like churches, the easiest method is ambient vibration test. Sensors are placed at locations determined during the initial inspection and the ambient

vibration measurements are taken. The data obtained from the measurements is then analysed to determine the modal parameters of the structure.

3.3. Finite Element Analysis

The next part of the proposed methodology is the creation of the finite element model and its analysis. The reason for creating a finite element model is to be able to observe the behaviour of the structure under different loading conditions and determining the seismic performance of the structure. The finite element model is also used to determine the modal parameters of the structure, and even helps determine the material properties used in the construction of the structure.

Creating the finite element model requires a thorough inspection of the structure, making on-site tests a prerequisite for this step. The most important aspect of the model is that it should be similar to the real structure. To ensure that the model is as similar to the structure as possible, inspecting the structure is a necessity. If possible, the blueprints of the structures must also be obtained, however it is usually not possible with cultural heritage buildings. A building survey using 3D laser scanners was conducted to determine the dimensions and layout of the structural components.

The finite element model is created using the dimensions obtained from the building survey. There are also some simplifications made to the model, without changing any major features. There are three types of analysis planned to be conducted on the model. First, a static structural analysis is done under gravitational loads. This analysis will be the initial conditions for the following analysis types. After determining the initial displacements and stresses on the structure, a modal analysis is conducted. The modal analysis will mainly be used for the calibration of the model parameters by changing the material properties and support conditions. All of the details about modelling and calibration will be explained in Chapter 6. The mode shapes and their respective modal frequencies, or more commonly known as natural frequencies, will be compared with the results obtained from the ambient vibration test to check how well the model represents the actual structure.

For seismic assessment, the model will be subjected to a response spectrum analysis. The response spectrum analysis is important due to two reasons. First of all, by comparing the stress concentration locations with the actual damaged locations in the structure, we can confirm if the solutions obtained from the model are viable or not. Secondly and most importantly, possible damage zones in the structure in case of an earthquake can be predicted and that is also the main reason for conducting a response spectrum analysis.

4. SMALL SCALE TEST

4.1. Introduction

Small scale tests or laboratory tests are used to conduct experiments which are not possible or practical to conduct on the real structure. Real structures usually are cultural heritage buildings and they can't be harmed in any way. In laboratories, destructive tests can also be conducted in addition to the non-destructive tests. For destructive tests, flat-jack test and cyclic loading test were conducted. The non-destructive tests which was conducted was the ambient vibration and forced vibration test.

4.2. Laboratory Tests

Masonry walls are the main structural elements in most of the cultural heritage buildings. There are also masonry columns and pillars but most of such structures are composed of masonry walls. Understanding the behaviour and failure mechanisms of these walls is of critical importance, if the task is to determine the seismic performance and reliability of the structure.

Laboratory tests on small scaled walls are used to provide information about the behaviour of the material. The most important part in these laboratory tests is to use relevant materials while creating the small scaled structure. These materials can be hard to obtain since construction techniques changed drastically since these structures were constructed. Also, in-lab constructed structures would be made by professional masons, therefore there would be very little inconsistencies within the wall. In the case of the wall used in our laboratory tests, the stones were cut in perfect rectangular prisms. In real life structures, the units usually have different shapes and sizes. There are many factors which can change the laboratory result and the result obtained from the real structures. Some of these factors are the materials used during the construction, the techniques of construction, weathering effects during the long

years, the previous damages the structure suffered and many more. Although there are many variables to consider, good approximations can be made using laboratory tests.

To research of elasticity modulus of stone masonry, a research was conducted in Boğaziçi University [22]. In this thesis, the results obtained and methods used for this research were also used. A wall with the dimensions of 1.5 m x 1.5 m x 0.3 m was constructed using pre-cut limestone blocks with the dimensions of 0.3 m x 0.3 m x 0.15 m and 0.15 m x 0.3 m x 0.15 m. The wall was constructed on a concrete slab. The mortar used in the construction consists of mainly lime. There is almost no cement in the mortar mixture. After the construction was over, the wall was left to cure for a month.



Figure 4.1. The Wall Under Construction

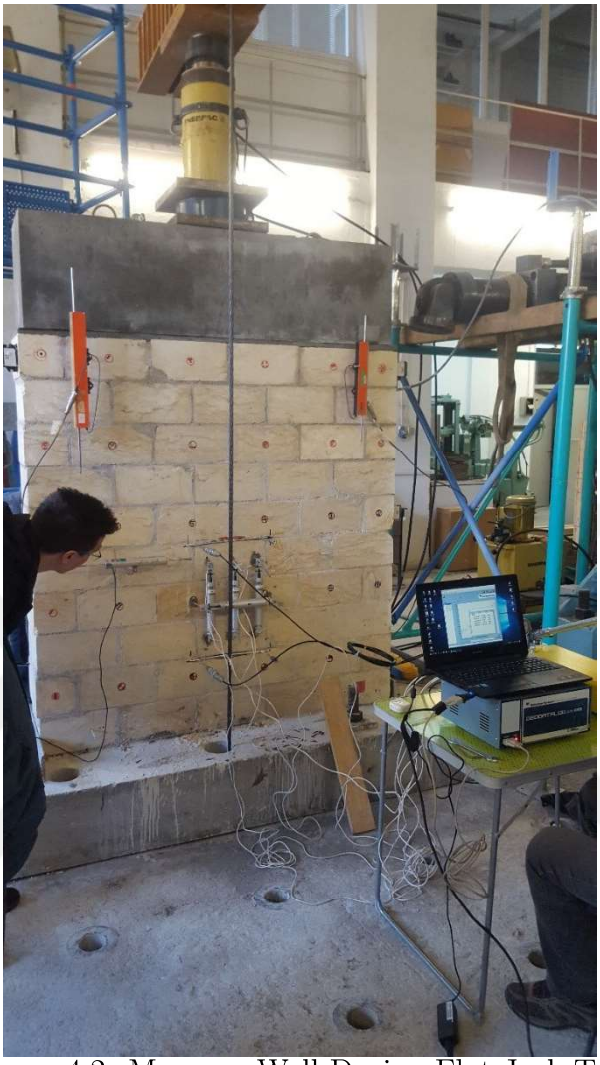

Figure 4.2. Masonry Wall During Flat Jack Test

In Figure 4.2, the preparations for the testing can be seen. There is a concrete slab underneath the wall and a concrete beam over the wall. On top of the concrete beam is the piston and another steel beam. They are used to create the compressive forces on the wall. Steel cables are connected to the steel beam and to the ground. When the piston tries to push the steel beam upwards, the cables hold the steel beam in-place, exerting compressive forces on the wall. Before the actual cyclic test, a flat jack test was done on the wall under the compressive forces to determine the material properties of the masonry. Separate tests on brick and mortar specimens were also conducted to determine their individual material properties.

Before the cyclic loading test, the wall was prepared for the ambient vibration test. Four accelerometers were placed on the sides of the wall. Two sets of short timed measurements were taken. The first measurement was taken in ambient environment. After that, the wall was hit by a hammer to generate responses in both the transverse and longitudinal directions. In Figure 4.3 the location of the accelerometers and the dimensions of the wall are shown. The dimension are greater than previously mentioned due to the thickness of the mortar.

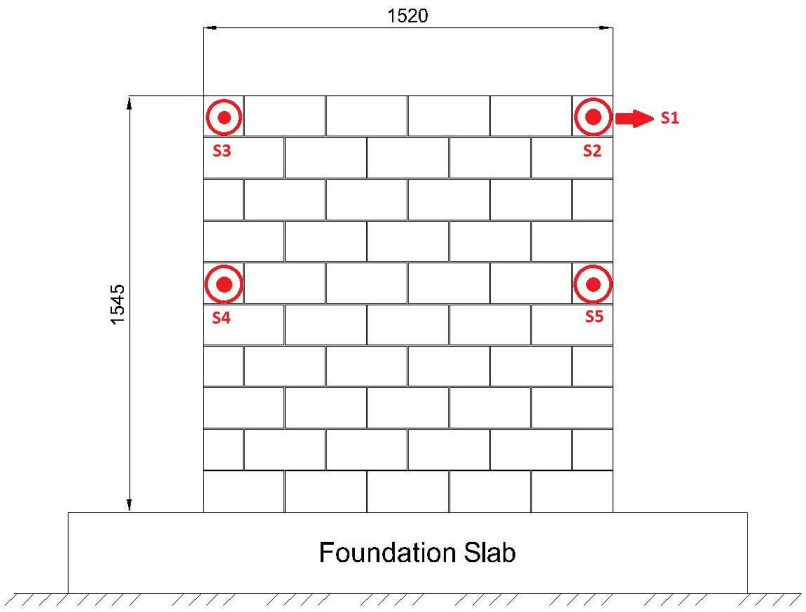

Figure 4.3. Accelerometer Layout

After the ambient vibration test, the preparations for the cyclic test started. The head of the hydraulic press is bolted to a steel plate. The plate was placed so that the hydraulic press would push at a location in between the top of the wall and the concrete beam. Before starting the test, strain gauges and LVDTs are placed at both face of the wall. There were also LVDTs measuring the displacement of the foundation slab, since the system can slide. The final testing system and its sketch with the instrumentation layout are shown in Figure 4.4 and Figure 4.5.



Figure 4.4. Final Testing System

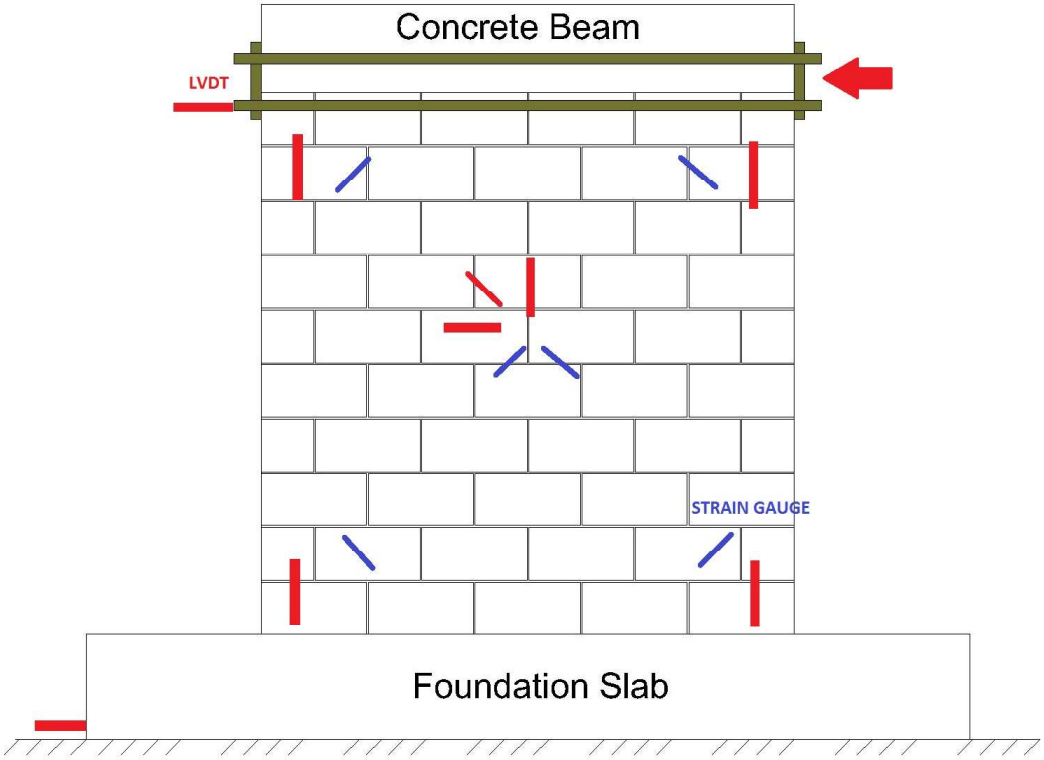

Figure 4.5. Final Testing System Sketch

Before the cyclic test started, the wall was loaded with 20 tons of vertical loading. the load pattern for the cyclic loading test was very simple. Starting from very small displacements (<1 mm), the displacement value was gradually increased. The wall was pushed to the target displacement value, then was returned to initial state, and then was pulled to the target displacement value. For each displacement value, this cycle was repeated for three times. After the cycles of the first two displacement values, which were both smaller than 1 mm, the cycle for a displacement value was conducted once, until vbisible damages started occurring on the wall. At every stage of the loading, the state of the wall was inspected. Any occurring damages were noted down with its corresponding displacement value. The test was over after the wall was heavily damaged. After that, to determine the natural frequencies of the damaged wall, measurements with accelerometers were taken.



Figure 4.6. Damaged Wall After The Test

In Figure 4.6, it can be clearly seen that the failure of mortar created a stair-shaped pattern on the face of the wall. This failure progressed as the wall was being pushed to its ultimate limit. The first stair-shaped failure occurred at the displacement value of 9.6 mm. The length of the failure was only four steps (by steps it is meant that the failure travelled four bricks in vertical direction). The test was concluded at the displacement value of 19.2 mm. Figure 4.6 shows the wall after the removal of the LVDTs and safety equipment.

4.3. Finite Element Model

4.3.1. Creating the Model

It is important to remind that the main purpose of this process is to establish an analysis method for the real structure. For a wall built of such regular and identical blocks, it is really simple to create a micro model, however, as previously noted that is not the purpose of this process. Therefore, the finite element model of the wall was created as a macro model. First of all, modal analysis was made on the wall to determine valid material properties. After the modal analysis, cyclic testing of the model was made.

4.3.2. Modal Analysis and Results

One of the best ways to determine if a finite element model is similar to the actual structure is to perform a modal analysis. By conducting a modal analysis, it is possible to check whether the finite element model and the real structure have similar natural frequencies. Structures having similar natural frequencies for the same failure modes behave similarly under deformations.

Before analysing the finite element model under deformations, it must be made sure that it will behave similarly to the real structure. Therefore a modal analysis was made with the following material properties.

- Density, ρ= 2300 kg/m^3
- Young's Modulus, E = 1500 MPa
- Poisson's Ration, $\nu = 0.18$

For the analysis settings, the support were chosen as fixed and only the first three modes are found. The results obtained from the signal processing compared with the modal results are shown in Table 4.1.

Table 4.1. Modal Results Comparison

Mode Number	**Experimental Freq. (Hz)**	**Numerical Freq. (Hz)**	**Error (%)**
1	17.82	17.09	4.08
2	38.38	38.74	0.93
3	57.47	57.50	0.06

The first and second modes are the first and second modes in the transverse direction. The third mode of the wall is in the longitudinal direction. Taking these results into consideration, the finite element model can be used for further analysis and it is expected to yield applicable results. The mode shapes are shown in Figure 4.7, Figure 4.8 and Figure 4.9.

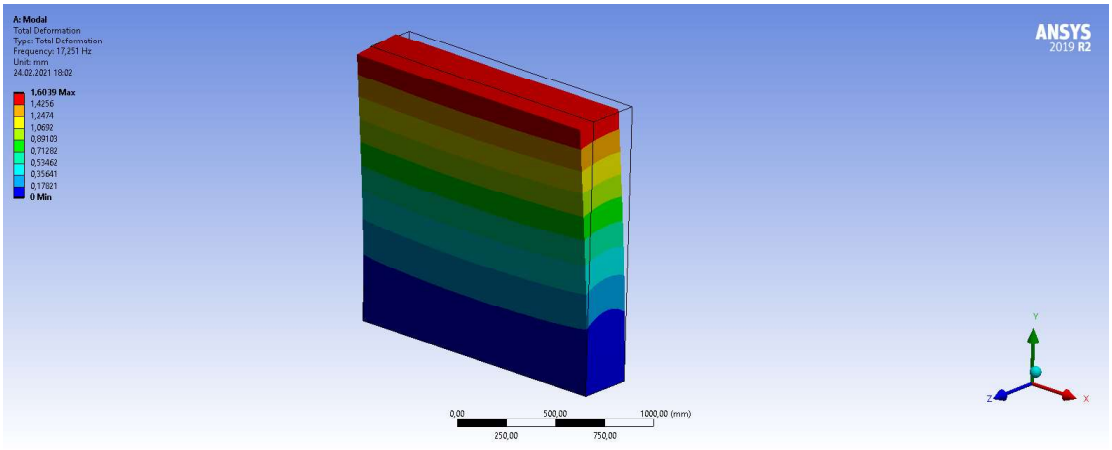

Figure 4.7. First Mode, 17.09 Hz

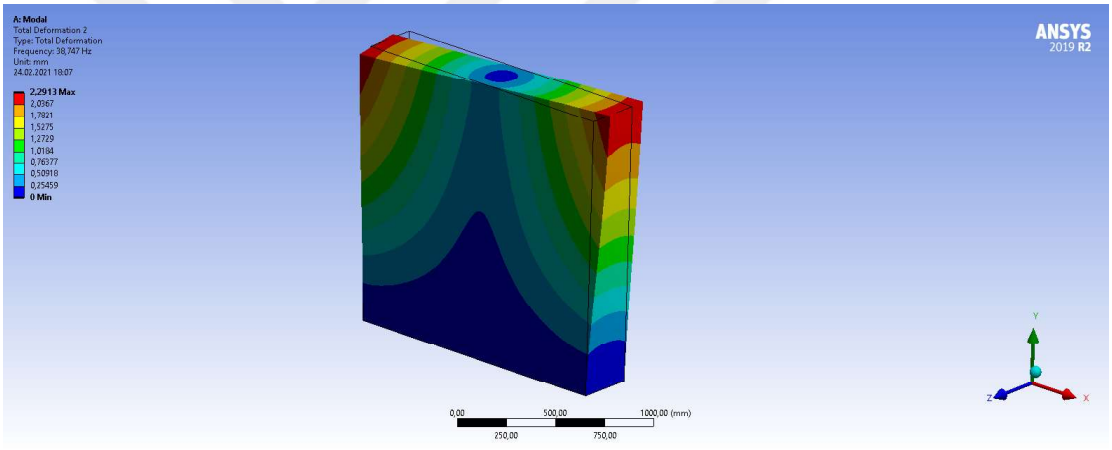

Figure 4.8. Second Mode, 38.74 Hz

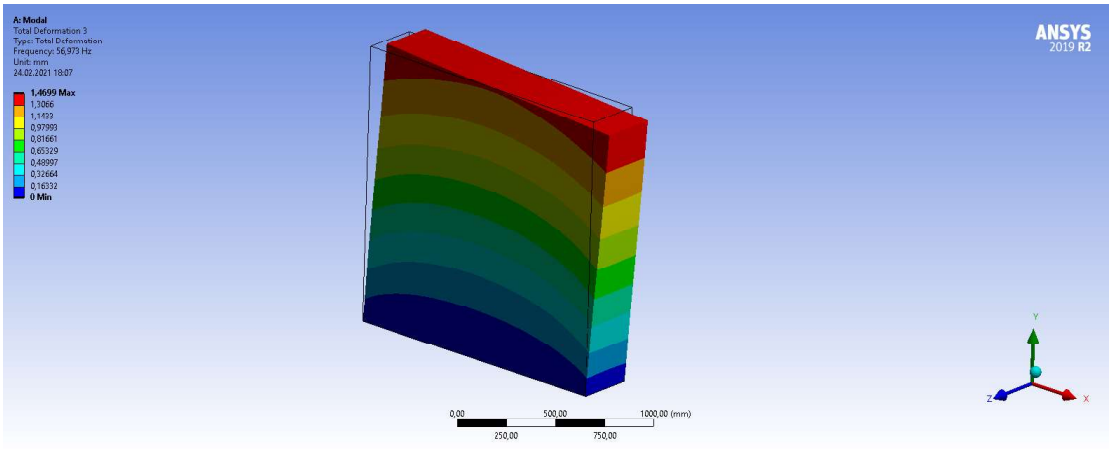

Figure 4.9. Third Mode, 57.50 HZ

4.3.3. Cyclic Loading Analysis and Results

First of all, the hysteresis curve obtained from the cyclic loading test must be inspected. In Figure 4.10, the hysteresis curve is shown. Here, it is evident that the Young's Modulus of the wall changes as the wall was being pushed to greater displacement values. The Young's Modulus gets smaller as more damage is accumulated on the wall.

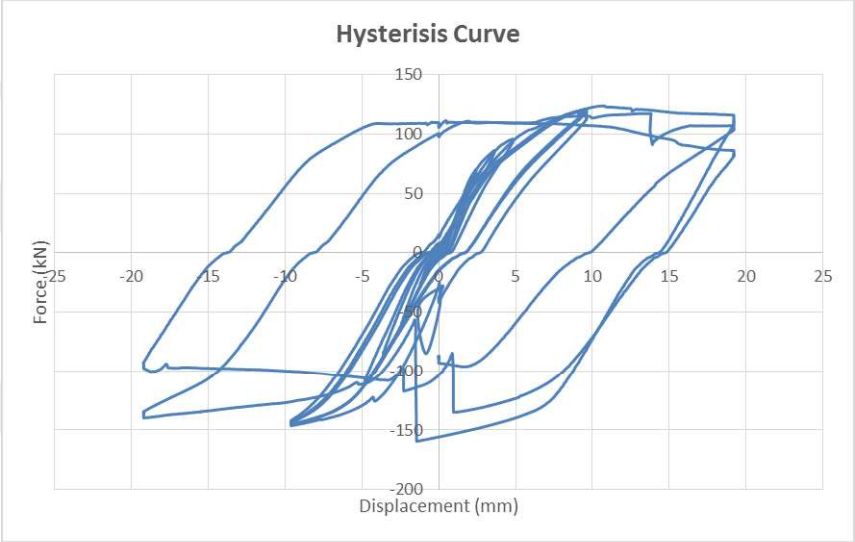

Figure 4.10. Hysteresis Curve obtained from Cyclic Test

For the macro model to give favourable results, the material used for the creation of the model has to have the characteristics of both the mortar and the brick. For this purpose, formula in EUROCODE 6 Section 3.6.1 Equation 3.2 was used to calculate the compressive strength of the masonry. This formula is given below:

$$\mathbf{f}_k = \mathbf{K} \cdot \mathbf{f}_b^{\alpha} \cdot \mathbf{f}_m^{\beta} \tag{4.1}$$

where:

f_k is the characteristic compressive strength of masonry,

f_b is the normalised mean compressive strength of a masonry unit,
f_m is the compressive strength of masonry mortar,
K is the constant according to EUROCODE 6 Section 3.6.1 Table 3.3.

For general purpose masonry, the constants of α and β are taken as 0.7 and 0.3, respectively. According to Table 3.3, for walls constructed with general purpose mortar and dimensioned natural stone, the value of the constant K is 0.45.

f_b and f_m are taken as 23.2 MPa and 2.74 MPa respectively. These values are considered as the approximate mean values for the used materials. Then the final value for f_k becomes:

$$\mathbf{f}_k = 0.45 \cdot 23.2^{0.7} \cdot 2.74^{0.3} = 5.502 \quad \mathbf{MPa} \tag{4.2}$$

The stress-strain graph of the created model is shown in Figure 4.11

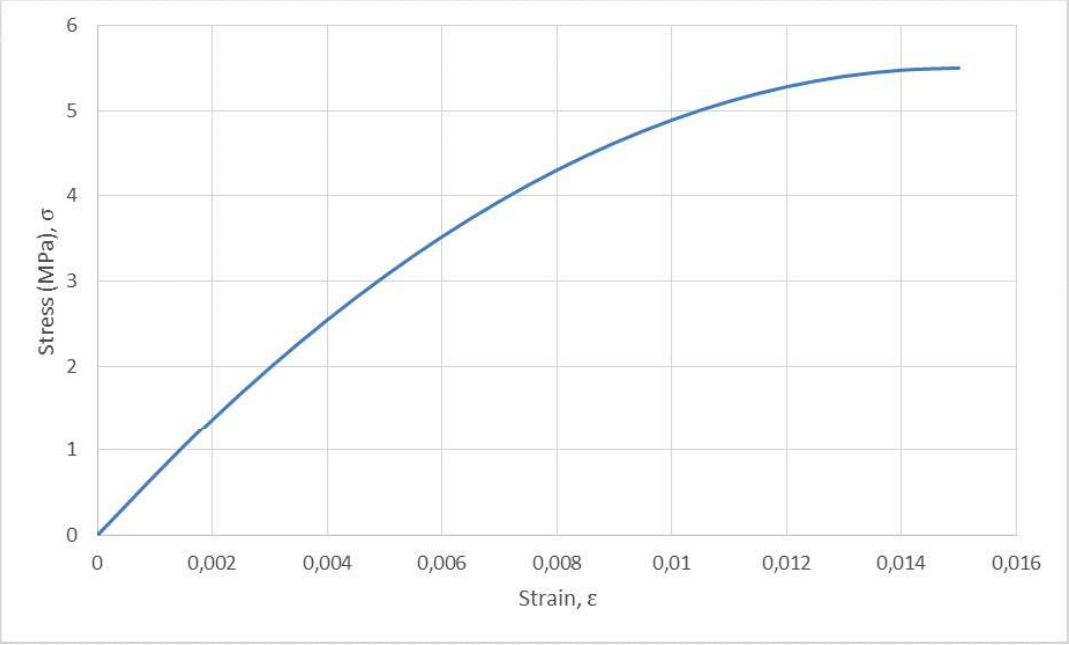

Figure 4.11. Stress-Strain Curve Of Masonry Model

The initial Young's Modulus was determined after the modal analysis results as 1500 MPa. However, the Young's Modulus value in Figure 4.11 is actually 700 Mpa. The reason for that will be explained later. The wall was modelled with a compression-only support and two different loading methods; surface displacement and nodal displacement. The most relevant result was chosen from these 2 options to create the force-displacement curve. The dimensions of the model was the same as the actual wall, 1.5mx1.5mx0.30m. The meshed model is shown below in Figure 4.12

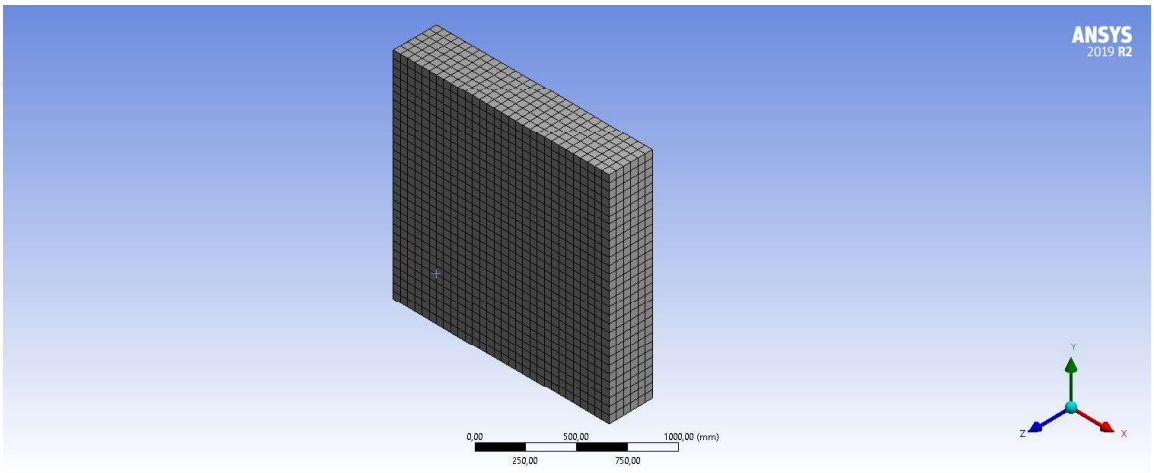

Figure 4.12. Meshed FEM Of The Wall

The mesh size is 50mm. The reason for taking the mesh size so small is that the geometry of the wall is very regular. The overall size of the wall was also small so the computational time does not increase too much when the mesh size gets smaller.

The dimensions and meshing were the simplest part of the modelling. Determining the support and loading types were more challenging. In the case of real life structures, the foundations do not work as fixed supports. Foundation systems of real life structures work more like compression only supports, instead of fixed supports. Therefore, the support at the base of the wall is taken as compression-only support. During the test, the wall was restrained to move in the longitudinal and transverse directions at the support. Considering this fact, displacement restraints were also added to the base of the model.

The next step in creating the model is to define the loading conditions. First of all, the gravitational load is added. In the lab test, a concrete beam was placed on top of the wall and the wall was put under constant compression with the help of a piston. To model the compressive forces, a constant pressure of 0.5 MPa acting on top of the wall was added. The displacement was acted on the side of the concrete beam. Since the machine was not directly pushing the wall, different types of displacement methods were used to simulate the process. The types of displacement depend on the surface they are acted and called Surface Displacement and Nodal Displacement. In the case of Surface Displacement, the displacement acts on the top surface of the wall, shown in Figure 4.13

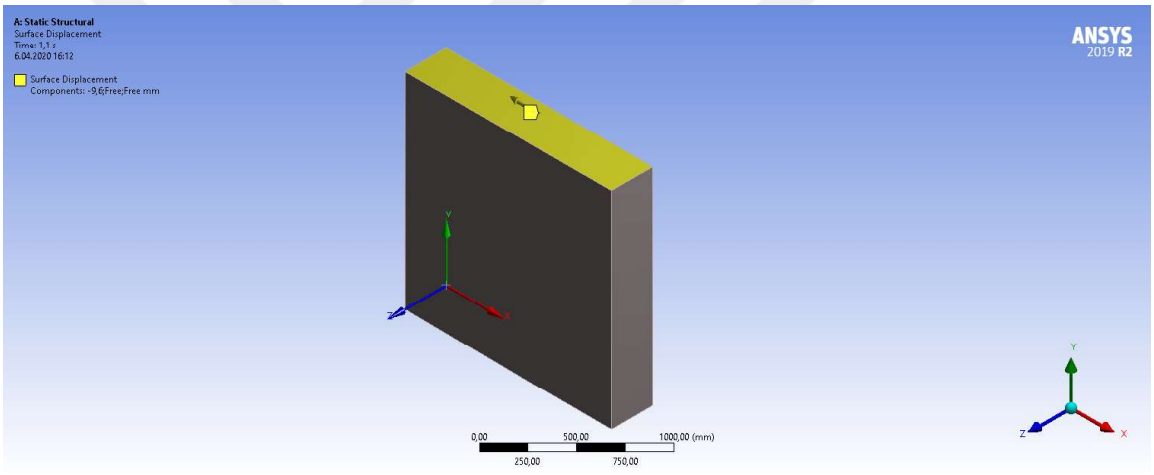

Figure 4.13. Surface Displacement Case

For Nodal Displacement, nodes on the side of the wall were chosen to act the displacement. The choice of nodes depend on the lab test. In the lab test, the displacement acts on a plate placed on the intersection of the concrete beam and the wall. The nodes are shown in Figure 4.14

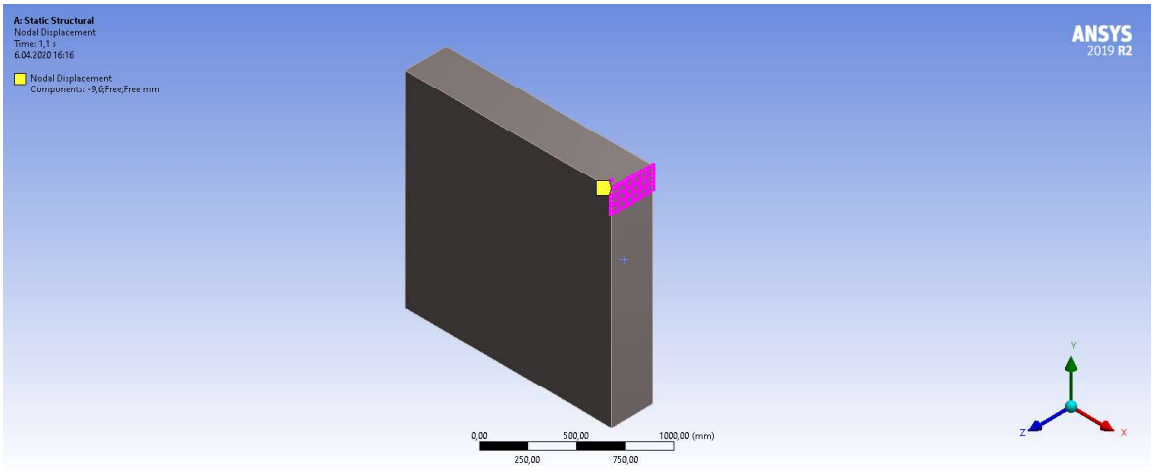

Figure 4.14. Nodal Displacement Case

After determining the displacement methods, the loading type was defined. In the lab test, the displacement value was steadily increased. From the lab test, it is known that the initial failure of the wall occurred at the displacement value of 9.6 mm. Since the wall was loaded at a constant speed during the lab test, the same method was used in the finite element model. To make the load steps more identical, the displacement was acted on the wall in 0.1 second intervals, increasing 1 mm after each interval in a total of 1.1 second duration. At the last interval, the displacement increases 0.6 mm. The model was complete and ready for static structural analysis after defining the loads and support conditions.

To create pushover curves, force reaction in the longitudinal direction at the bottom support of the wall was taken. The displacement values were already known for the creation of the model. In the next part, the results are discussed.

4.4. Results Comparison and Interpretation

The finite element model was made to mimic the behaviour of the wall used in the lab test. The main failure criteria was shear failure, because during the test, the wall failed at the mortar. There were initial crushing in the stones at the corners, but the main failure occurred due to mortar failure, creating a stair shape, as seen in Figure

4.15 The initial failure locations and the cracking pattern can be easily observed.



Figure 4.15. Stair Cracking Pattern

In the figures below, the shear failure criteria for the finite element models depending on the loading types can be seen. The lowest factor of safety is distributed diagonally on the face of the wall. Comparing the final state of the wall with the results obtained from the finite element model, we can clearly see that the failure locations overlap with the highest stress concentration locations. The crack locations on the lab test are shown with the black lines on the finite element models.

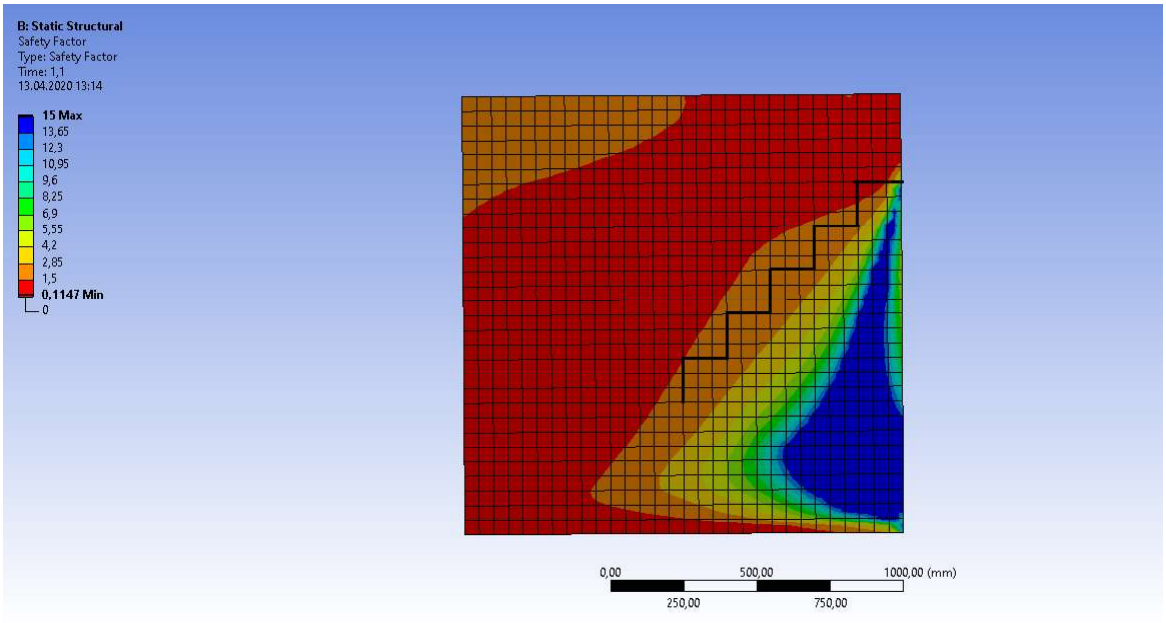

Figure 4.16. Nodal Displacement Result

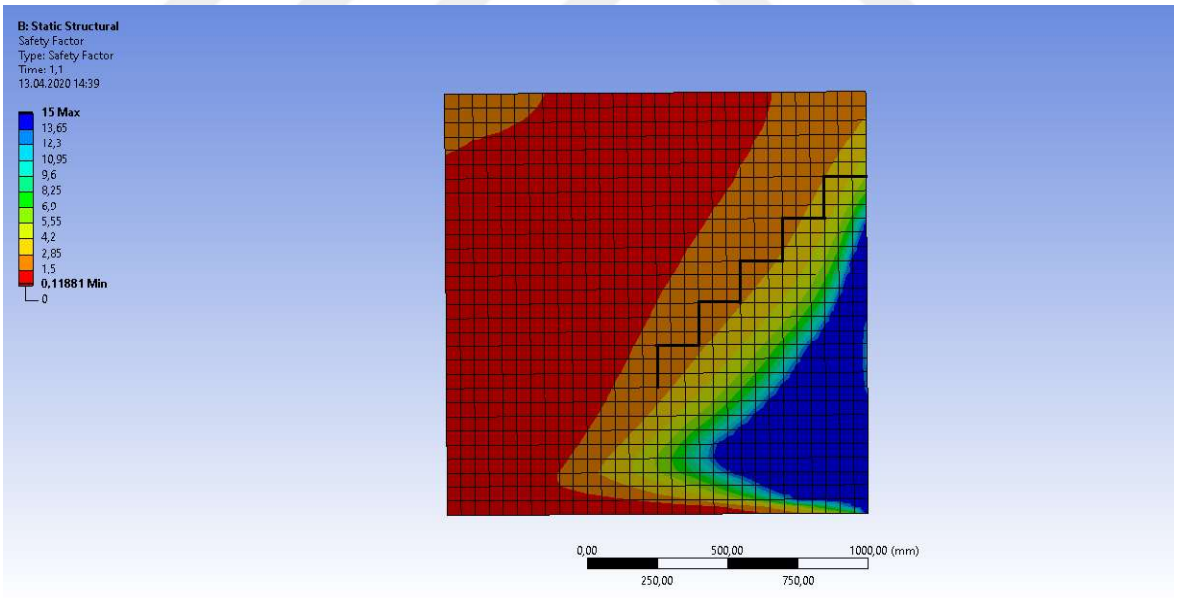

Figure 4.17. Surface Displacement Result

In the finite element models, a maximum shear strength of 0.5 MPa was used while determining the safety factors. Starting with the case of the nodal displacement, as seen in Figure 4.16, it is easily observed that the lowest values of factor of safety, ranging from 1.5 to 0.1, are in the middle of the wall, splitting the face of the wall

diagonally. The starting location of the failure in the lab test is on a red location. The stair shape of the failure fits really well on the red zones of the results obtained from the finite element model. For the second case, which uses the surface displacement as the deformation property, the failure place does not exactly match with the areas with the lowest factor of safety. However, this model also shows a diagonal failure plane.

The results show similarities and are a valid approximation for the real life situation. The differences between the finite element model results and lab results may arise from the following parameters. First of all, the used model is a macro model. Since the model considers the wall to be a homogeneous single block of stone, differences in the results are bound to happen. Secondly, the properties of mortar and the construction irregularities also play a significant role in the results. Lastly, there is a concrete beam on the top of the wall, which holds the last row of bricks together. There are also plates connected with steel rods squeezing the concrete beam and the last row of bricks, so that when they are pushed, they do not slide apart. All of the finite element model results show that the failure starts from the top of the wall and propagates diagonally along the face of the wall. Since the wall in the lab is constricted to fail on the top, the failure started from the side. The most important thing to note here is that the way the failure forms, which is diagonal on the face of the wall. This can be clearly observed in all of the finite element models.

The shear results are not the only parameters which were compared. While loading the wall to the predetermined displacement values during the lab test, the reaction forces were also recorded aside the displacement values. Using these reaction forces and the displacement values, pushover curves were created for the lab test and the individual finite element model cases. In Figure 4.18, the comparison of the actual test data and the data obtained from the finite element model cases are shown.

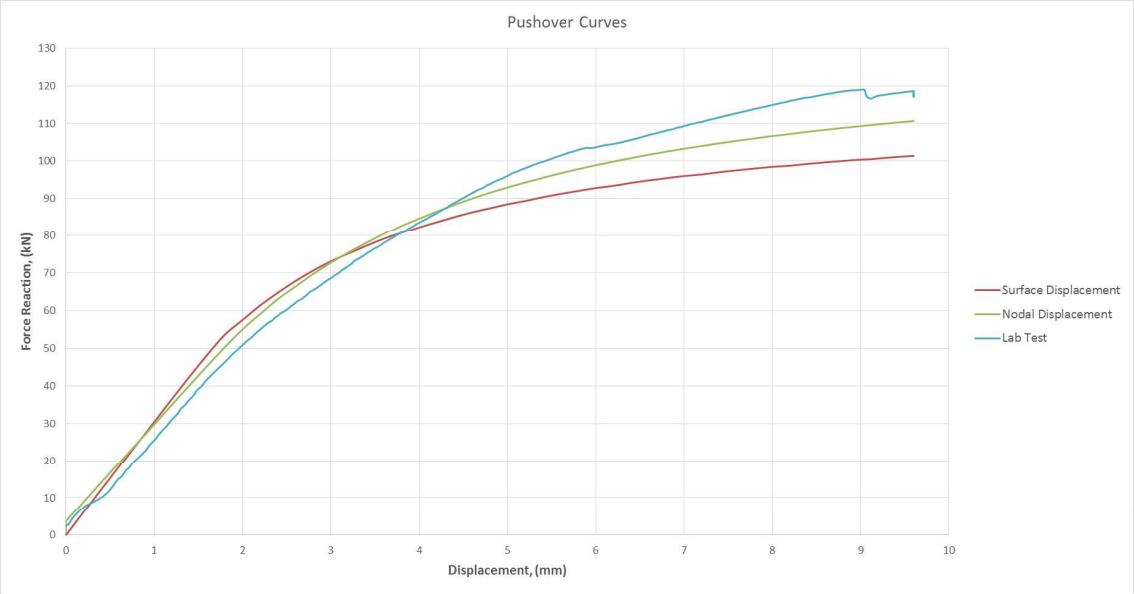

Figure 4.18. Experimental and Numerical Pushover Curves

Looking at Figure 4.18, it is clearly seen that the nodal displacement case gives the closest results to the actual test data. It is important to note here that the used Young's Modulus value of the material is 700 MPa, but the Young's Modulus value obtained from the modal analysis was 1500 MPa. Both of these Young's Modulus values correspond to the elastic part of the curve. However, during the modal analysis, the Young's Modulus value is very close to the origin point of the pushover curve, due to the fact that the vibration values are too small.

The change of the Young's Modulus can be seen in Figure 4.19. As the displacement values increase, the wall gets damaged and the Young's Modulus value grows smaller. The curves for smaller displacements values such as 1.2 mm and 0.6 mm follow the same path of the displacement value of 2.4 mm, therefore they are not shown. The finite element model was pushed to smaller displacement values to obtain the curves with the dashed lines. The solid lines are the results from the cyclic test. The results from the finite element model were shifted in the x-Axis to be able to better compare the slopes of the dashed and solid lines.

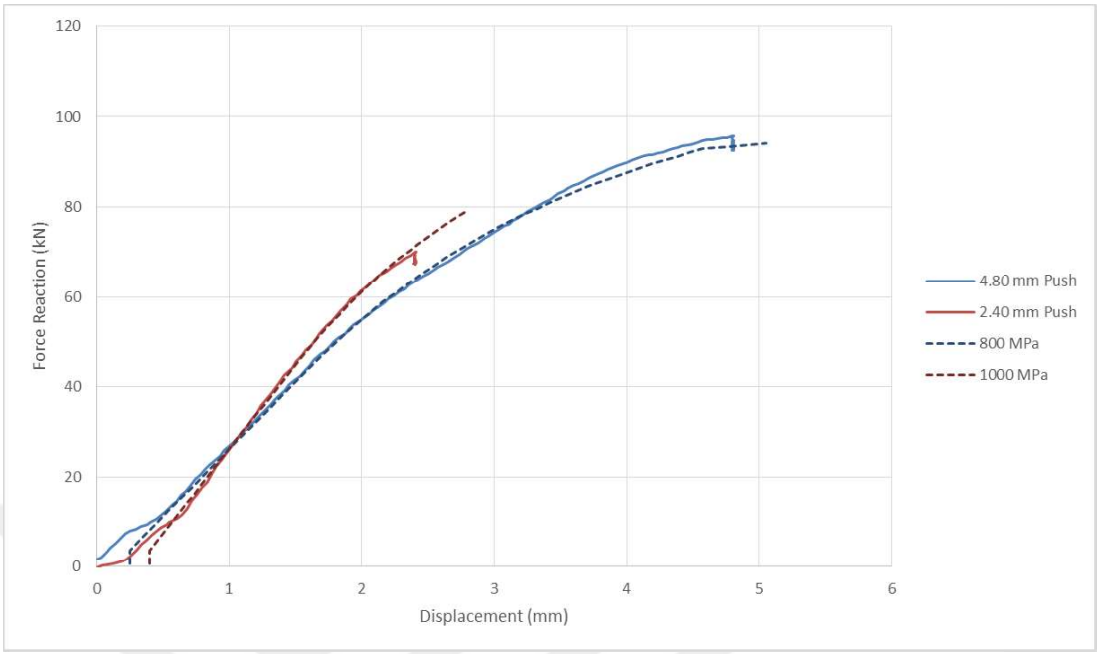

Figure 4.19. Young's Modulus Change

It is evident that for the displacement value of 2.40 mm, a Young's Modulus value of 1000 MPa would be the best fit, whereas when the displacement value is increased to 4.8 mm, a Young's Modulus value of 800 MPa fits better to the curve obtained from the lab tests. For the last displacement value, 9.6 mm, the Young's Modulus value was found to be 700 MPa. These results clearly showed that as masonry elements accumulate damage, their Young's Modulus values decrease.

To sum up, if both the shear failure criteria and the force-displacement curves are considered, the best assumption is made with the finite element model utilizing nodal displacement method. Although the pushover curve is a little lower than curve obtained from the lab results, the failure pattern matches very well. The difference between the pushover curves is also not much. The finite element model starts with greater force values but stays under the lab results as the displacements increase. The error in the forces is around 8% at the failure point. Overall, the behaviour and the reaction force values match well and it can be said that the model represents the actual structure fairly well.

4.5. Conclusion

Finite element models can be created using many different techniques. Considering this circumstance, there are many different approaches for a single problem. In this case, a simple pushover test for a masonry wall can be modelled using three different techniques, namely macro modelling, mezzo modelling and micro modelling. All methods have their benefits, along with their shortcomings.

The main purpose of comparing the different methods with the lab test was to probe that if it is possible to obtain meaningful results from finite element models, if the structure in question was a masonry structure. Depending on the materials, construction techniques and other parameters, there is a trial and error period while creating the model. Stone and mortar impurities also have effects on the results. Therefore, material properties had to be changed to obtain favourable results. Different methods in loading and impact points were compared in order to obtain the best results, without changing the material properties too much. For a small structure like this wall, the results may not be perfect, but it still gives a good approximation.

Considering the obtained results, it can be said that macro modelling techniques can be used while analysing masonry structures. For historical structures, the determination of material properties will be more difficult, but the results obtained from the small scale test agree well with the results obtained from the finite element models, so it is possible to implement this method to massive masonry structures.

5. ON-SITE TEST

5.1. Hagia Irene

The church of Hagia Irene is a monument from the Byzantine Empire and serves as a perfect example of Constantinapolitan imperial and religious architecture. The name of Hagia Irene or Hagia Eirene means "Holy Peace" in Byzantine Greek. It is one of the three churches dedicated to the peace of God, the other two being Hagia Sophia and Hagia Dynamis. The Greek Eastern Orthodox church is located in the courtyard of Topkapı Palace, Istanbul.

5.1.1. History

The church of Haiga Irene was built in the 4th century, during the reign of Emperor Constantine I. There existed a smaller church on the site, but the emperor decided to enlarge and dedicate it to Hagia Irene. The church was completed at around the end of the emperor's reign in year 337. It served as the main cathedral of the Patriarchate before the opening of Hagia Sophia in 360. The church burned down in 532, like the majority of Constantinople, during the Nika revolt. After the end of the revolts, Emperor Justinian I ordered the church to be rebuilt in 548. However, the church was transformed into a domed basilica during the rebuilding. The church was also damaged by an earthquake in 740 and was reconstructed shortly after. The interior of the basilica was decorated with frescoes and mosaics, some of which have survived to this day.

The church was never turned into a mosque after the capture of the city by the Ottoman Empire in 1453. It served as an armoury during the entire Ottoman rule. It is now inside the courtyard of Topkapi Palace and mainly serves as a concert hall and museum.

5.1.2. Architecture

Rebuilt in 548, 15 years after its destruction during the Nika riots, Hagia Irene is a phenomenal example of the early era Byzantine domed basilicas. Although it could never rival the magnificence of Hagia Sophia, it remains the second largest Constantinopolitan church which has survived until today. The base plan of the church measure around 58 m x 30 m, without the atrium. The church is defined as a paradigmatic domed basilica with two aisles and a nave. The aisles and the nave open into the central space. The large dome which is still present in its original state nowadays, has a diameter of approximately 15 m. With a height of 35 m, the dome rests on four brick arches on four sides supported by four massive pillars. It has twenty windows, but most of them are closed. The smaller dome also rests on four arches supported by four pillars. It is almost 27 m high and has an elliptical plan with diameters of 11 and 14 m.



Figure 5.1. Hagia Irene from Outside

The apse of the church, which is now used as the stage for the concerts is 16

m wide. The amphitheatre structure is covered with a semi-dome. There are three giant windows on the wall which support the semi-dome. On the both sides of the amphitheatre, small passages exist to allow access to the aisles.

The aisles on the both sides of the central space are two storeyed and have rectangular plans. The dimensions are approximately 40 m in length and 5.50 m in width. The aisles are divided into subparts by arches. In the second floor, or the gallery floor, the aisles are divide into three subparts by the arches sitting on the pillars on both sides. The aisles are covered with two thick arches supporting the domes. The walls separating the aisles from the outside have numerous windows, especially the ones on the gallery floor.



Figure 5.2. Hagia Irene Inside

The narthex is between the space under the small dome and the atrium. Arches

supported by pillars divide the structure into five subparts. Three of these parts are in the centre of the narthex, with dimensions of approximately 7.5 m in length and 5 m in width. The remaining parts are covered with mirror vaults and have a square plan. Their dimensions are approximately 7 m x 7 m.

The last part to mention is the atrium. It is an open courtyard enclosed by halls. Like the church, the atrium also has a rectangular plan, around 50 m in length and 40 m in width. Nowadays, entry is permitted to the atrium.

5.2. Ambient Vibration Test

5.2.1. Introduction

Numerous methods are used to identify the modal parameters of a structure. There are both destructive methods and non-destructive methods. Being one of the non-destructive methods, ambient vibration test is pretty easy to conduct. The results can be obtained pretty fast too. One crucial reason for using ambient vibration test instead of any destructive methods is that the structure we are working with is a cultural heritage building. Therefore, it is important to note to damage the structure. Ambient vibration tests are made to estimate the dynamic features of the structure.

5.2.2. Procedure

The procedure can be explained in two main steps:

- Setting up the equipment,
- Recording data.

The most important part is setting up the equipment. The equipment used for the ambient vibration test is accelerometers, cables, data collection stations and GPS antennas. The first thing to do was to set up the recording stations, shown in Figure 5.3, on the second floor of the narthex. The measurements were to be taken during working

hours, so the equipment had to be placed somewhere it wouldn't be disturbed. There were two recording stations for the two aisles on the both sides of the gallery. First, the stations were connected to the GPS antennas and the clock inside the recording stations were updated and calibrated. Both of the stations must have the same time on their internal clocks, so that it would be easier to correlate the results obtained from the both stations afterwards.



Figure 5.3. Recording Station

Secondly, the accelerometers were placed. There were 10 accelerometers attached to each of the stations, in total 20 accelerometers. The accelerometers were placed in different locations on the walls or on the ground along the aisles. They were fixed in their locations using molten silicon. The fixed accelerometers are shown in Figure 5.4 and 5.5.

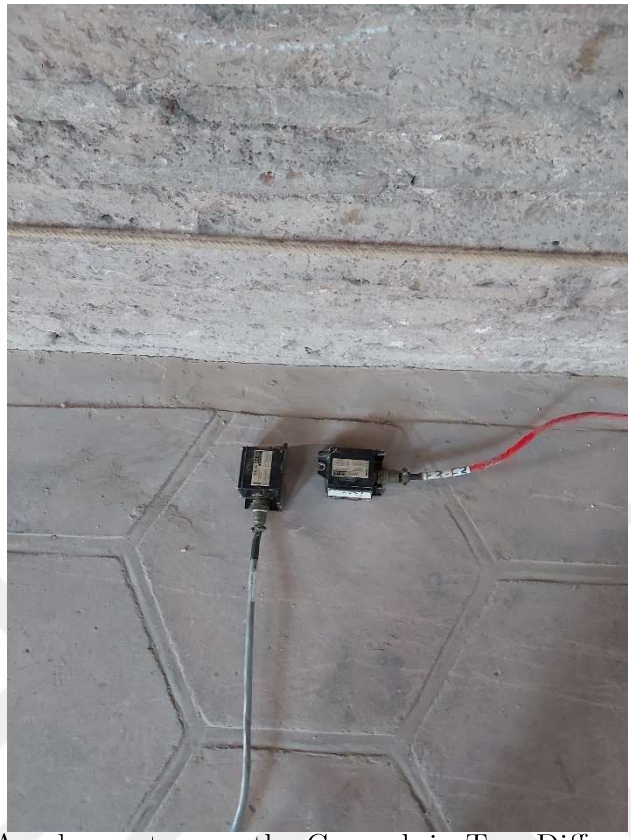

Figure 5.4. Accelerometers on the Ground, in Two Different Directions



Figure 5.5. Accelerometer on the Wall

The accelerometers were placed so that one part of them would take measurements in longitudinal direction, whereas the remaining one would take the measurements in transverse direction. For the first set of measurement, the locations of the accelerometers with their directions, shown as red dots and arrows, and the location of the recording stationas, shown as blue rectangle, are pointed out in Figure 5.6. The accelerometers which were directed in the transverse direction were all facing the centre of the church, so to say the main gallery. The locations of the accelerometers on the aisles can be seen in the figures below. The accelerometers in the longitudinal direction were all facing the narthex. Lastly, the data flow was monitored to see if there were any irregularities in the data coming from the accelerometers.

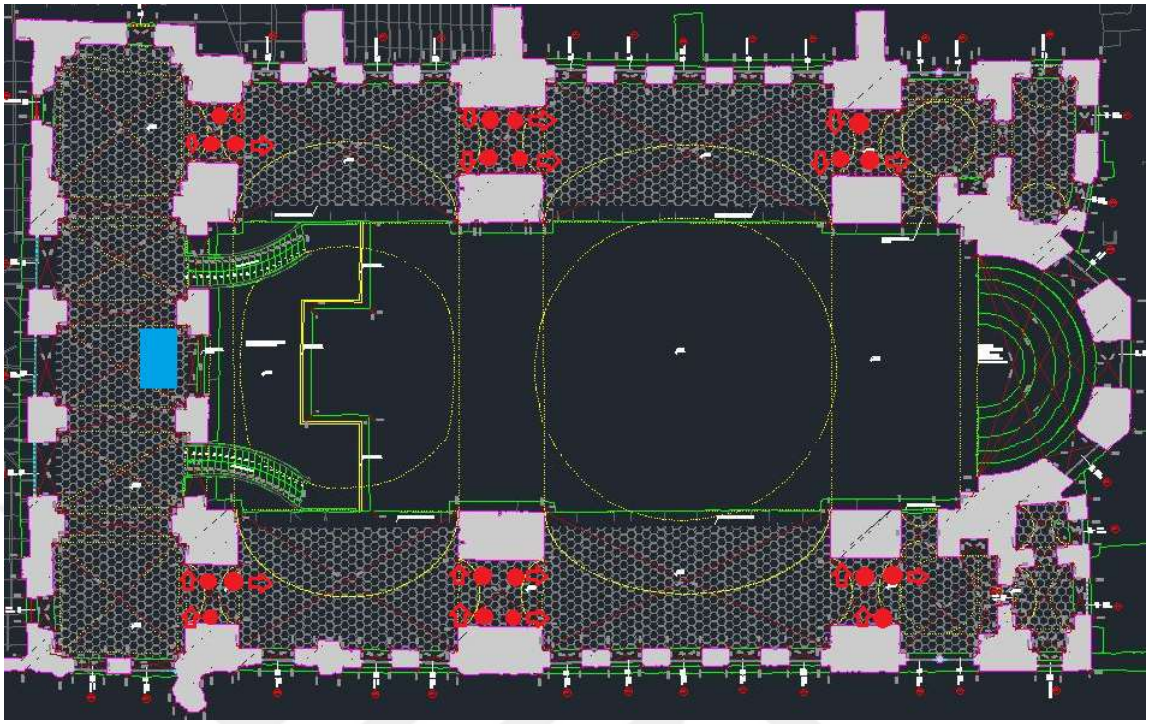

Figure 5.6. Layout of the Accelerometers

The next step is recording the data. The first sets of records were taken for one hour. Actually, the duration for a recording step was planned to be 3 hours, but due to the limited time on the site, the duration for the recordings were shortened. For Set 1, the accelerometers were placed all on the aisle floor. Half of the accelerometers were facing the longitudinal direction, directed at the narthex whereas the rest of them were facing the transverse direction. The accelerometers that are facing the transverse direction were all pointing towards the main hall of the structure, so to say the centre of the structure. For Set 2, 8 accelerometers were placed on the walls. The directions were the same for the accelerometers. The measurements for Set 3 were not taken in the second floor aisles. The apse of the church has a unique geometry, therefore one set of measurements was made for the apse only. 8 accelerometers were placed around the circumference of the apse, on the walls. Half of them were directed towards the centre of the apse or perpendicular to the curve, since it is considered to be a half circle, and the other half of the accelerometers were placed so that they were parallel to the cure of the apse. The recordings for the apse were taken for one hour, since the machinery were on the same floor as the common touristic area. Footsteps and other

environmental noises can affect the results and this is not wanted.

5.2.3. Signal Analysis and Results

The results of the ambient vibration test can be obtained through simple signal processing. For the signal processing, a code in MATLAB was developed. The code firstly reads the usable data from the source. After that, the data is converted to g values for further use. The next step in the analysis was to detrend and apply a high-pass filter to the signal. Detrending sets the mean of the signal to zero and a high-pass filter blocks the signals with a lower frequency than the cutoff frequency. With the raw data, the analysis results yield a very high peak at the 0 Hz frequency, making it impossible to detect any other peaks, however after the application of the high-pass filter, the peaks created by the modal frequencies could be observed.

After the signal was made ready for the analysis, Fast Fourier Transform (FFT) was performed on the signals to obtain the peaks. However, the results obtained after the analysis looked too complex. To counter this, a Savitzky-Golay filter was used to make the results more smooth. A Savitzky-Golay filter makes use of a convolution process by by fitting successive sub-sets of adjacent data points with a low-degree polynomial. This results in a smoother curve and increases precision without distorting the signal tendency.

Set 1 was chosen for the signal analysis and modal identification. The peaks show the fundamental frequencies of Hagia Irene in longitudinal and transverse directions. In Figure 5.7 and Figure 5.8 , the Fourier amplitude functions of the two directions can be seen. The effects of the Savitzky-Golay filter can also be clearly inspected in these figures. The peaks defining the modal frequencies were searched in the interval of 0 Hz to 5 Hz, resulting in the discovery of 8 modal frequencies in total.

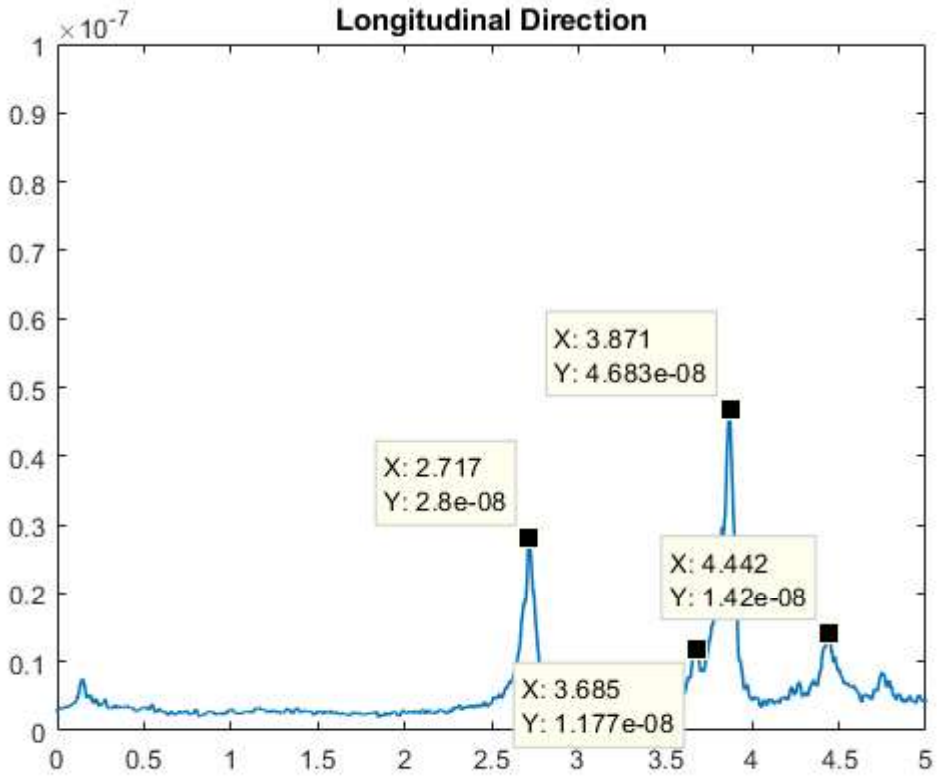

Figure 5.7. Peaks with Filter in Longitudinal Direction

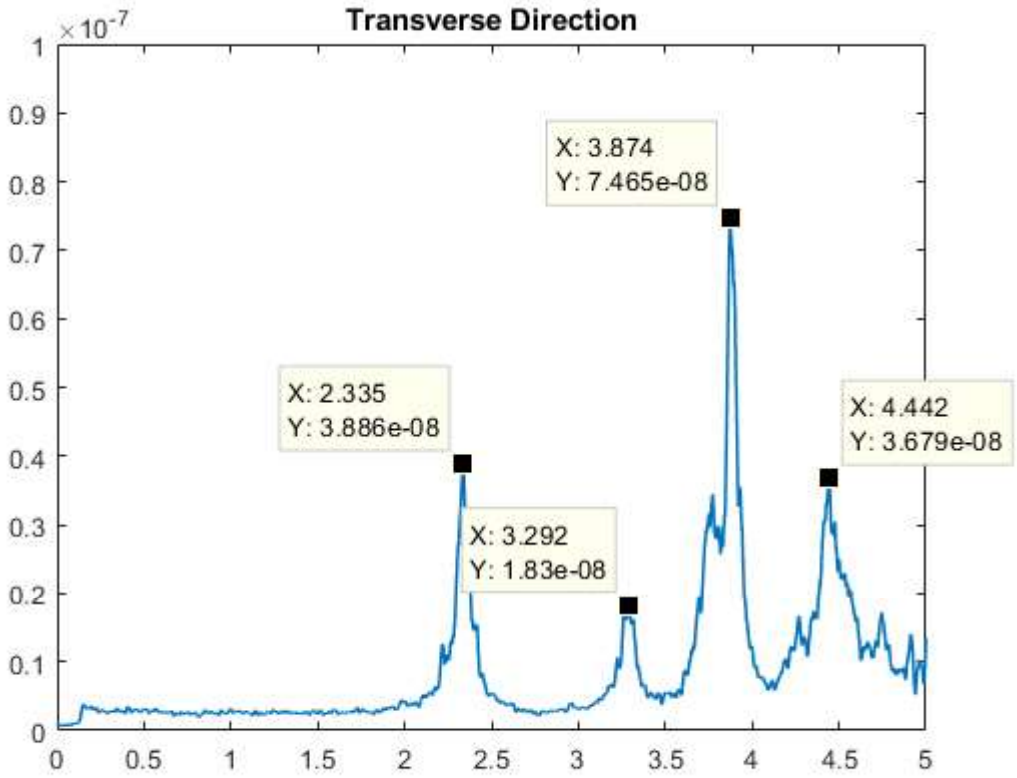

Figure 5.8. Peaks with Filter in Transverse Direction

The two smallest frequency values belong to the modal frequencies of the first displacement modes in the longitudinal and transverse directions. It can also be seen that the peak values of 3.87 Hz and 4.44 Hz appears in both of the directions. For this frequencies, it can be said that their modes are combined in both directions.

6. FINITE ELEMENT MODEL

6.1. Creating the Model

The creation of the finite element model of Hagia Irene is one of the most important steps. Ancient structures such as Hagia Irene are almost impossible to model with every small detail. The most important part of this task is the simplification of the model for the finite element program. Before starting to actually create the model, some simplifications were made:

- The model will be fully symmetric along the longitudinal axis. To this extent, the entrance part will not be modelled. The reason for not modelling the entrance part is that it is not an original part of the church. The entrance structure was built during the Ottoman Empire era.
- The base of the structure is assumed to be on levelled terrain. In reality, there is a 20 cm elevation difference along the longitudinal axis.
- The cross sections of the columns and structural elements are taken as simple as possible.
- Elements with similar dimensions are modelled as a single type, for example the circular columns in the first level.
- The roof panels, the wooden stair connecting the first two levels and other non-masonry elements are not modelled.

Hagia Irene is an ancient structure, therefore it does not have any building plans. A previously made building survey with laser spectrometers created the floor plans and numerous cross-sections of the church as AutoCAD drawing files. To ease the modelling process, the model was divided into four parts:

- The main structure of the church,
- Small dome,
- Large dome,
- Narthex.

First, the base of the entire church was created. To create it, the locations, shapes and dimensions of all of the structural elements such as walls and columns were noted down. Then while checking with the original plans, the base plan was drawn according to the previously taken notes. The base plan and the transverse and longitudinal axes can be seen in Figure 6.1. At this step of the project, the model was only two dimensional. It is important to note that only one half of the church was modelled. Then, the created model was mirrored along the longitudinal axis to complete the model.

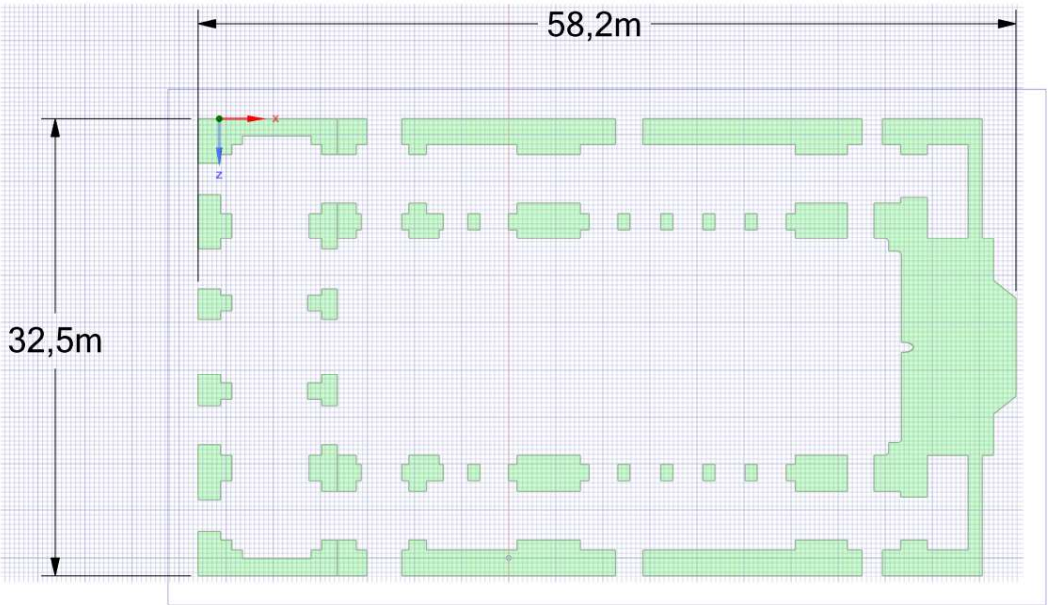

Figure 6.1. Base Plan of the FEM

After laying the base of the church, the first floor was modelled. During the modelling of the entire structure, the following method is used:

- A two dimensional "projection" of the element is drawn.
- The projection is extruded depending on the dimensions (width, height or depth) of the element.

The modelling of the first floor started with the modelling of the circular columns. Since all of the columns are somewhat different, they were simplified to a single type. After creating these columns, the pillars and outside walls were modelled up to the second floor. Before starting to model the second floor, the apse and the amphitheatre part of the structure was modelled. It is important to note here that the method used while creating the model is to model the structure until certain heights. The first floor was 7 m high, so the first 7 m of the entire church was modelled. The arches between the pillars and inside the walls were also modelled. All of the arches were different, so they were individually modelled. The only simplification made was that the arches were modelled as half circles or ellipses.

After creating the first 7 m of the church, the side walls were modelled. As seen in Figure 6.2 and Figure 6.3, there are two main side walls at each side of the church. A single type of window was modelled on each wall, to make the modelling process simpler. After creating the side walls, the pillars were created. After creating the pillars and the walls, the archways are modelled similar to the first floor. The most important part was to create the arches which supported the domes, since they bear the load of the domes and the roof. It is important to model the pillars and arches as a single structure. Creating contact zones between the structural elements makes the analysis more complicated. After creating the arches and pillars, the remaining part of the apse and the semi-dome were modelled. With the modelling of the apse, the modelling of the main part of the church is concluded. The finished model is shown in below figures, from different perspectives.

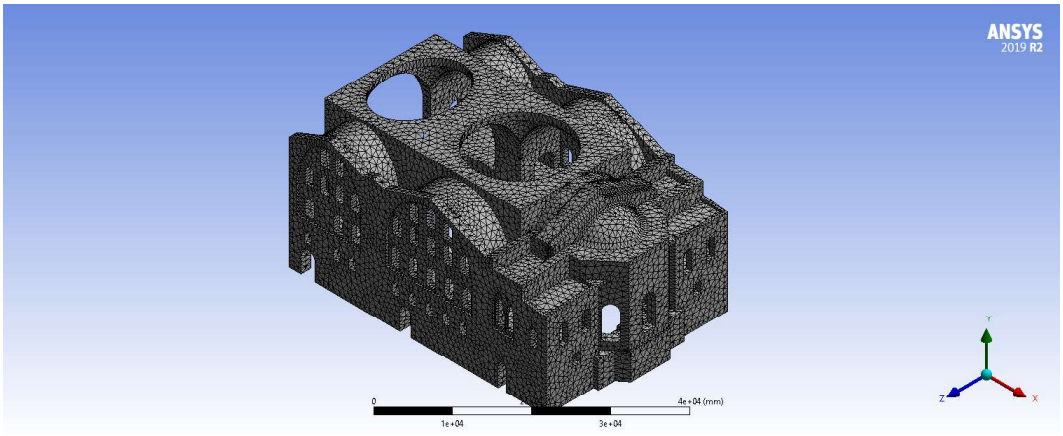

Figure 6.2. Main Structure Model 1

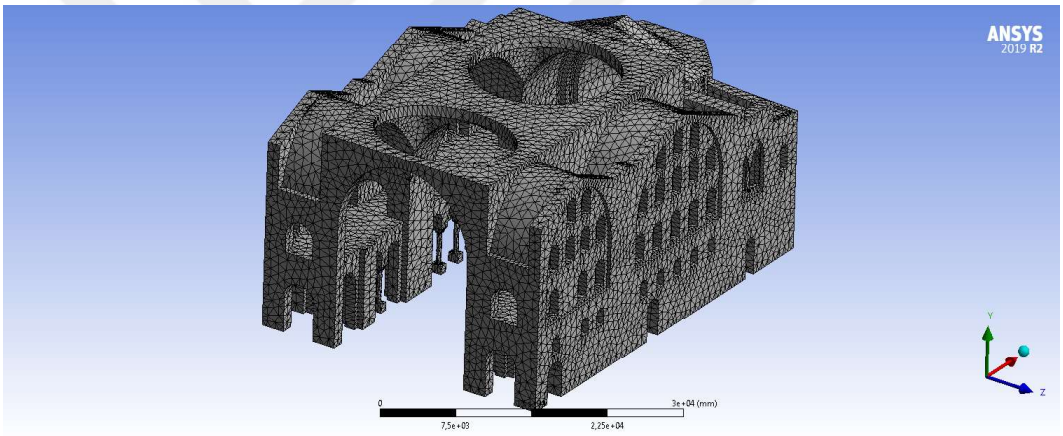

Figure 6.3. Main Structure Model 2

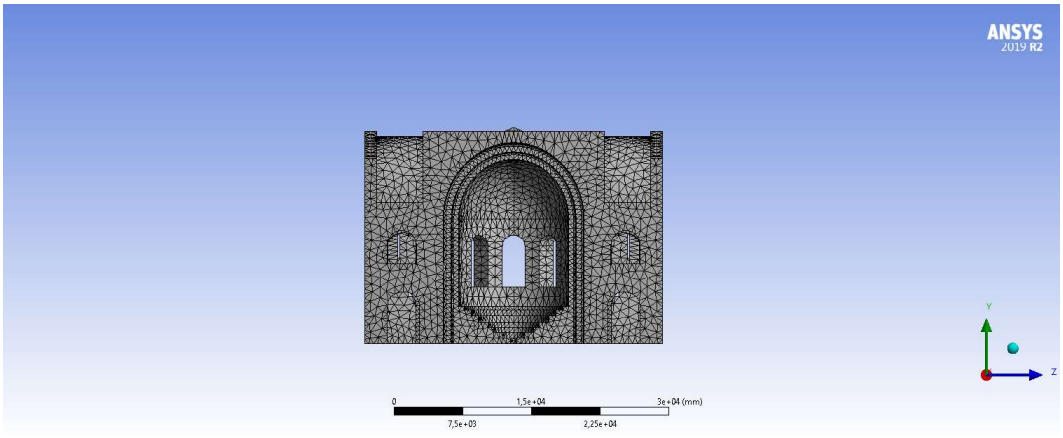

Figure 6.4. Main Structure Model 3

It is important to note here that ANSYS could not mesh the model at first. This was due to the sharp edges on the boundaries of the arches and curved surfaces. They were smoothened so that a mesh could be formed on the body.

After the main part of the church was modelled, the narthex was modelled. The procedure was the same as the main part. First, the walls, columns and pillars are modelled. Second, openings like archways and windows are placed in their correct places. Finally, the roof is closed and modelling is concluded. The finished model of the narthex is shown in Figure 6.5.

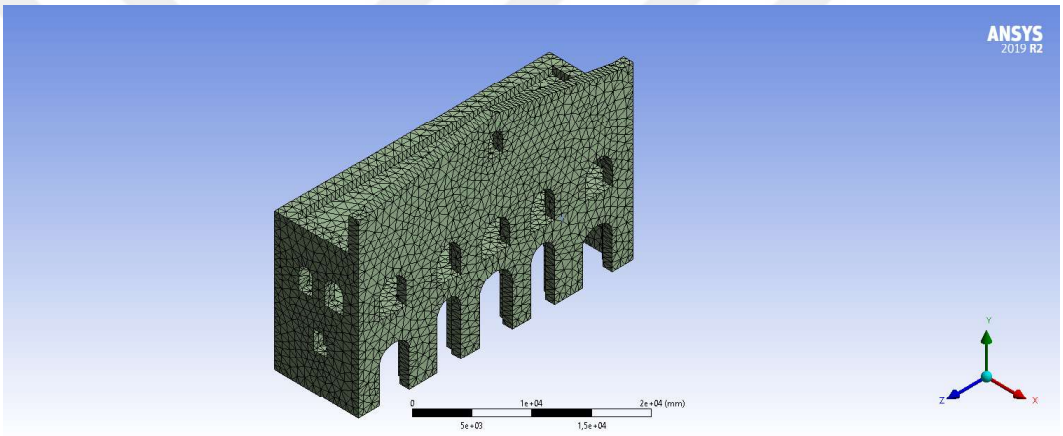

Figure 6.5. Model of the Narthex

The modelling of the domes were more difficult than the modelling of the narthex or the main body. The first problem was that the base of the domes were not perfect circles. The second problem was that the cross-sections of the walls of the domes were not identical throughout the circumference of the domes. Due to this fact, the small dome was modelled in quarters. Both of the domes have open tops. This detail is used to make the modelling process easier and meshing of the domes possible. The model of the small dome is shown in Figure 6.6 and the model of the large dome is shown in Figure 6.7.

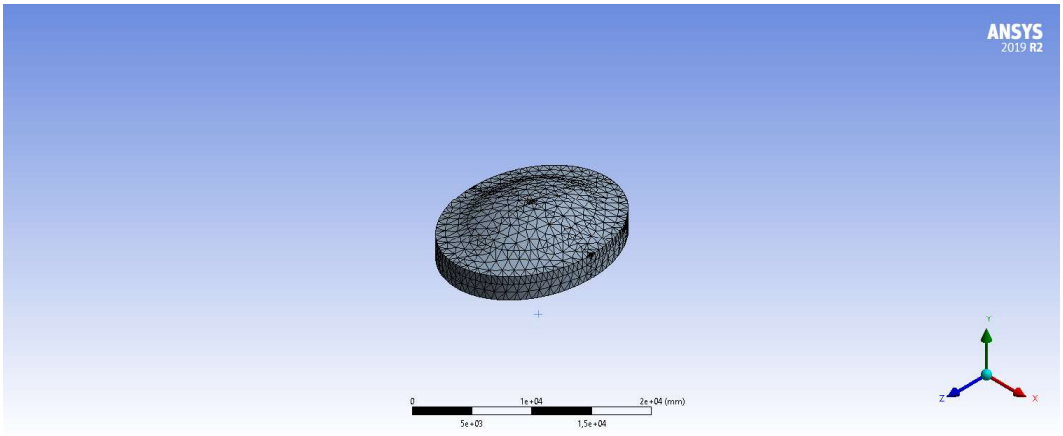

Figure 6.6. Model of the Small Dome

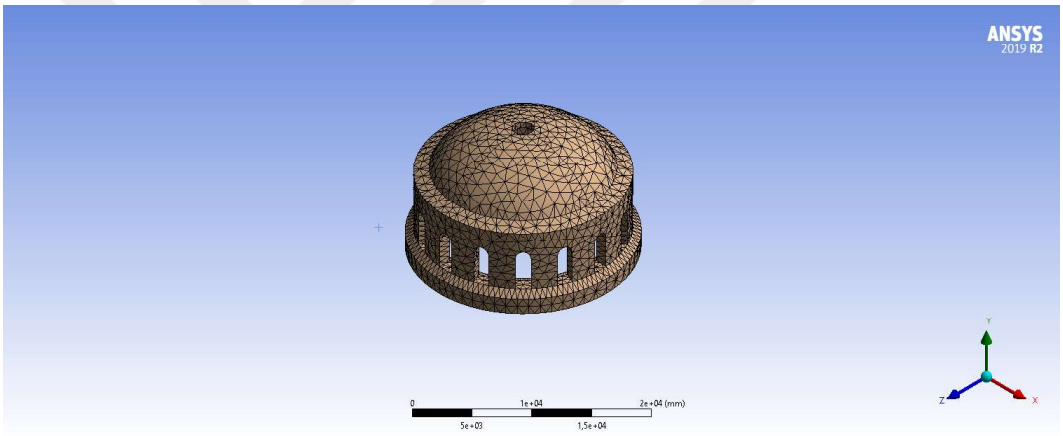

Figure 6.7. Model of the Large Dome

The interaction between these parts is also important. The contact surfaces were defined as bonded. There are other contact types such as frictional contact, but bonded contact type was chosen to ensure that the bodies would act as a single part. In Figure 6.8 the final finite element model and in Figure 6.9 the cross-sectional view along the longitudinal axis can be seen.

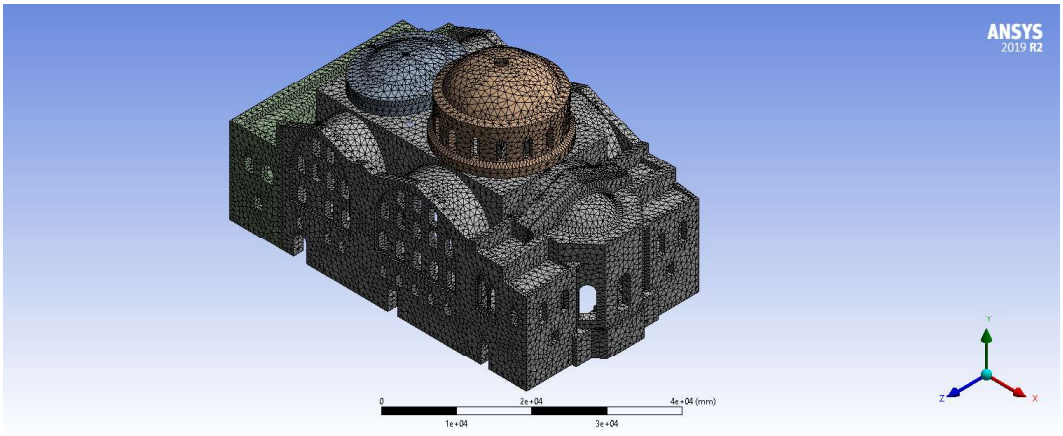

Figure 6.8. Model of the Entire Structure

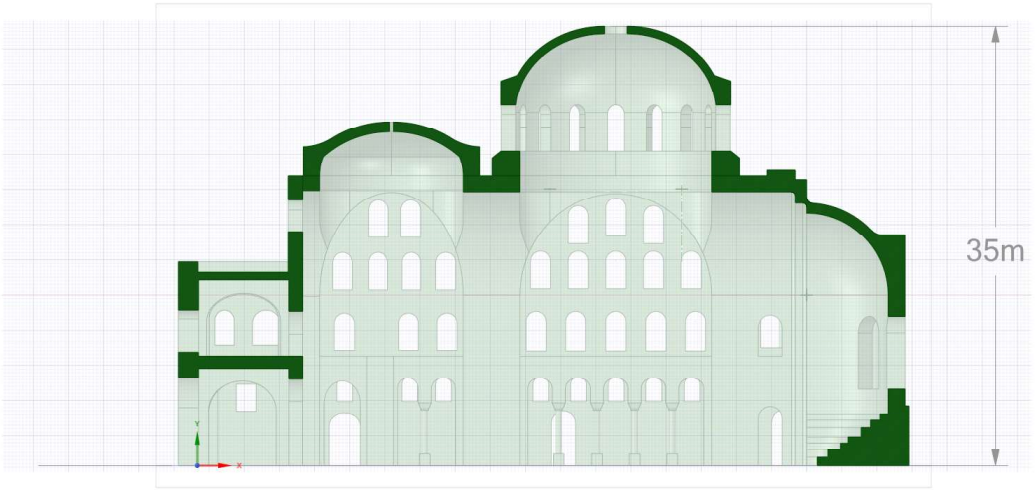

Figure 6.9. Longitudinal Cross Section

This model will be used for modal analysis and response spectrum analysis of the structure.

6.2. Summary of FEM Results

6.2.1. Modal Results

After creating the finite element model of Hagia Irene, a preliminary modal analysis was made. According to the results obtained from this analysis, material properties and support conditions were changed to obtain results closer to the ambient vibration results. The factors which were changed to affect the results were:

- Support Conditions: Support types play the greatest role in creating a realistic model. Choosing the entire contact surface between the structural elements and the ground greatly affects the results.
- Material Properties: The modal results depend heavily on the Young's Modulus of the material.

A preliminary modal analysis was made with the following assumptions:

- Fixed supports at all contact surfaces
- E = 3000 MPa
- ρ = 2400 kg/m^3
- Poisson's Ratio $\nu = 0.18$
- Initial conditions: Static gravitational loads

The results of this analysis set the reference point. The modal results and their comparison with the ambient vibration results are given in Table 6.1.

Table 6.1. Preliminary Results Comparison

Mode Number	**Experimental Freq. (Hz)**	**Numerical Freq. (Hz)**	**Error (%)**
1	2.34	3.28	40.34
2	2.72	3.99	47.18
3	3.29	4.92	50.18
4	3.68	5.46	48.51
5	3.87	6.10	57.78
6	4.44	6.14	38.50

After this result, more combinations of density and Young's modulus were used with fixed supports. The conclusion obtained from those trials were:

- Increasing Young's Modulus increases the hardness of the structure, therefore increases the natural frequencies of the modes. To reach the values obtained from the ambient vibration analysis, Young's Modulus must be decreased.
- Increasing the density of the structure makes it heavier. As the structure gets heavier, the natural frequencies of the modes decrease.
- First two modes are the first modes of the transverse and longitudinal axes, respectively.

The final results obtained by using fixed supports are given below in Table 6.2.

Table 6.2. Final Results Comparison

Mode Number	**Experimental Freq. (Hz)**	**Numerical Freq. (Hz)**	**Error (%)**
1	2.34	2.246	3.99
2	2.71	2.72	0.47
3	3.28	3.36	2.63
4	3.68	3.74	1.66
5	3.86	4.16	7.77
6	4.43	4.19	5.45

This combination is named as Set 1. For this set, the material properties were:

- E = 2000 MPa
- ρ = 2400 kg/m^3
- Poisson's Ratio ν = 0.18

The mode shapes are shown in the following figures.

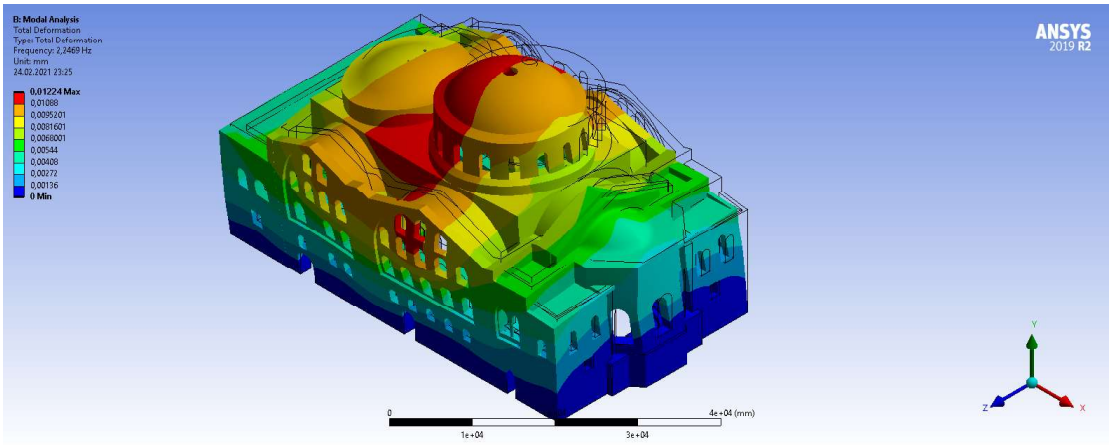

Figure 6.10. Mode 1, 2.34 Hz

The first mode shape is the swaying motion in the transverse direction. It is the dominant mode in this direction. In Figure 6.10, the deformed shape of the church can

be clearly seen. Similarly, the second mode is the dominant mode in the longitudinal direction, as seen in Figure 6.11.

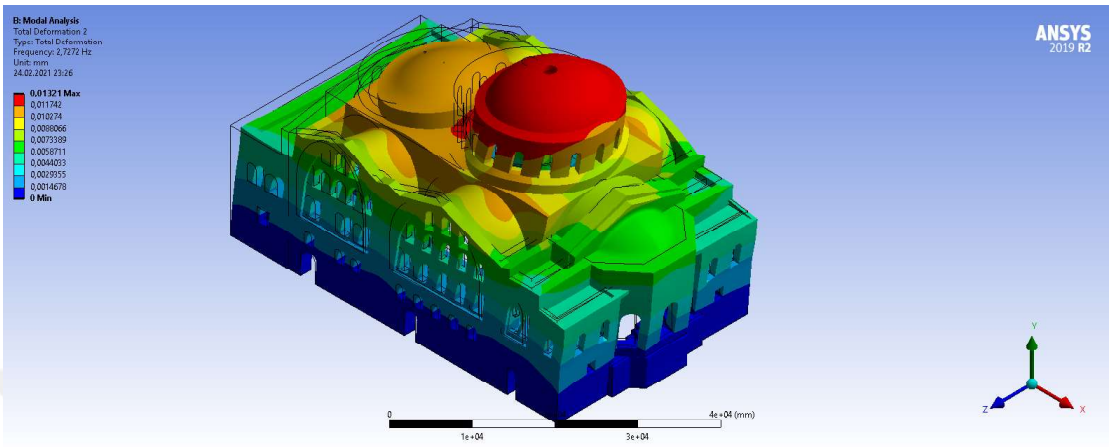

Figure 6.11. Mode 2, 2.71 Hz

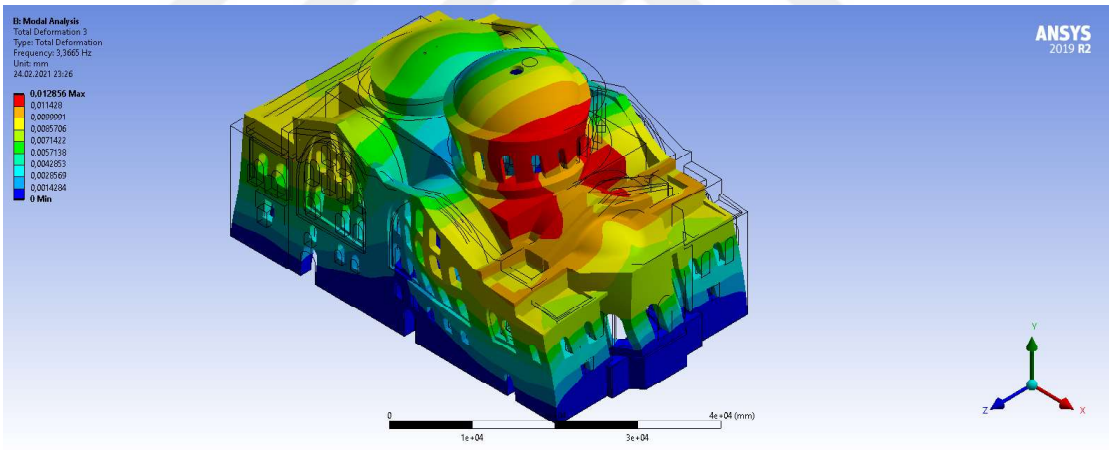

Figure 6.12. Mode 3, 3.28 Hz

Like the first and second modes, the third and fourth modes are their second modes in their respective directions, as can be seen in Figure 6.12 and Figure 6.13.

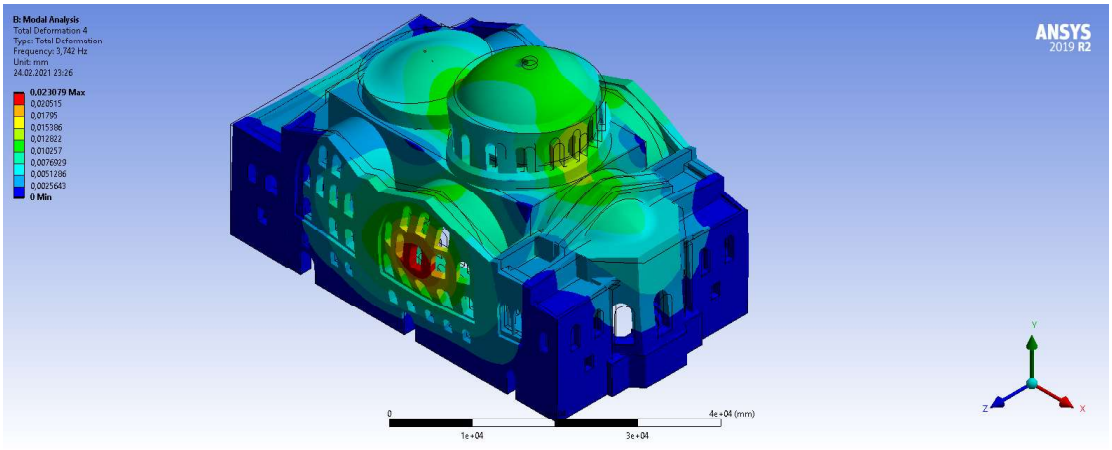

Figure 6.13. Mode 4, 3.68 Hz

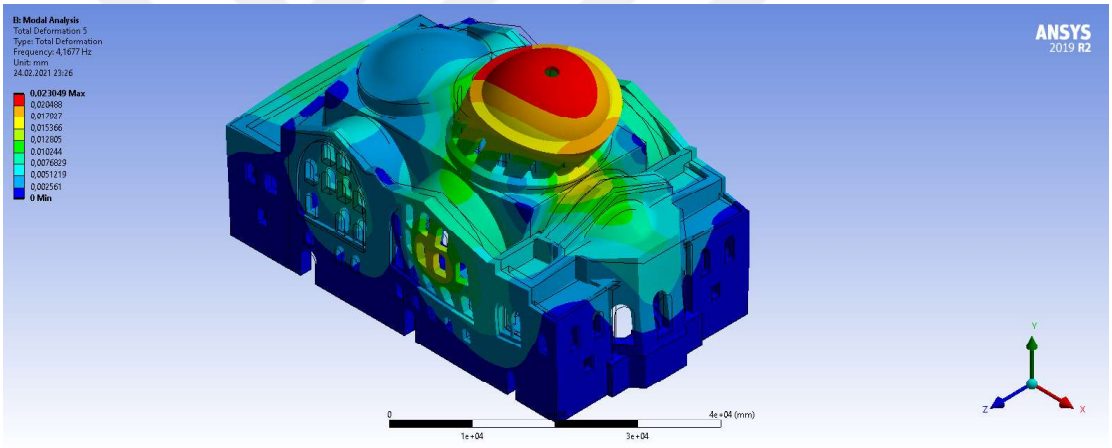

Figure 6.14. Mode 5, 3.86 Hz

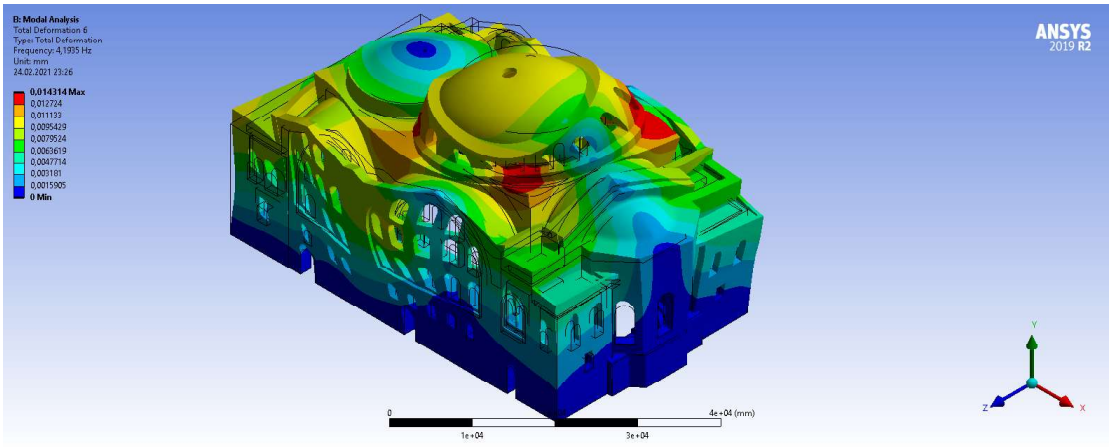

Figure 6.15. Mode 6, 4.43 Hz

Two other support conditions were used too to get similar results. The main reason for choosing other support types is mainly due to keeping the values of the material properties in a certain range. In these cases, the material properties were fixed as the following:

- E = 3000 MPa
- $\rho = 2400$ kg/m^3
- $\nu = 0.18$

The support conditions of the second set, Set 2, is the following:

- Elastic supports at all soil-structure contact surfaces
- Displacement restraints in transverse direction at all contact surfaces
- Displacement restraints in longitudinal direction shown in Figure 6.16 as the yellow surfaces. Four surfaces do not have this support type.

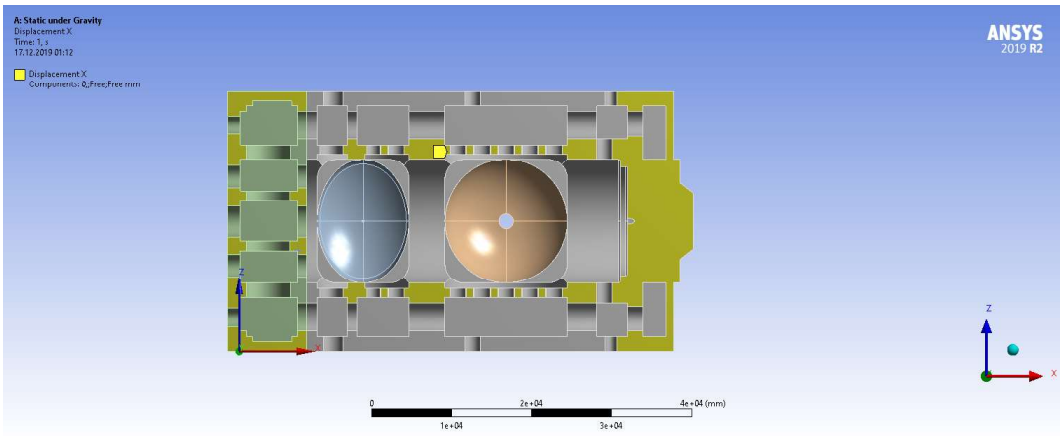

Figure 6.16. Support Conditions for Set 2

As seen in Figure 6.16, four side walls are free to move along the longitudinal axis. This was done according to the results obtained from the previous results. One of the previous results is given below in Table 6.3, with the accompanying material properties and the support conditions.

- E = 3000 MPa
- $\rho = 2400$ kg/m^3
- $\nu = 0.18$
- Elastic support with 0.5 MPa stiffness and displacement restraints along both axes (transverse and longitudinal) at all contact regions

Table 6.3. Trial Frequency Results

Mode Number	**Experimental Freq. (Hz)**	**Numerical Freq. (Hz)**	**Error (%)**
1	2.34	2.49	6.41
2	2.71	3.40	25.46
3	3.28	4.00	21.95
4	3.68	4.48	21.73
5	3.86	5.29	37.04
6	4.43	5.32	20.09

We assume that the first two modes are the primary modes in the transverse and longitudinal axes. Therefore, according to the ambient vibration results, the frequencies for the first two modes should be $f_1 = 2.3403$ Hz and $f_2 = 2.7142$ Hz. Since the difference between the first two frequencies are too large, the structure had to be softened in the longitudinal direction. The reason for "releasing" the four side walls was to obtain modal frequency results similar to those obtained from the ambient vibration tests. The results obtained using given material properties and previously explained support conditions are shown below in Table 6.4.

- E = 3000 MPa
- $\rho = 2400$ kg/m^3
- $\nu = 0.18$
- Elastic support with 0.2 MPa stiffness

Table 6.4. Set 2 Results Comparison

Mode Number	**Experimental Freq. (Hz)**	**Numerical Freq. (Hz)**	**Error (%)**
1	2.34	2.34	3.99
2	2.71	2.72	0.47
3	3.28		N/A
4	3.68		N/A
5	3.86	3.86	0.07
6	4.43	4.49	1.34

Two modal frequencies obtained from the ambient vibration analysis do not have a match in the set of results obtained from the finite element model. The other results, however, are almost identical. The error percent is less than 1.5% for all obtained modal frequencies and it is important to note that errors up to 20-25% is also acceptable at such small natural frequency values.

The third and last set of results, Set 3, were obtained using a mixed type of support types. The parameters were:

- E = 3000 MPa
- ρ = 2400 kg/m^3
- ν = 0.18
- Elastic supports and displacement restraints in both axes appointed at all soil-structure surfaces except one.
- Fixed support appointed under the apse/amphitheatre part.

The modal frequency results are given below in Table 6.5.

Table 6.5. Set 3 Results Comparison

Mode Number	**Experimental Freq. (Hz)**	**Numerical Freq. (Hz)**	**Error (%)**
1	2.34	2.10	3.99
2	2.71	2.93	0.47
3	3.28		N/A
4	3.68	3.97	8.05
5	3.86	4.04	4.48
6	4.43	4.64	4.64

6.2.2. Response Spectrum Analysis and Results

The response spectrum analysis was made using the following conditions:

- The initial condition is the static gravitational load.
- E =2000 MPa
- $\rho = 2400$ kg/m^3
- Poisson's Ratio $\nu = 0.18$
- All soil-structure contact surfaces are fixed supports.

The reason behind choosing Set 1 is actually quite simple. All modal frequencies obtained using this set have a pair in the set of results obtained from ambient vibration testing. Apart from that, Set 2 has have supports free to move in a direction. Response spectrum analysis results obtained using Set 2 differ too greatly with the results obtained from Set 1 and Set 3.

Before the response spectrum analysis, the design spectrum of the site of Hagia Irene and the recorded response spectrum of an actual earthquake was compared. The main reason for this comparison was to choose which spectrum to use for the analysis. The real-life earthquake used for this comparison was the Kocaeli Earthquake, which

occurred on August 17, 1999. The comparison of the Kocaeli Earthquake Spectrum and the DD-2 Earthquake Spectrum is shown in Figure 6.17. The first six experimentally determined modal frequencies of Hagia Irene are also pointed out.

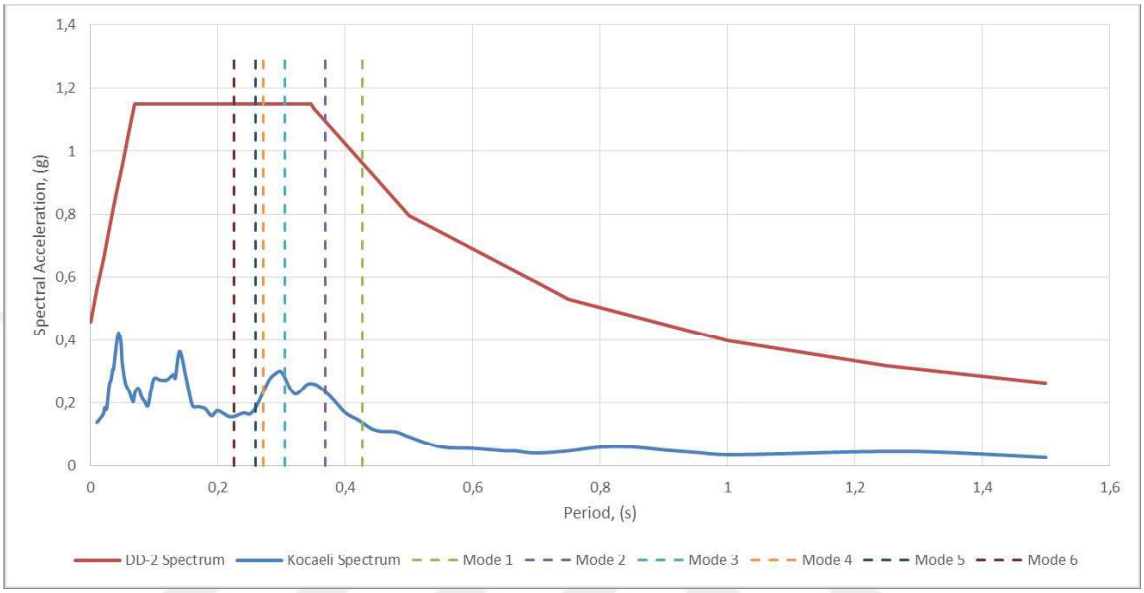

Figure 6.17. Spectra Comparison and Modal Frequencies

The reason for choosing the Kocaeli Earthquake was that it affected the cities of Düzce, Kocaeli and Istanbul very severely. The spectrum shown in Figure 6.17 belongs to the measurements taken at the Fatih Station in Istanbul, which is the closest station to the site of Hagia Irene. Looking at Figure 6.17, it is clearly seen that the results obtained from an analysis using the Kocaeli Earthquake would be much smaller than those obtained from the design spectrum. For all of the modal frequencies, the spectral acceleration values values of the design spectrum far exceed the values from the Kocaeli Earthquake. Therefore, response spectrum analysis will be conducted using the following two spectra:

- Horizontal Design Spectrum of a DD-2 Type Earthquake based on Turkish Earthquake Code 2018
- Vertical Design Spectrum of a DD-2 Type Earthquake based on Turkish Earthquake Code 2018

The spectra for the design earthquake are shown in the figures below.

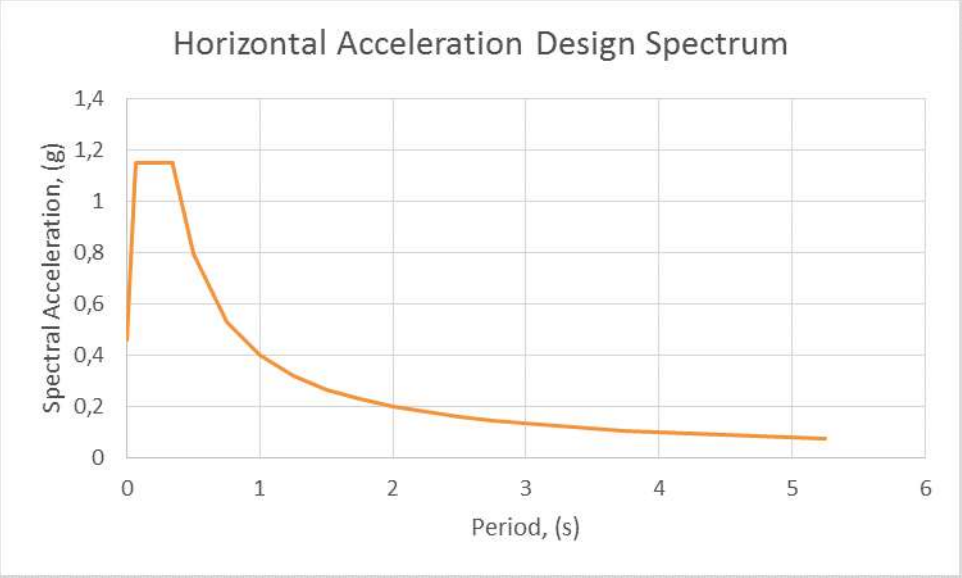

Figure 6.18. Horizontal Acceleration Spectrum DD-2 Earthquake

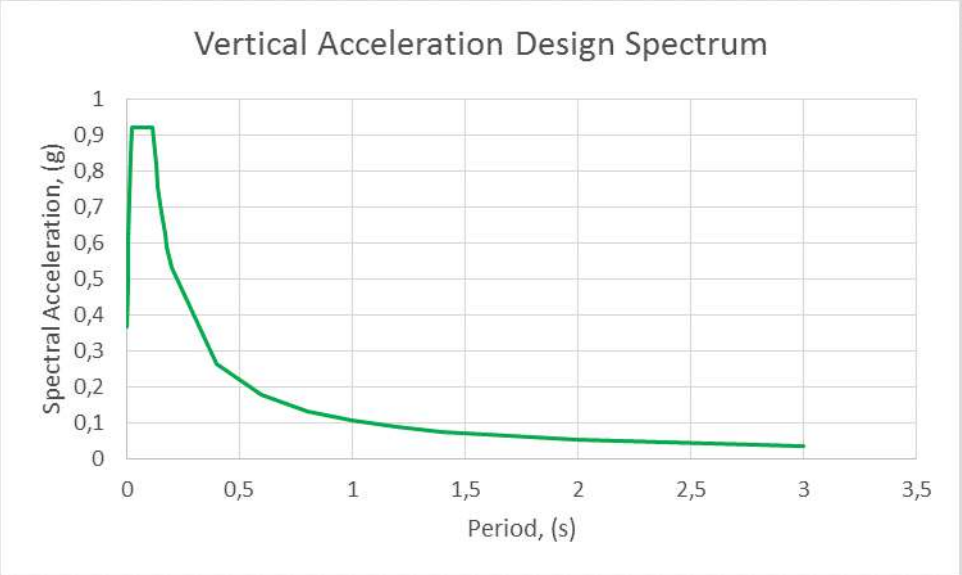

Figure 6.19. Vertical Acceleration Spectrum DD-2 Earthquake

Only one spectrum can not be used while making a response spectrum analysis. During an earthquake, acting forces vary depending on the direction they are acting from. Therefore, it is necessary to use a vertical response spectrum apart from a

horizontal response spectrum. The spectra are combined using the 30 % rule. The formulae used for the combination of the spectra are given below:

- $X + 0.3Y + 0.3Z$
- $0.3X + 0.3Y + Z$
- $0.3X + Y + 0.3Z$

Here, X and Z are the longitudinal and transverse directions, respectively. That is the reason why the coefficients for them are taken as 1 in their respective cases. There are 3 loading cases regarding the combinations of the spectra. The results are shown in the figures below.

The following results were obtained from the response spectrum analysis:

- Total Deformation (mm)
- Shear Stress (MPa)
- Maximum Principal Stress (MPa)
- Minimum Principal Stress (MPa)

Here, the maximum principal stress value represents the compressive forces acting on the elements, whereas the minimum principal stress value represents the tensile forces.

DD-2 Earthquake Spectrum Results, Loading Case: $X + 0.3Y + 0.3Z$

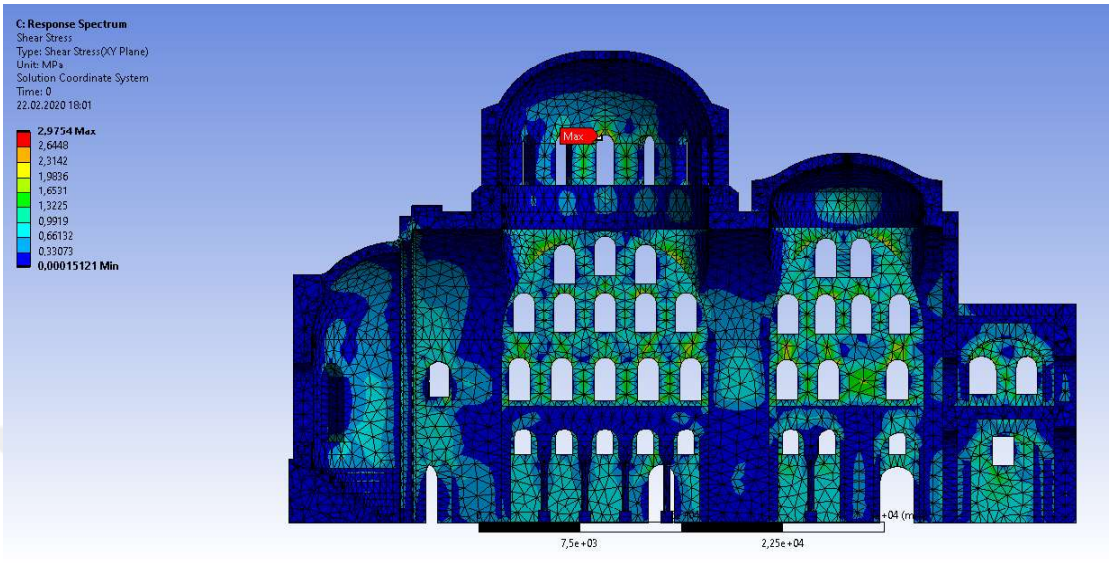

Figure 6.20. Shear Stress

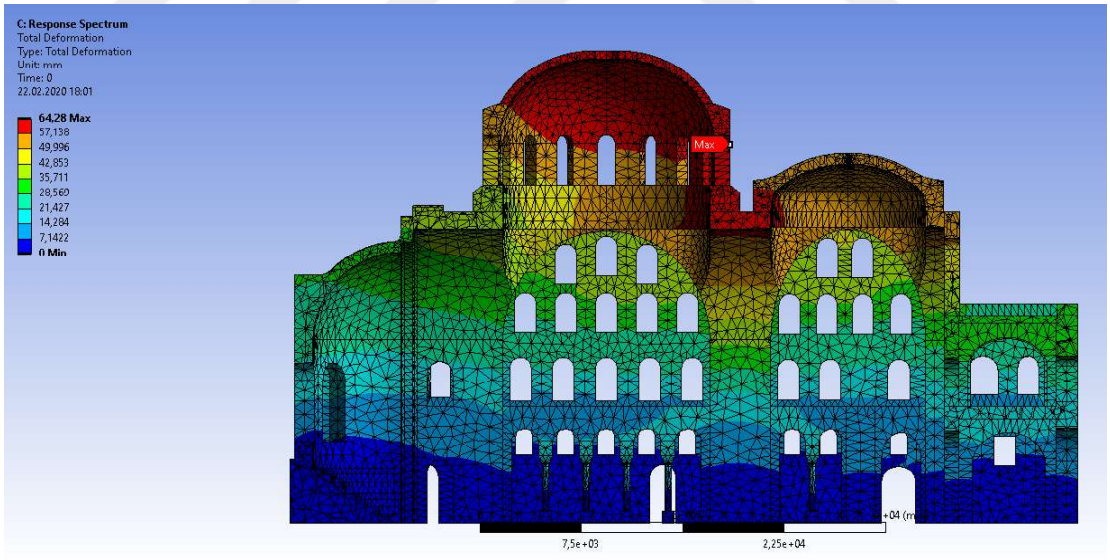

Figure 6.21. Total Deformation

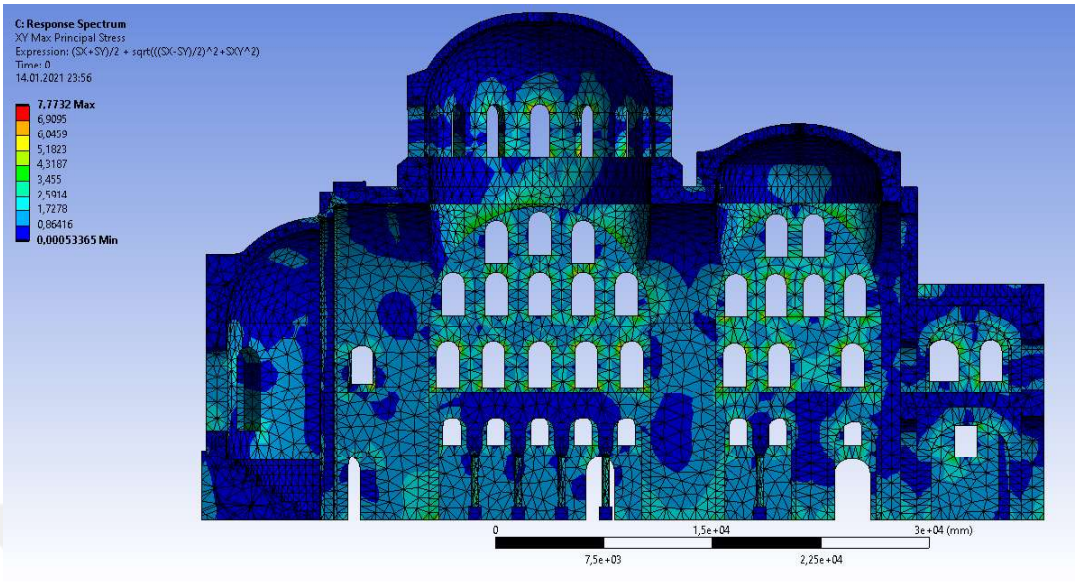

Figure 6.22. Maximum Principal Stress

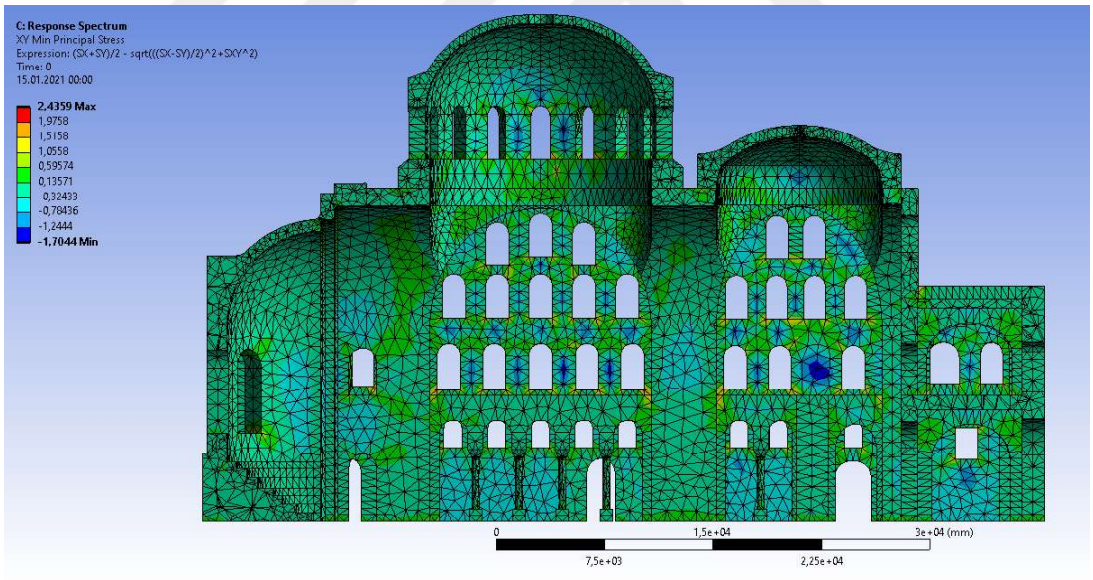

Figure 6.23. Minimum Principal Stress

DD-2 Earthquake Spectrum Results, Loading Case: $X + 0.3Y + 0.3Z$

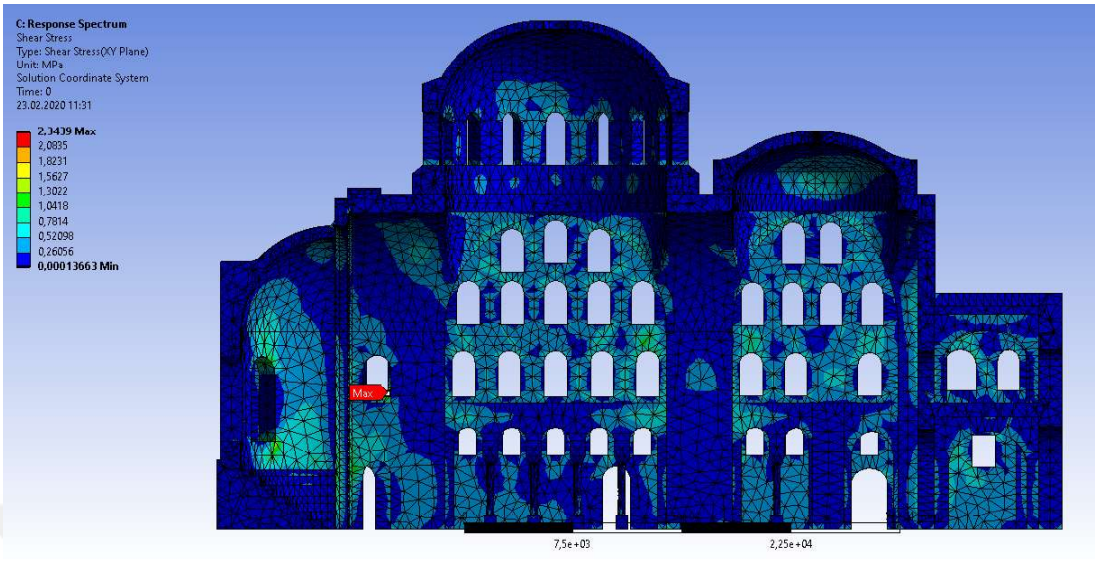

Figure 6.24. Shear Stress

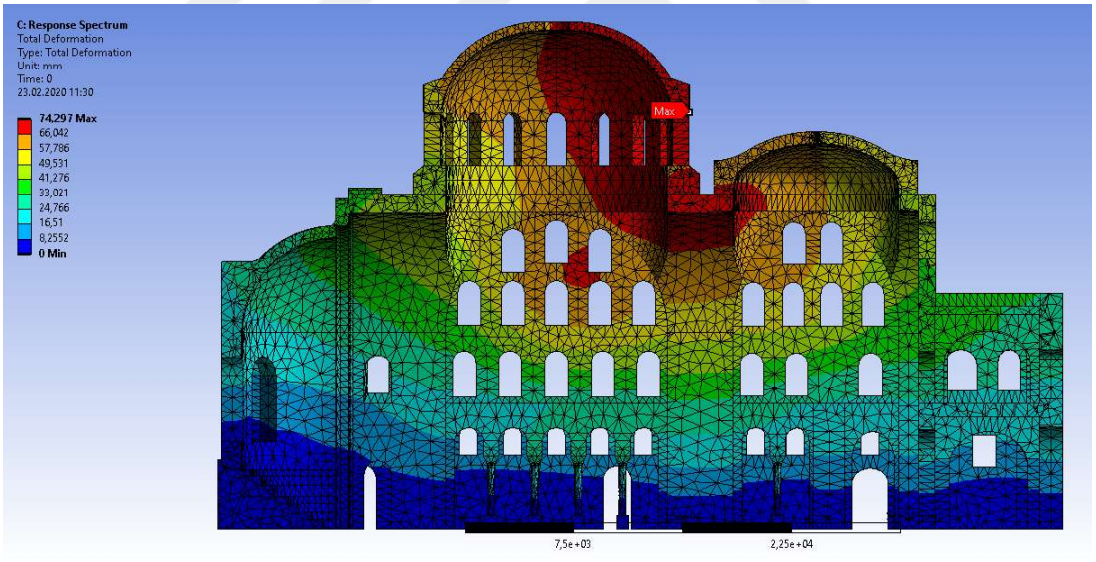

Figure 6.25. Total Deformation



Figure 6.26. Maximum Principal Stress

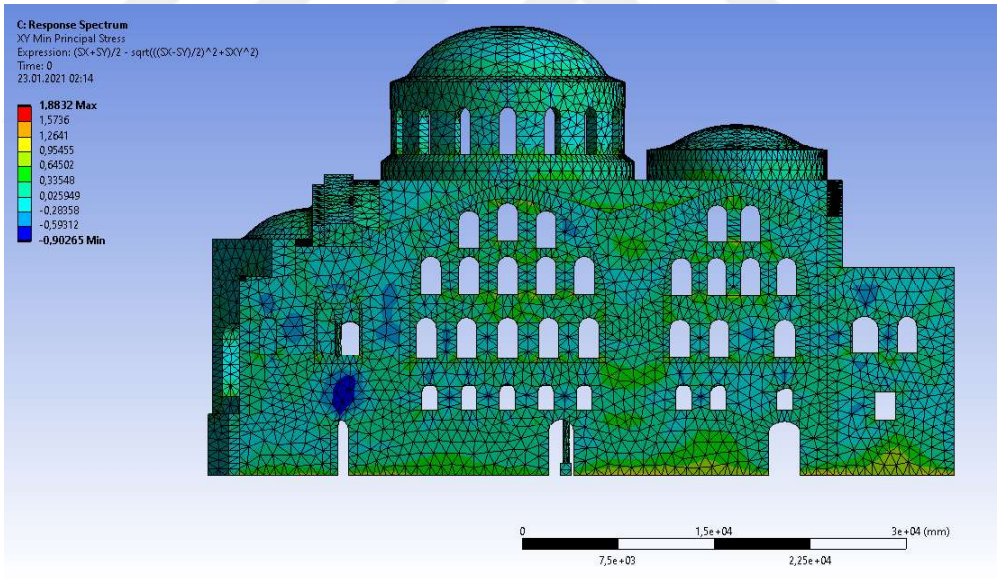

Figure 6.27. Minimum Principal Stress

DD-2 Earthquake Spectrum Results, Loading Case: $0.3X + Y + 0.3Z$

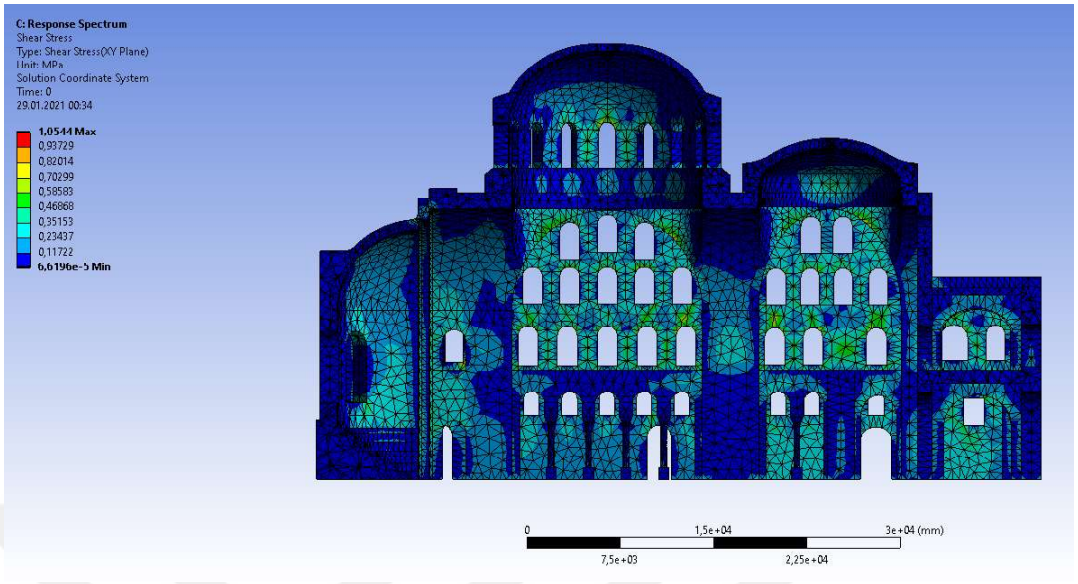

Figure 6.28. Shear Stress

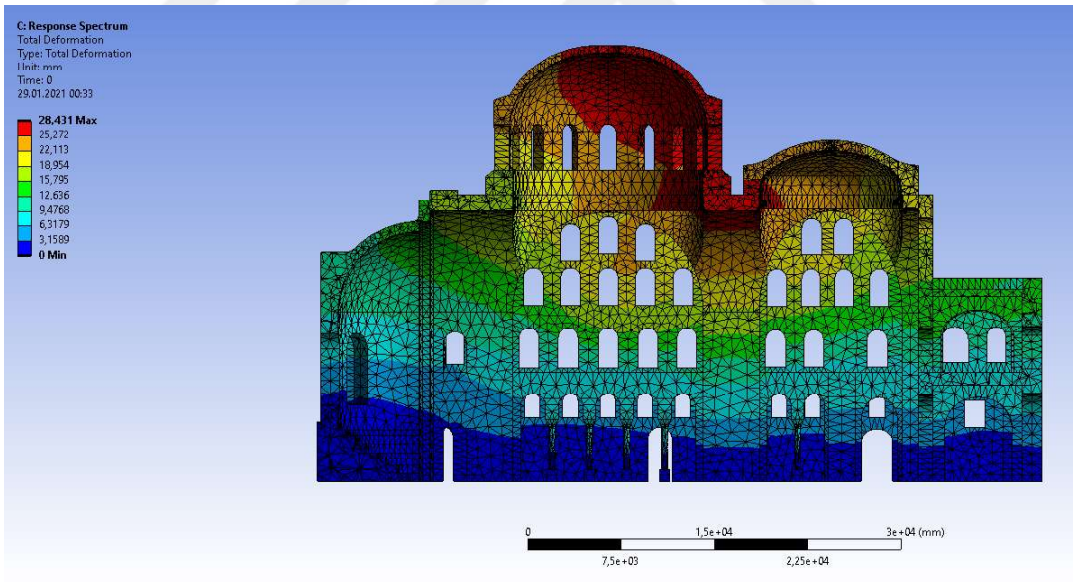

Figure 6.29. Total Deformation

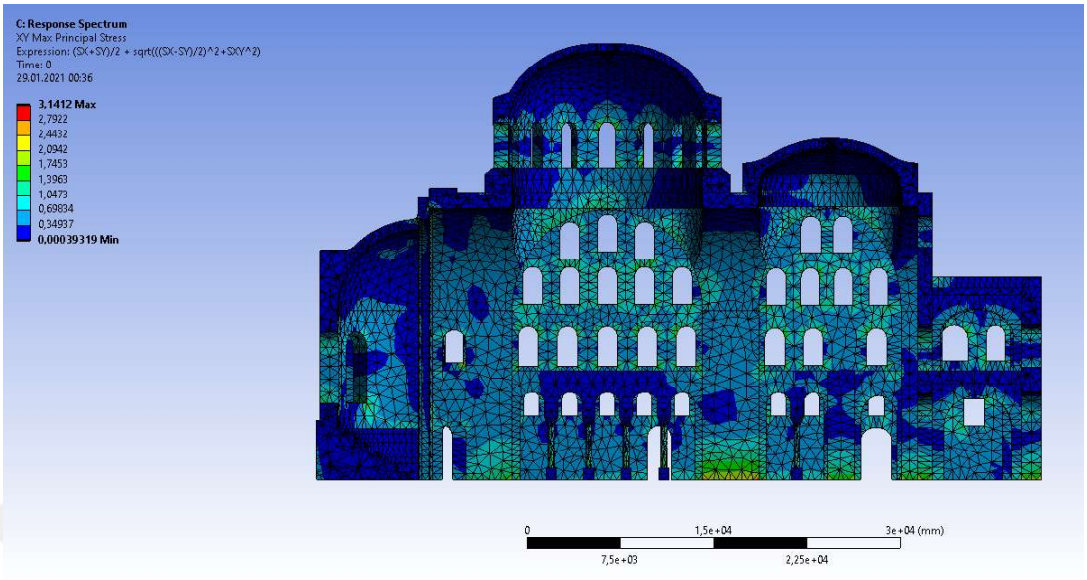

Figure 6.30. Maximum Principal Stress

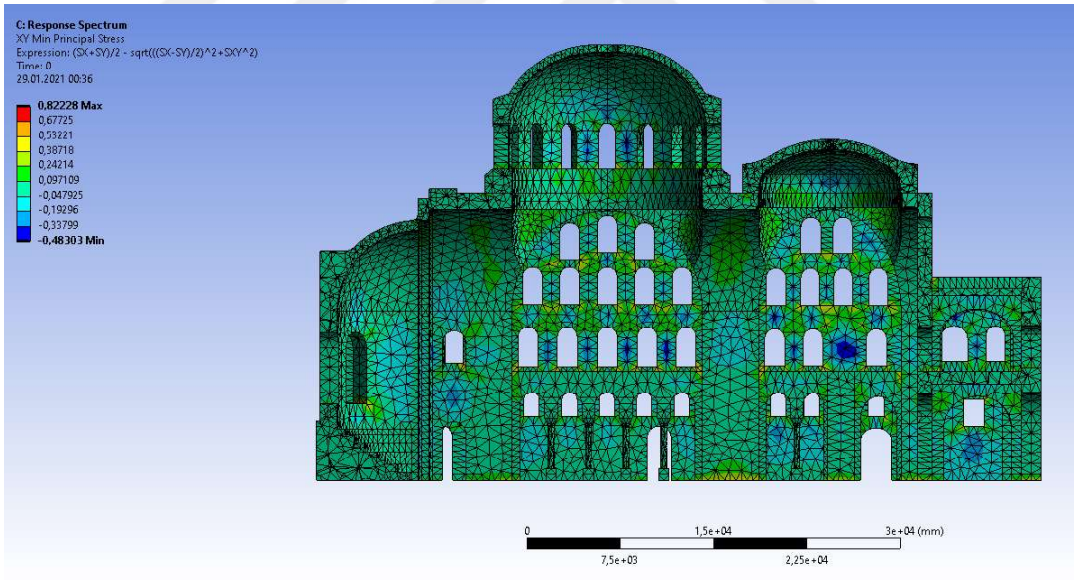

Figure 6.31. Minimum Principal Stress

The maximum for the stresses and deformations for the individual cases are given below, in Table 6.6. Here, Case 1 is the load combination $X+0.3Y+0.3Z$, Case 2 is the load combination $0.3X+0.3Y+Z$ and Case 3 is the load combination $0.3X+Y+0.3Z$.

Table 6.6. Response Spectrum Results Peak Values

	DD-2 Earthquake		
	Case 1	**Case 2**	**Case 3**
Shear Stress	2.97	2.34	1.05
Total Deformation	64.28	74.29	28.43
Max. Principal Stress	7.77	9.92	3.14
Min. Principal Stress	-1.70	-2.14	-0.48

7. RESULTS DISCUSSION

In this chapter, the finite element model results will be compared to the actual structure. This is particularly important because in the event of a new earthquake, the performance of the structure must be known, in order to take adequate precautions.

To determine the possible damage zones, it is important to know whether the finite element model gives correct assumptions on the damage zones. To this extent, places where the displacements are too great or stress concentration zones will be compared to the damaged zones in the actual structure. All of the previously mentioned variables will be inspected while determining the possible damage zones.

7.1. Possible Damage Zones

The damage zones will be determined according to the results obtained from the finite element model. Since the results obtained from the both response spectra look similar, the damage zones will be determined using only the results obtained from the analysis using the design earthquake. For the design earthquake, the dominant component of the response spectrum will be in the longitudinal direction (X-Axis). The first variable to consider will be the *Total Deformation*.

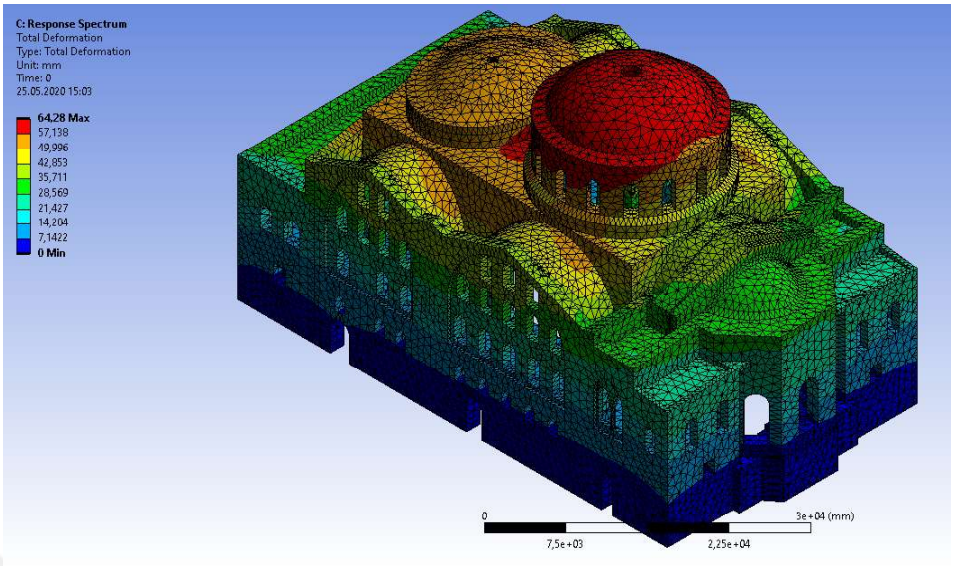

Figure 7.1. Total Deformation (mm)

Looking at the entirety of the church, it is clearly seen that the total deformation is directly proportional to the height. This is valid for most of the structures. Looking at the finite element model more detailed, the minimum displacement is at the bottom of the structure. The entire first floor of the structure undergoes displacement values lower than 10 mm. Since the supports are taken as fixed supports, these results are not surprising. In the case of real life, the foundations act as compression-only supports or spring supports, since the soil also moves.

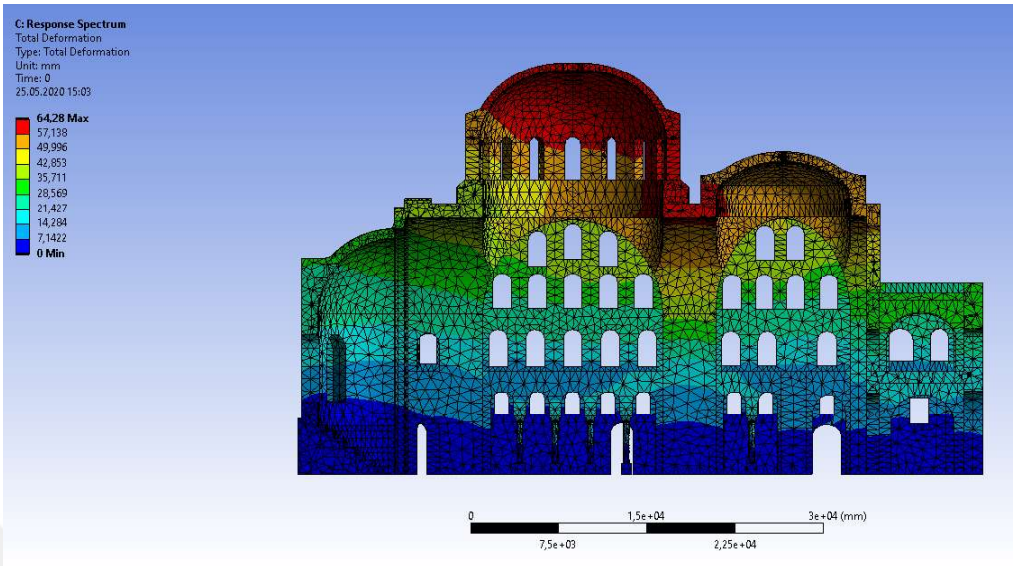

Figure 7.2. Longitudinal Cross-Section

In Figure 7.2 it can be seen that the total deformation increases fastest on the main arch, which carries both of the domes. The deformations on the main arch reach 40 mm faster than the surrounding areas of the arch. Due to this difference, damages may occur in the area. Apart from the main arch, the circular columns and the arches connecting them to each other and the second floor slab may also suffer damages. The two columns on the each side of the main arch are particularly prone to suffering damages due to the fact that the displacements focus on this area.

The displacement results give a rough estimation for the possible damage areas. To make a more concrete estimation, the stress results must also be inspected. To this end, the results for shear stress and maximum and minimum principal stresses will be used. First, the results for the case of maximum principal stress will be inspected. As previously mentioned, maximum principal stress represents compressive stresses. In Figure 7.3, the longitudinal cross-section of the church is shown.

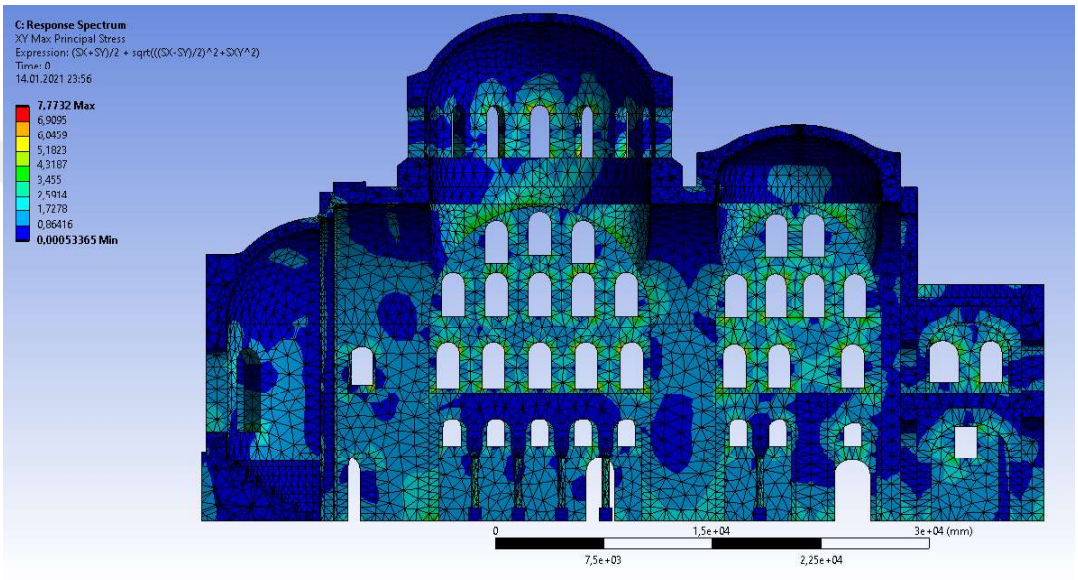

Figure 7.3. Maximum Principal Stress

The first thing that catches attention is the fact that the maximum principal stresses do not develop on the domes. The distribution of stresses is completely different than the distribution of displacements. Stresses start developing at the base of the structure and do not increase linearly with the height of the structure. Examining the entire structure, it is clear that the compressive stresses are maximum at the base of the pillars and side walls.

Apart from the stresses at the base of the structure, there are also peaks in the stress concentrations around the arched structures. These arched structures are not limited with the main arches which support the entire structure. Window holes on the walls are also shaped like archways. These stresses can cause cracks starting from the top of these arches. At the windows, apart from the top of the arches, there are also

stress concentrations at the bottom of the windows. They can be seen as insignificant, but such cracks on the main arches supporting the domes can expose the structure to more serious damages. This can be said due to the fact that the modelled material has a compressive strength of 5 MPa, but the model shows stress values up to 7.77 MPa.

Looking at the subparts of the structure, it is possible to see that at the apse the stresses concentrate around the windows. There are hardly any stresses on the dome and on the amphitheater steps. However, there are considerable stresses on the bases of the pillars supporting the domes. The stresses in the narthex are similar to the rest of the structure.

After the maximum principal stresses or the compressive stresses are checked, it is important to check the minimal principal stresses or what they represent, namely the tensile stresses. It is important to check the tensile stress because masonry structures have very low tensile strength, usually around 0.5-2 MPa. In Figure 7.4, the minimum principal stress distributions can be seen.

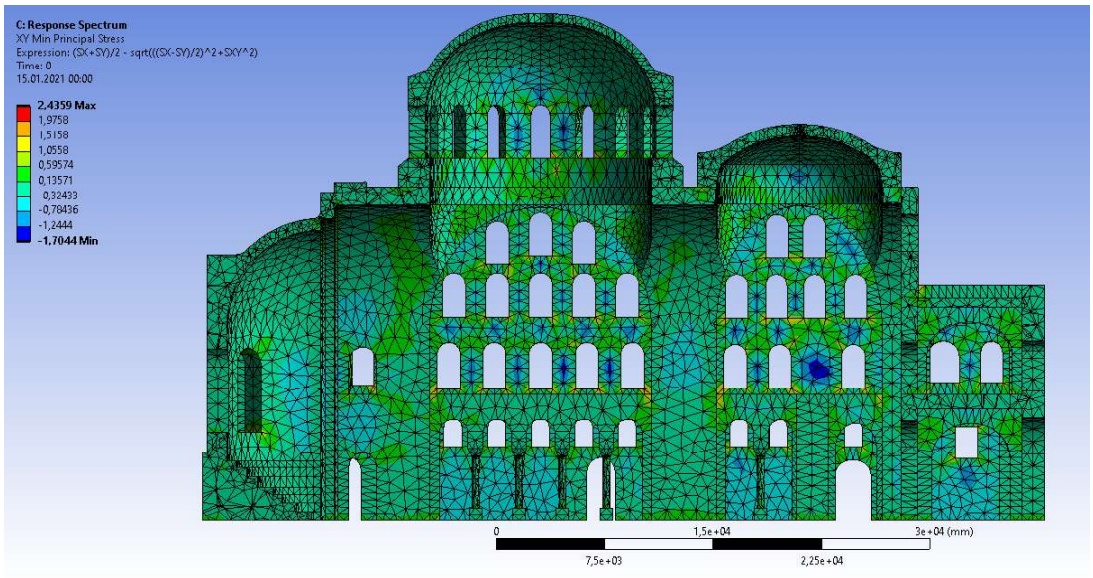

Figure 7.4. Minimum Principal Stress

For minimum principal stress case, the minimum stress values must be inspected. Here, the minimum values reach up to -1.7 MPa, which far exceeds the tensile yield

strength of the modelled material. Here, it can be clearly seen that the smallest values of minimum principal values occur between the windows and the walls. The most critical location is between the two windows at the first row of the windows in the second floor. First floor walls can also be categorized as critical locations, because there are tensile stresses going up to 1 MPa in those locations. Apart from the maximum principal stresses and the minimum principal stresses, shear stresses are also a very important variable to consider. The shear stress concentrations and distributions can be seen in Figure 7.5.

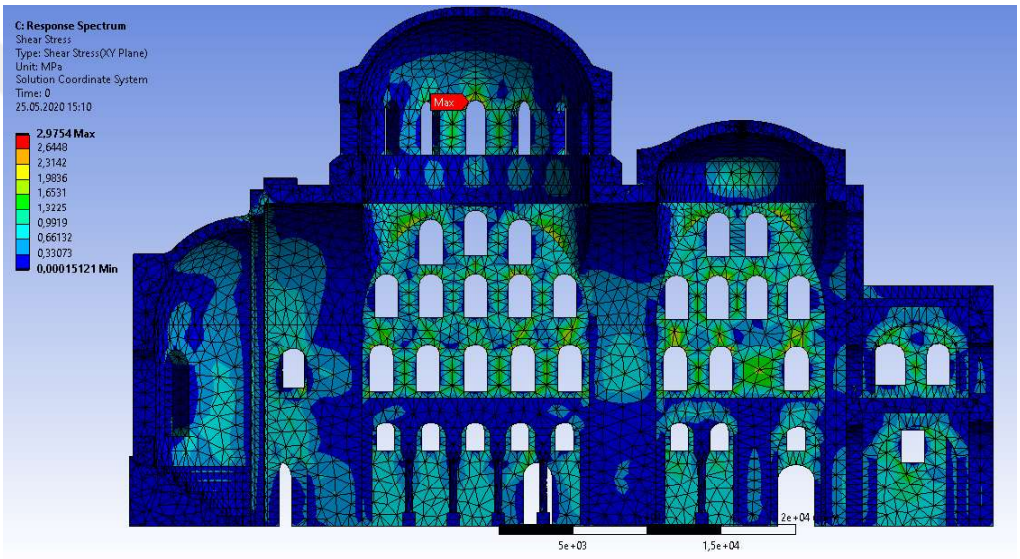

Figure 7.5. Shear Stresses

Looking at Figure 7.5, the most apparent thing is that shear stresses are concentrated on the side walls. It is apparent that the shear stresses increase at the highest point of any type of arched structure. These arched structures include the window holes and the arches carrying the domes. The stresses do not concentrate only on the arches. There are shear stress concentrations on the walls near the base of the structure, between windows and also on the pillars at the height of the second level.

Comparing the shear stress and principal stress distributions, the following comments can be made. Maximum principal and shear stress locations overlap greatly, mainly around the windows and arches. This is important to take note of, since the

shear capacity of masonry structures are usually very small. The shear stress capacity of masonry is limited by the normalized mean compressive strength of a masonry unit, in accordance to the EUROCODE 6 Section 3.6.2 Equation 3.5. The formula for characteristic shear strength of masonry, f_{vk} is shown in Equation 7.1.

$$\mathbf{f}_{vk} = \mathbf{f}_{vko} + \mathbf{0.4}\sigma_d \tag{7.1}$$

but not greater than $0.065 f_b$ or f_{vlt} where:
f_{vko} is the characteristic initial shear strength, under zero compressive stress;
f_{vlt} is a limit to the value of f_{vk};
σ_d is the design compressive stress perpendicular to the shear in the member at the level under consideration, using the appropriate load combination based on the average vertical stress over the compressed part of the wall that is providing shear resistance;
f_b is the normalized compressive strength of masonry units, as described in the EUROCODE 6 Section 3.1.2.1, for the direction of application of the load on the test specimens being perpendicular to the bed face.

The strength of materials were defined according to the materials used by the Byzantine Empire. In Byzantine Empire, bricks made of mud or clay and lightweight mortar were commonly used. According to Table 3.4 of EUROCODE 6, the characteristic initial shear strength of masonry structures consisting of clay bricks with lightweight mortar must be taken as $fvko = 0.15$ MPa. Looking back at Figure 7.3, it can be seen that the maximum compressive stress obtained from the analysis is 7.7 MPa. A mean value of 4 MPa was taken to determine the characteristic shear strength of the masonry. Inserting these values into Equation 7.1, the following results is obtained:

$$\mathbf{f}_{vk} = 0.15 + 0.4 * 4 = 1.75\,\mathbf{MPa} \tag{7.2}$$

The limit of $0.065 f_b$ must be checked before going forward with this calculated value. For clay bricks, the normalized mean compressive strength varies between 20-40 MPa. Taking the damages and the weathering of the materials in Hagia Irene into account, the normalized mean compressive strength of a brick was taken as $f_b = 20$ MPa. According to this value, the shear strength can have a maximum value of $f_{vk} = 1.3$ MPa. The limit value of $f_{vk} = 1.3$ MPa was taken for further inspection of the finite element analysis results. Looking at the shear stress values after calculating the shear strength, it is clearly evident that there will be damages in the previously mentioned locations due to shear stress.

The possible damage zones are summed up and given as a list below to simplify the process of comparing them with the real life damaged areas:

(i) At the first floor of the structure, the finite element model results show very small levels of displacement values at the base of the structure. Defining the contact surfaces between the soil and the structure as fixed supports causes the pillars and walls to act as cantilevers, however in real life, the soil acts as a spring. Therefore, there will be some displacements, still they are expected to be too small to cause any type of damage. The only places which can suffer damages at the first floor are the windows in the apse, narthex and the windows on the side walls. These damages are expected to occur due to shear stresses.

(ii) The second level side walls undergo moderate amounts of displacements, however great amounts of shear stresses occur at the window arches and the walls in general. Considering these, damages are expected to occur at the top of the windows where the shear stress and maximum principal stress peaks. Damages due to displacement are not expected to occur at these walls. The only exception is the walls supporting the main dome, where they undergo excessive directional

displacements in transverse direction. These movements can cause slip failure at the higher parts of the wall, however they are unlikely.

(iii) The narthex will suffer similar damages like the side walls. Tensile stresses mainly determine the damages in the narthex. Near the windows and at the archways, shear cracks will form, apart from that, nothing special is expected to occur at the narthex.

(iv) The amphitheater part of the apse is an arched structure, and like all of the arched structures in the church, it may suffer damages. However, these damages are expected to be very small and insignificant, since the amphitheater is at the ground level. It also has no structural function.

(v) The windows at the apse are expected to suffer damages due to shear stresses. These damages are expected to occur at the top of the windows and move in the vertical direction, as if they are trying to snap the arches in half.

(vi) All of the domed structures are expected to suffer damages. The apse, the main dome and the small dome are all susceptible to damages caused by swaying motions. The damages on the domes will have the same characteristic like the ones in at the window arches. The cracks will run vertical on the inner surface of the dome. However, horizontal cracks and failures may occur at the main dome due to the excessive displacements.

(vii) The damages on the pillars will most likely start at the base due to compressive stresses.In Figure 7.3, the stresses occurring at the bases of the pillars are visible. Comparing the maximum principal stress distribution with the shear stress distribution, it is apparent that the stresses occurring at the base of the pillars are not shear stresses. Therefore, it is safe to assume that there are compressive stresses acting at the bases of the pillars.

(viii) On the main pillar, which is in the middle of the both domes, the deformation values increase too fast, which can cause a damage due to the drift.

(ix) The last set of damage zones are the arches. Due to the concentrated shear stresses on the top of the arched structures, cracks will occur. This is valid for the main arches supporting the domes and the arches connecting the marble columns.

7.2. Comparing the Results with the Damages in Hagia Irene

In the previous section, the possible damage zones are listed. The finite element model results will be compared with the damages in the actual structure. In Figure 7.6, the longitudinal cross-section of Hagia Irene is shown. The cracks are shown in cyan color. The damages in Entry 1 is shown with white circles. As mentioned, there are no cracks apart from those occurring at the arches and the bases of the pillars. The finite element model result for maximum principal stresses of the same cross section is shown in Figure 7.7. The possible damage zones and the amount the stresses exceed the limit value are shown with different colored circles:

(i) Green: Very close to the limit value, does not exceed the limit value.
(ii) Yellow: Exceeds the limit less than 50% of the limit value.
(iii) Red: Exceeds the limit more than 50% of the limit value.

It is possible to see the stress concentrations at the narthex and the pillar bases. The stress values coded by the colors yellow and orange pass the compressive strength limit of the material model. However, there are little to no stresses developing around the arches on top of marble columns.

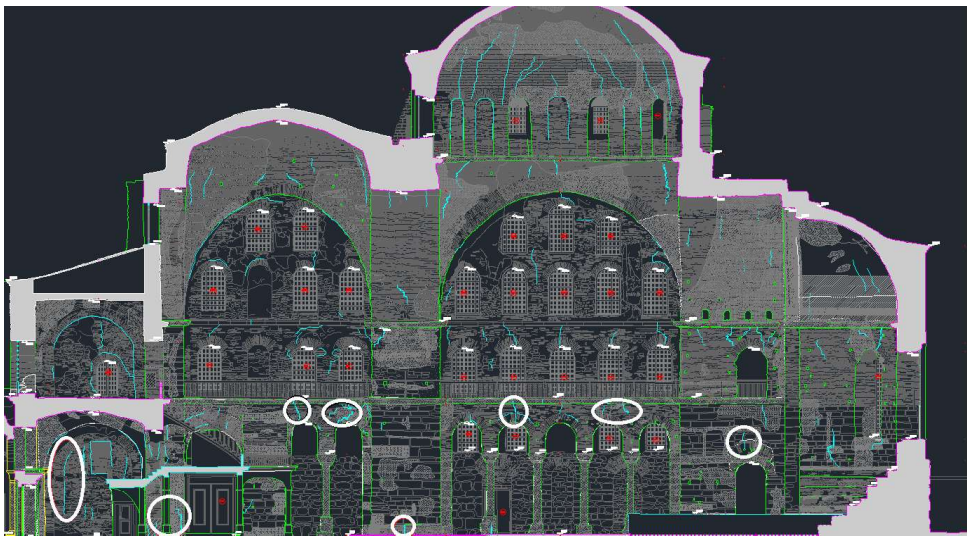

Figure 7.6. Entry 1 Damages

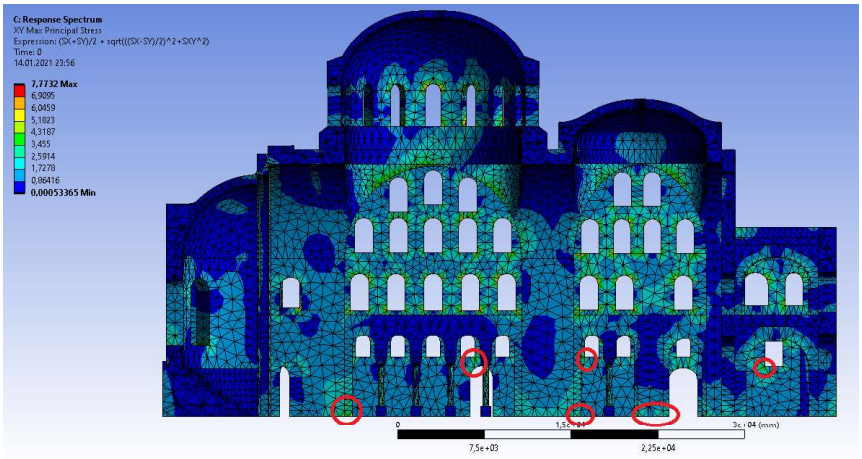

Figure 7.7. Entry 1 Damages FEM Results

For Entry 2, the cracks in the structure are shown in Figure 7.8 with red circles around them. There are more similar cracks to those which are encircled, but all of them are not encircled to avoid overcrowding the figure. As mentioned before, the cracks start from the top of the window arches and move vertically. The cracks at the bottom corners of the windows can also be seen in both the FEM results and the church. These damages are related to the compressive stresses. In Figure 7.8, the damages in Hagia Irene corresponding to this entry are shown. In Figure 7.9, the damages caused by compressive stresses are shown.



Figure 7.8. Entry 2 Damages

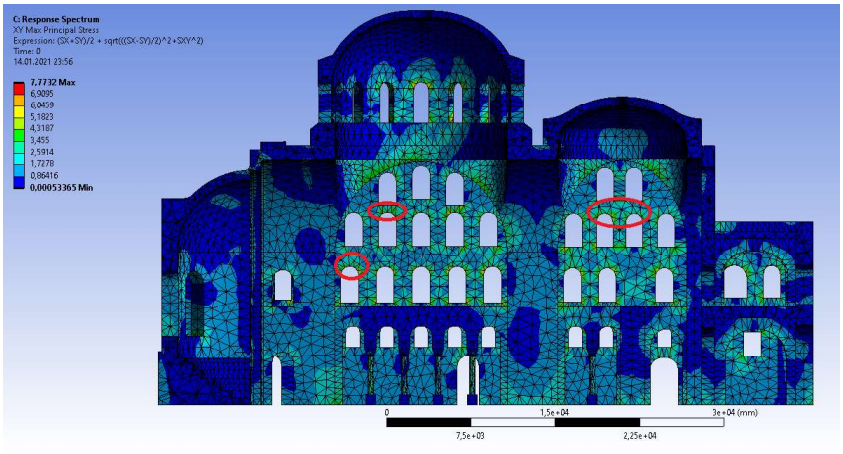

Figure 7.9. Entry 2 Damages, Compressive Stresses

Apart from these damages, there are also cracks between the windows as mentioned in the related entry. However, these damages are related to the tensile stresses occurring at these locations, shown in Figure 7.10.

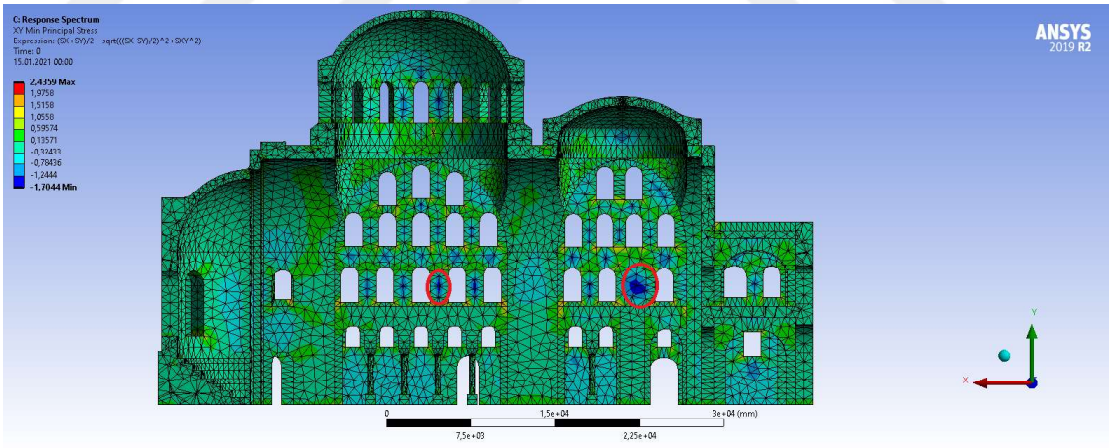

Figure 7.10. Entry 2 Damages, Tensile Stresses

These damages can very well caused by shear stresses, however tensile stresses greatly exceed the limit value of 0.5 MPa. Stress values close to 1.5 MPa can be observed at the Looking at Figure 7.11, it can be seen that there are shear stress values passing the limit of 1.3 MPa.

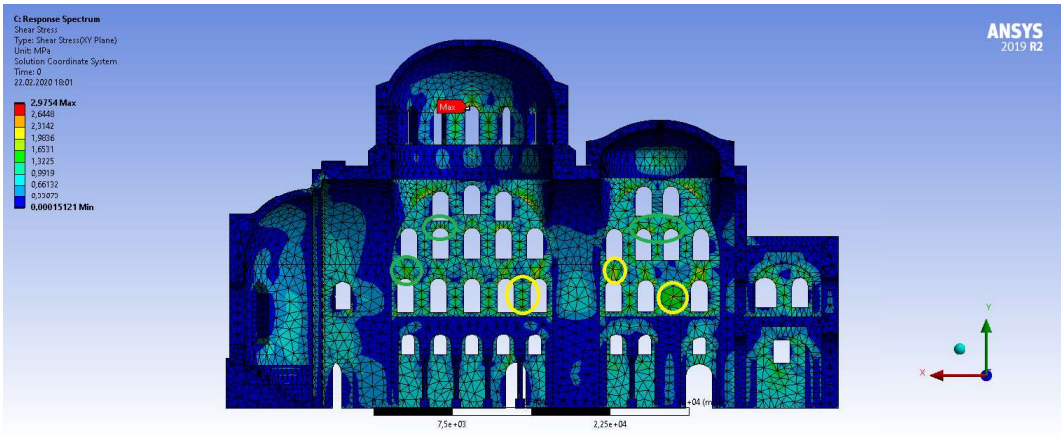

Figure 7.11. Entry 2 Damages, Shear Stresses

Comparing the figures, it is evident that at the crack locations, shear stresses concentrate and reach values between $1.3 - 1.9$ MPa. Previously, the maximum value of shear stress was calculated to be $f_{vk} = 1,3$ MPa. Considering the maximum shear stress, damages may occur at these locations. For Entry 2, the results obtained from the finite element model and the damages in the structure mostly coincide.

Continuing with Entry 3, Figure 7.12 shows the transverse cross-section of the narthex. The damaged locations are shown as before.

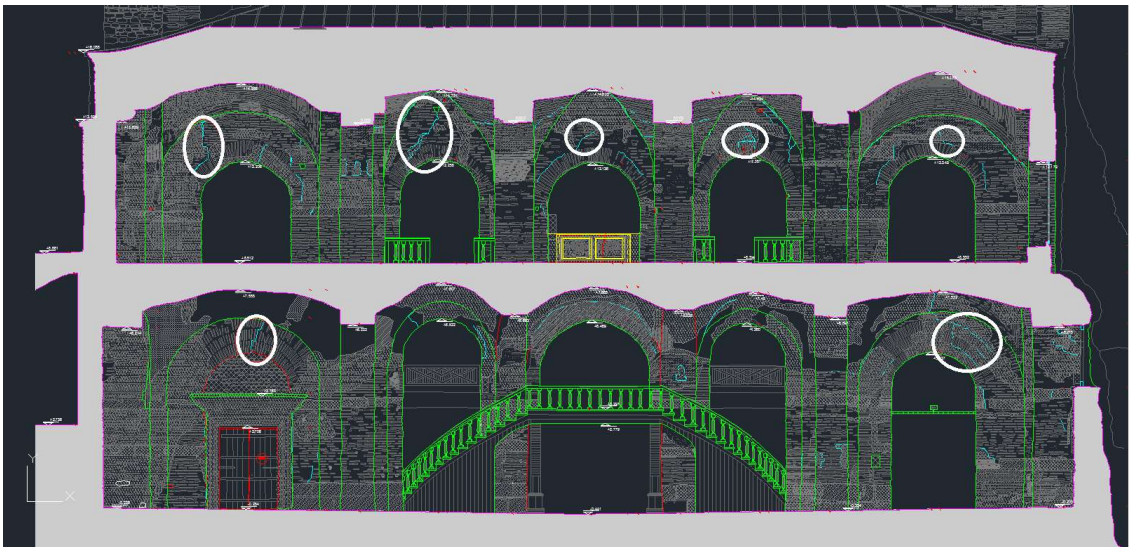

Figure 7.12. Entry 3 Damages

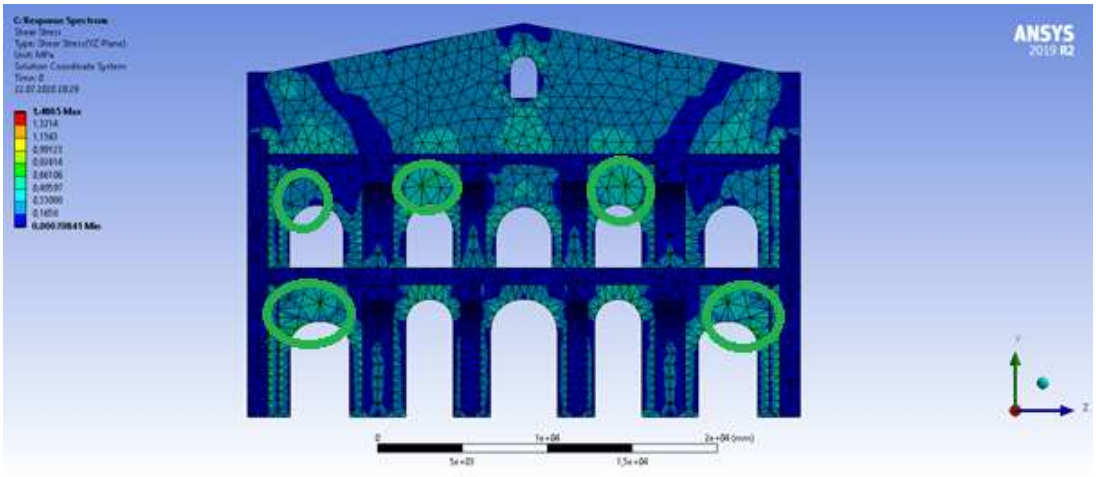

Figure 7.13. Entry 3 Damages FEM Results

Comparing the highlighted areas in the narthex and the model of the narthex, it is clearly evident that the model gives reasonable results. However, it is very important to note that the shear stress in the YZ plane is taken into consideration. If the shear stress in XY plane is taken, the stresses cannot be seen, as shown in Figure 7.14.

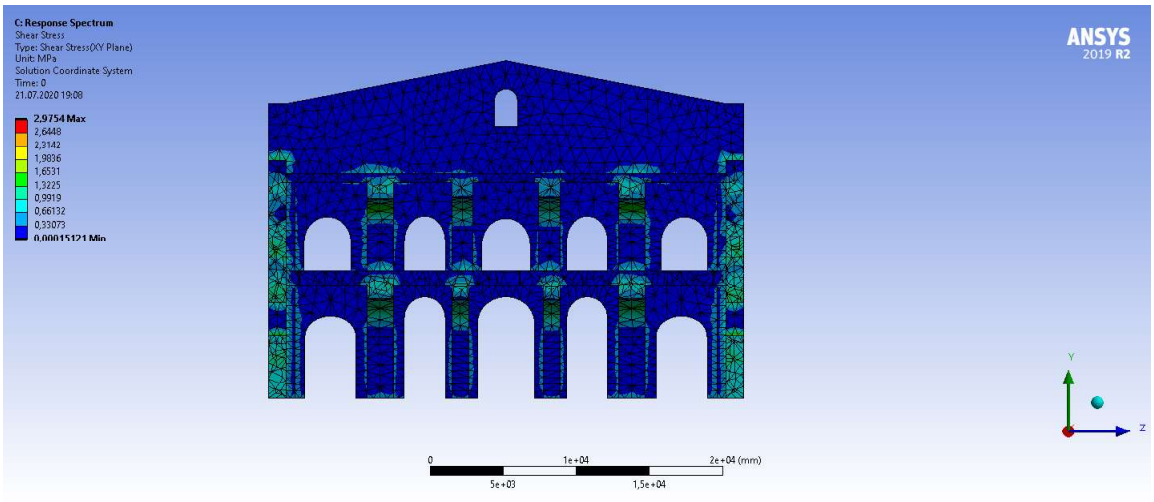

Figure 7.14. Narthex Shear Stresses, XY Plane

To inspect the side walls of the narthex, the cross sections used in Entries 1 and 2 are used. Figure 7.15 shows the damages in the actual structure, whereas in Figure 7.16 the FEM results of these damages are shown. For the comparison, the minimum

principal stress case is used. Comparing the locations shown in the actual building at the results obtained from the finite element model, it is evident that the cracks are located at places where the model gives high tensile stress values, far passing the limit of 0.5 MPa.

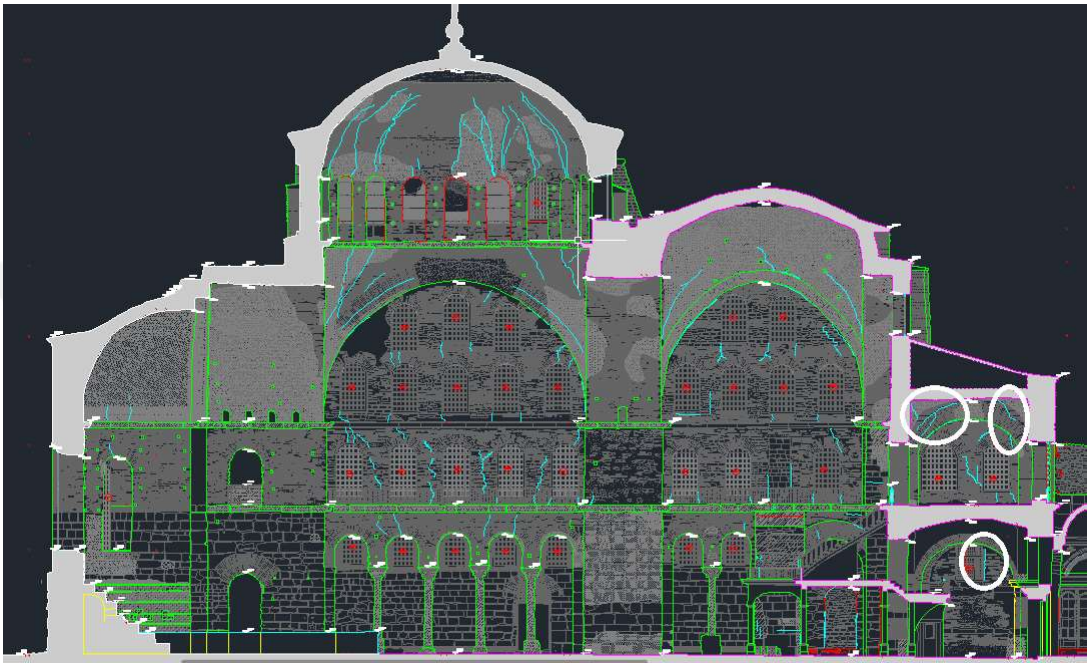

Figure 7.15. Narthex Damages, Longitudinal Cross Section

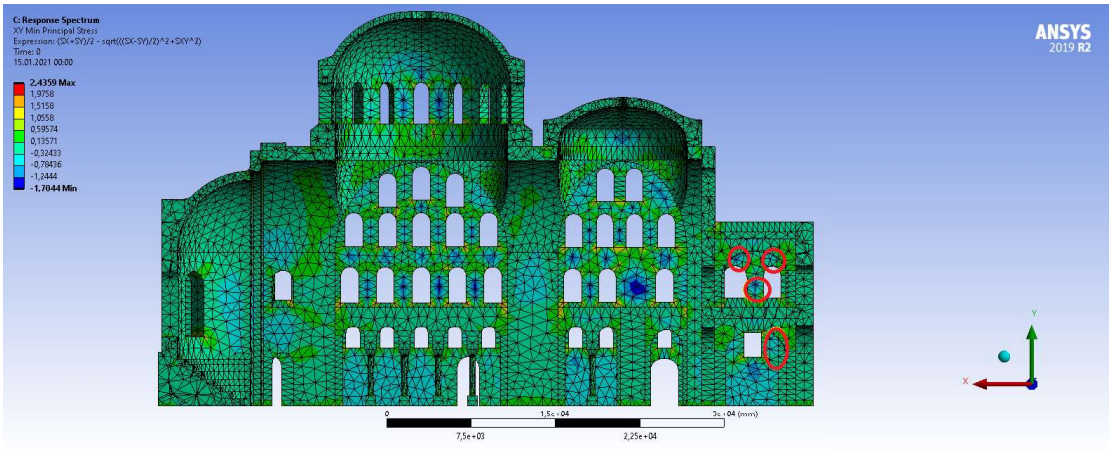

Figure 7.16. Narthex FEM Results, Longitudinal Cross Section

Entries 4, 5 and 6 will be inspected together. Entry 4 focuses on the amphitheater of the structure. As previously mentioned, the amphitheater isn't a structural

element. However, it is an important part of the interior of the church. The concerts are performed using the amphitheater as the stage. For Entry 5, the windows in the apse are the main focus. The window holes are also arched structures, so damages are expected to occur at the windows too. Lastly in Entry 6, the main dome and the half dome in the apse will be inspected. In Figure 7.17 and Figure 7.18, the cracks on the amphitheater, around the apse windows and in the dome are shown. There are also cracks on the intersection part between the main arch and the apse dome.

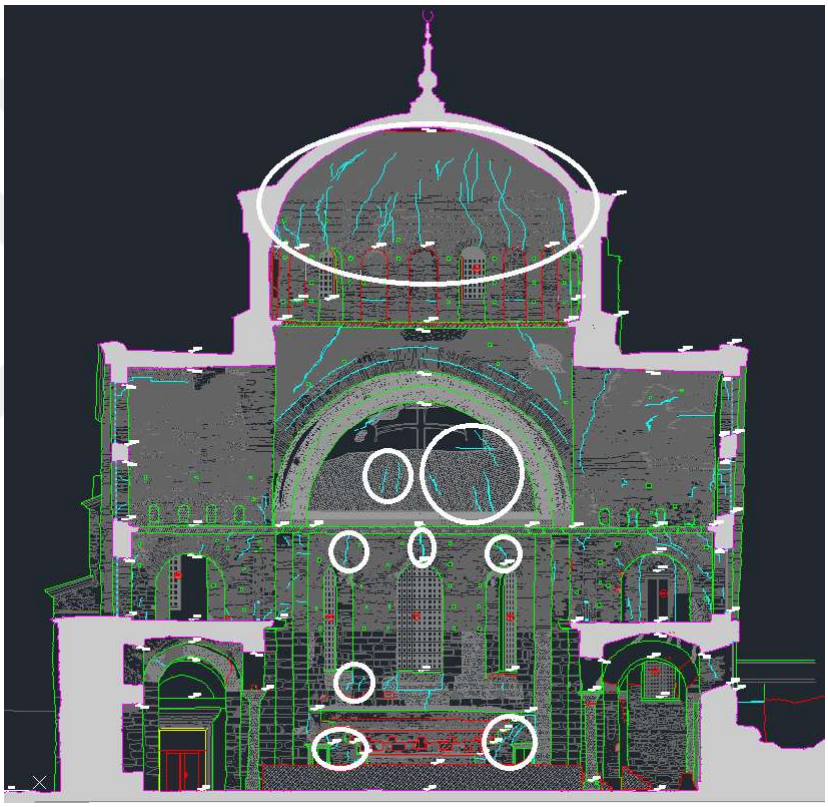

Figure 7.17. Entries 4,5 and 6 Damages

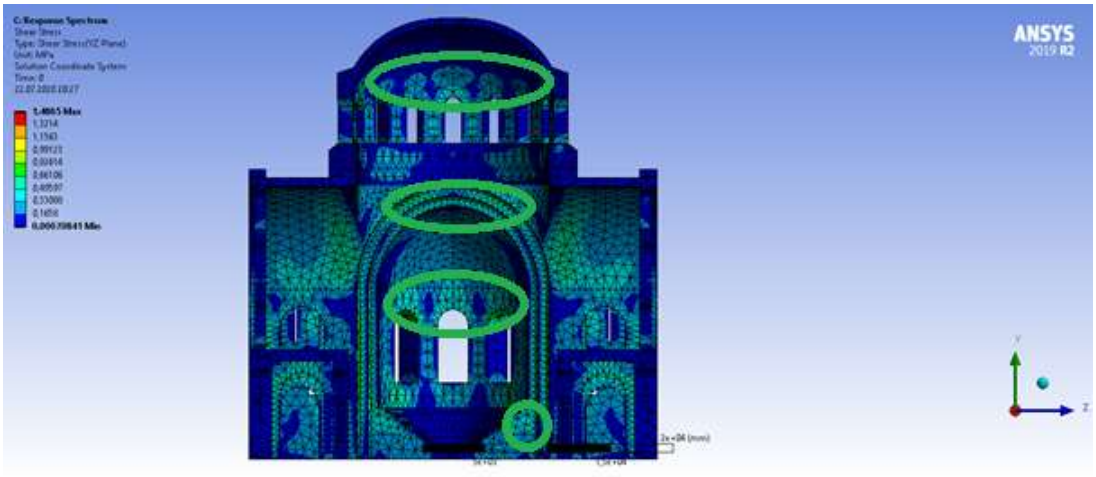

Figure 7.18. Entries 4,5 and 6 FEM Results

The finite element model results show the shear stress in YZ plane. Starting the inspection from the bottom of the structure, it can be seen that there are low shear stresses at the amphitheater. In the cross-section of the structure, the crack locations are in the same areas as the critical locations shown in the finite element model, however the stress values do not exceed the limit value. The damages on the amphitheater do not affect the structural integrity of the entire church, however it is important for its use as a stage. Moving upward, the on the apse are heavily focused around the windows and the arched areas, especially the half dome. Looking at the model results, the interior of the dome, the arches on the windows and between the pillars are critical locations where high values of shear stresses are expected, however these stresses also do not exceed the limit value. It can be said that shear stresses will not be causing great damages in these parts. The last part for this entry is the dome. The dome is the most critical part of the entire structure. The swaying motion of the structure during a potential earthquake creates the highest displacement values in the dome. As seen in Figure 7.17, the number of cracks inside the dome is very high. In the model, there are only stresses at the top of the windows, however the cracks are much longer in the actual structure. It can be assumed that the cracks occur due the shear and compressive stresses and advance vertically due to high displacement values. In this case, the window arches can be defined as the critical points.

Entries 7 and 8 focus on the pillars of the structure. Looking at the building survey, there are very small number of cracks on the main pillars of the structure. The main pillars can be seen in Figure 7.19. There are no visible cracks on the pillars. The model shows small stress values for the pillars, apart from the connection parts with the arches. Therefore, the pillars are not expected to suffer huge damages after an earthquake.

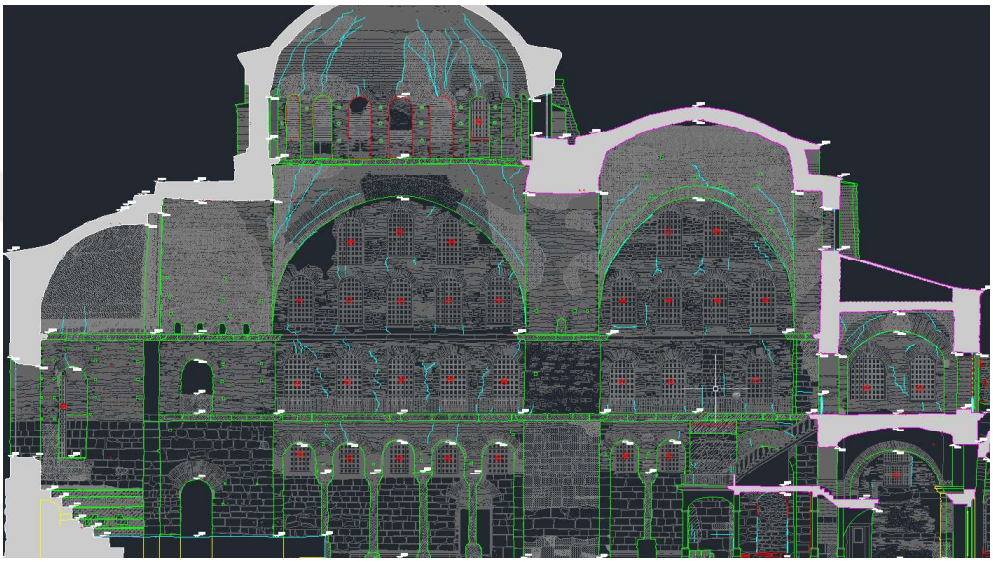

Figure 7.19. Damages on the Pillars

The last entry, Entry 9, focuses on the arches in the entire structure. The arches above the windows, between the marble columns and in the apse are already inspected. The remaining arches are the ones between the pillars. They are also the arches which carry the weight of the domes and the roof of the church. In Figure 7.20, the damaged areas on the main arches are shown with red circles.

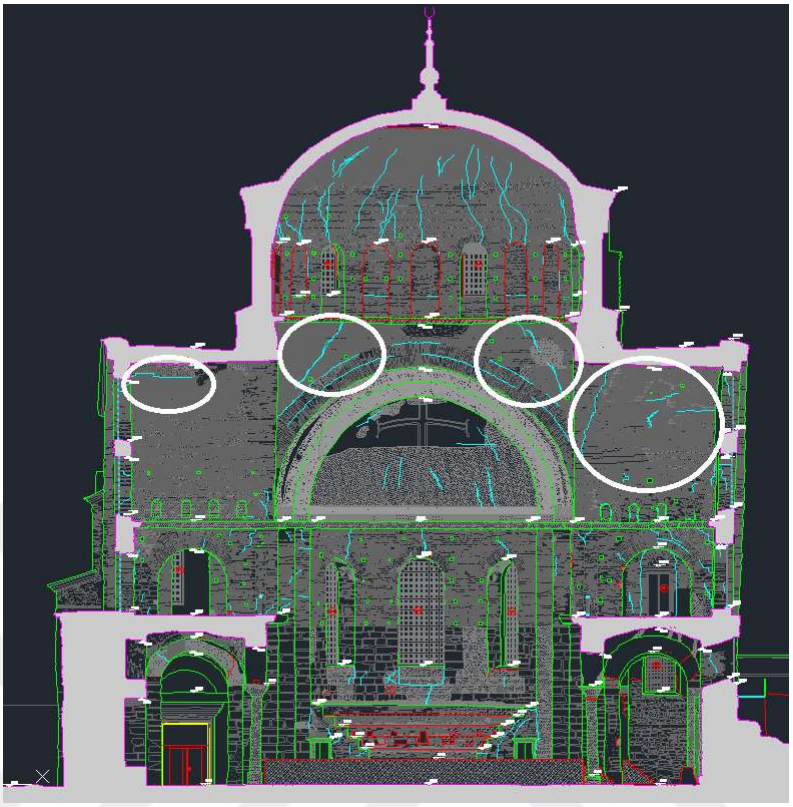

Figure 7.20. Damages on the Arches

It is clearly seen that there are numerous cracks on the arches supporting the roof and the domes. They are mainly located at the top of the arches. The cracks at the top of the arches are usually known to occur due to high shear stresses. This can be seen by looking at the according finite element model results.

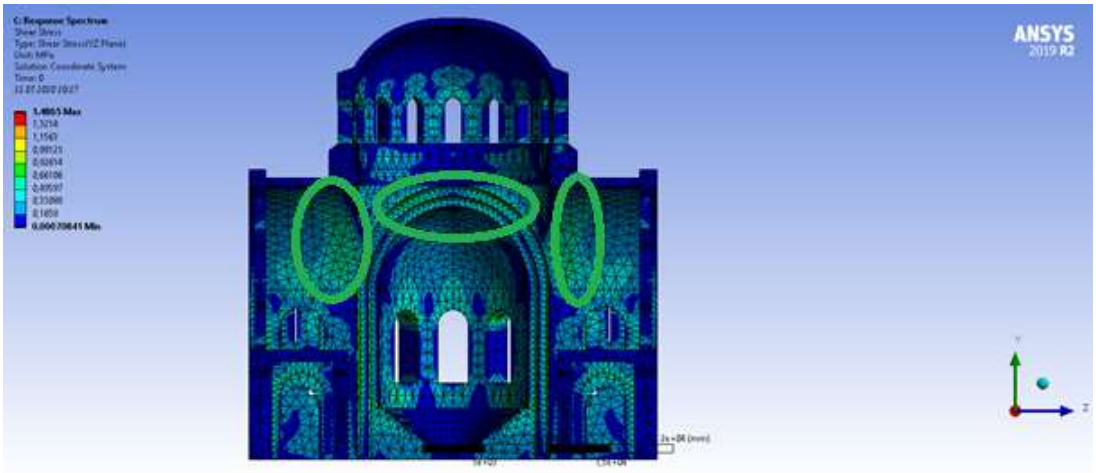

Figure 7.21. Damages on the Arches FEM Results

In Figure 7.21, the stress concentration on the arches are shown. This figure shows the equivalent stresses occurring on the arches supporting the main dome. It is evident that high stress values are located on the actual crack locations. The arches are structural elements, therefore the damages and stresses in these elements must be thoroughly inspected.

8. CONCLUSION

In this thesis, the question "*Are regular seismic assessment methodologies applicable to masonry cultural heritage buildings?*" was tried to be answered. These methodologies include ambient vibration testing for structural identification and finite element model for seismic assessment. Looking back at the obtained results, it can be clearly said that the methods used for regular structures can be applied to masonry heritage buildings.

The process of applying conventional seismic assessment methodologies to masonry structures was found out to be much more challenging than regular reinforced concrete structures. Applying ambient vibration test is trivial for any structure, however creating a finite element model of a masonry structure was the tricky part. The first reason for this is the material properties. The properties of the individual building components like the stones and mortar can be determined via laboratory tests, but when they are combined, it becomes much more complicated. This is mainly due to the fact that masonry elements are heavily reliant on the construction process. Human factor plays a crucial role during the construction of masonry structures. The thickness of the mortar joints, the quality of the mortar mixture, the placement of the stones or bricks all have an influence on the mechanical properties of a masonry element. This was inspected during the construction of the panel wall, which was later used for the small scale test explained in Chapter 4. Mortar thickness changed with each level of brick due to reasons like the fatigue of the mason and decrease of the ready mortar.

The second reason is the modelling strategy. By separating the materials from each other in the model (micro-modelling), the problem of defining material properties for the combination of materials can be tackled. However, the ultimate goal is to apply the methodology on a heritage building and micro modelling an entire structure brick by brick is simply impossible. To tackle these problems and to check whether macro-modelling strategies are applicable to masonry buildings, the small-scale test was made. In this test, a wall panel was constructed in laboratory conditions and the

subjected to tests. After obtaining the test results, the same conditions were created in a finite element model. After comparing the results of the lab tests and FEM analysis, it was concluded that macro models give acceptable results for masonry elements.

The small scale test set the path for the monitoring of Hagia Irene. During the field tests, which lasted for three days, the interior of the structure was inspected and ambient vibration measurements were taken. After analyzing the vibration data and extracting modal parameters, the finite element model was created. Since there was no possibility of conducting material tests on the site, the properties from the small test were used as a starting point. The reliability of the finite element model was controlled by comparing both the modal results and the results obtained from response spectrum analysis. The results from the FEM analysis agreed well with the ambient vibration test and the present damages on the structure.

Macro models for masonry cultural heritage buildings give good results which can be used for further seismic assessments. During the modelling process in both Chapter 4 and Chapter 6, many different techniques and conditions were applied. It is made evident that different approaches to material models, support and loading conditions, analysis types and modelling methods can achieve similar results. Also it is important to note that every cultural heritage building is unique and require its own way of tweaking the conventional seismic assessment methods. Trying different approaches gives a better understanding to the structure and problem at hand. Limiting to one approach is not feasible while discussing a multidisciplinary subject like SHM.

Although the results of this research may be satisfactory, there is room for much improvement. The model created in this thesis was a linear model considering the structure a whole. Like previously discussed in Chapter 2, some models divide the structure into parts and use different material properties for these individual parts. Different material properties and characteristics can be assigned to these parts to obtain better results.

The previous discussion about assigning different material properties opens up

a discussion for a very important topic, which is the determination of these material properties. The material properties used in this thesis were calibrated according to the model results. Although this is used in many different cases in Chapter 2, there are other way to calibrate the material properties, mainly the Young's Modulus. Damages and cracks affect the value of Young's Modulus greatly. Damaged location must be modelled with lower Young's Modulus values to represent these areas more realistically. In the case of Hagia Irene, there were no localized cracks or damages, therefore the Young's Modulus values for the entire church was taken lower than actual. Even if the material properties were to be determined by using destructive or non-destructive methods, it is always necessary to include the affects of the cracks and other damages by calibrating these material properties.

The interaction between soil and masonry structures can be examined as a whole different topic. In the model, soil-structure interaction surfaces were taken as fixed supports. That is not the case in real life structures. In reality, soil acts as a spring, so it could be modelled as an elastic support or a compression only support. However, there were no usable site tests, which can be used to model the soil medium.

One last improvement to the model could have been the detail level of the structure and its components. In historical structures, the structural elements have all different dimensions along their lengths or spans. The church is also not symmetrical like the finite element model. The best way to create a perfectly detailed model is to create a 3D CAD model and then exporting it to a finite element analysis program.

The protection of cultural heritage buildings is very important because these buildings represent the history and culture of civilizations which resided on those ground before. Protecting these structures means protecting the memory of a civilization and a part of the history of the world. This topic is really important for Turkey because Anatolia was home to thousands of hundreds and cultures. Seismic assessment methods are continuously improving and the maintenance of cultural heritage buildings and researches in these areas are becoming more sophisticated as time goes by. Even if construction and seismic assessment methods may change in the future,

maintenance of cultural heritage buildings which represent the history and culture of country will always be needed.

REFERENCES

1. Farrar, C. R. and K. Worden, "An introduction to structural health monitoring", *Philosophical Transactions of the Royal Society A: Mathematical, Physical and Engineering Sciences*, Vol. 365, No. 1851, pp. 303–315, 2007, https://royalsocietypublishing.org/doi/abs/10.1098/rsta.2006.1928.

2. Doebling, S., C. Farrar, M. Prime and D. Shevitz, "Damage Identification and Health Monitoring of Structural and Mechanical Systems From Changes in their Vibration Characteristics: A Literature Review", *Technical Report No. LA-13070-MS*, Vol. 30, 05 1996.

3. Brownjohn, J., "Structural health monitoring of civil infrastructure", *Philosophical Transactions of the Royal Society A: Mathematical, Physical and Engineering Sciences*, Vol. 365, No. 1851, pp. 589–622, 2007, https://royalsocietypublishing.org/doi/abs/10.1098/rsta.2006.1925.

4. Gentile, C. and A. Saisi, "Ambient vibration testing of historic masonry towers for structural identification and damage assessment", *Construction and Building Materials*, Vol. 21, pp. 1311–1321, 06 2007.

5. Bassoli, E., L. Vincenzi, A. D'Altri, S. Miranda, M. Forghieri and G. Castellazzi, "Ambient vibration-based finite element model updating of an earthquake-damaged masonry tower", *Structural Control and Health Monitoring*, Vol. 25, 02 2018.

6. Erdogan, Y., "Discrete and Continuous Finite Element Models and Their Calibration Via Vibration and Material Tests for the Seismic Assessment of Masonry Structures", *International Journal of Architectural Heritage*, Vol. 11, 05 2017.

7. Cimellaro, G., S. Piantà and A. De Stefano, "Output-Only Modal Identification of Ancient L'Aquila City Hall and Civic Tower", *Journal of Structural Engineering*,

Vol. 138, pp. 481–491, 04 2012.

8. Ubertini, F., N. Cavalagli, A. Kita and G. Comanducci, "Assessment of a monumental masonry bell-tower after 2016 Central Italy seismic sequence by long-term SHM", *Bulletin of Earthquake Engineering*, Vol. 16, p. 775–801, 02 2018.

9. Ramos, L., L. Marques, P. Lourenco, G. De Roeck, A. Costa and J. Roque, "Monitoring historical masonry structures with operational modal analysis: Two case studies", *Mechanical Systems and Signal Processing*, Vol. 24, pp. 1291–1305, 07 2010.

10. Ceravolo, R., A. De Marinis, M. Pecorelli and L. Zanotti Fragonara, "Monitoring of masonry historical constructions: 10 years of static monitoring of the world's largest oval dome", *Structural Control and Health Monitoring*, Vol. 24, 12 2016.

11. Lombillo, I., H. Blanco Wong, J. Pereda, L. Villegas, C. Carrasco and J. Balbás, "Structural health monitoring of a damaged church: design of an integrated platform of electronic instrumentation, data acquisition and client/server software: Integrated Platform for the Structural Health Monitoring of a Church", *Structural Control and Health Monitoring*, Vol. 23, 05 2015.

12. De Matteis, G. and F. Mazzolani, "The Fossanova Church: Seismic Vulnerability Assessment by Numeric and Physical Testing", *International Journal of Architectural Heritage*, Vol. 4, pp. 222–245, 07 2010.

13. Cigada, A., L. Dell'Acqua, B. Castiglione, M. Scaccabarozzi, M. Vanali and E. Zappa, "Structural Health Monitoring of an Historical Building: The Main Spire of the Duomo Di Milano", *International Journal of Architectural Heritage*, Vol. 11, 12 2016.

14. Casarin, F. and C. Modena, "Seismic Assessment of Complex Historical Buildings: Application to Reggio Emilia Cathedral, Italy", *International Journal of Architectural Heritage*, Vol. 2, No. 3, pp. 304–327, 2008,

https://doi.org/10.1080/15583050802063659.

15. Abbiati, G., S. Massetto, L. Zanotti Fragonara, G. Pistone and R. Ceravolo, "Vibration-Based Monitoring and Diagnosis of Cultural Heritage: A Methodological Discussion in Three Examples", *International Journal of Architectural Heritage*, Vol. 10, 09 2014.

16. Pelà, L., A. Aprile and A. Benedetti, "Seismic assessment of masonry arch bridges", *Engineering Structures*, Vol. 31, No. 8, pp. 1777 – 1788, 2009, http://www.sciencedirect.com/science/article/pii/S0141029609000716.

17. Conde, B., L. Ramos, D. Oliveira, B. Riveiro and M. Solla, "Structural assessment of masonry arch bridges by combination of non-destructive testing techniques and three-dimensional numerical modelling: Application to Vilanova bridge", *Engineering Structures*, Vol. 148, pp. 621–638, 10 2017.

18. Gönen, S. and S. Soyöz, "Seismic analysis of a masonry arch bridge using multiple methodologies", *Engineering Structures*, Vol. 226, p. 111354, 2021, http://www.sciencedirect.com/science/article/pii/S0141029620339559.

19. Aytulun, E., S. Soyoz and E. Karcioglu, "System Identification and Seismic Performance Assessment of a Stone Arch Bridge", *Journal of Earthquake Engineering*, pp. 1–21, 11 2019.

20. Costa, C., A. Arêde, A. Costa, E. Caetano, A. Cunha and F. Magalhães, "Updating Numerical Models of Masonry Arch Bridges by Operational Modal Analysis", *International Journal of Architectural Heritage*, Vol. 9, 11 2014.

21. Senthivel, R. and P. Lourenço, "Finite element modelling of deformation characteristics of historical stone masonry shear walls", *Engineering Structures*, Vol. 31, No. 9, pp. 1930 – 1943, 2009, http://www.sciencedirect.com/science/article/pii/S0141029609000753.

22. Gonen, S. and S. Soyoz, "Investigations on the elasticity modulus of stone masonry", *Structures*, Vol. 30, pp. 378–389, 2021, https://www.sciencedirect.com/science/article/pii/S2352012421000394.